AUS DER KLINIK UND POLIKLINIK FÜR NEUROLOGIE
PROF. DR. ULRICH BOGDAHN
DER FAKULTÄT FÜR MEDIZIN
DER UNIVERSITÄT REGENSBURG

THE ROLE OF THE PROTEOGLYCAN VERSICAN IN HIGH-GRADE GLIOMAS

Inaugural – Dissertation
zur Erlangung des Doktorgrades
der Medizin

der
Fakultät für Medizin
der Universität Regensburg

vorgelegt von
Julia Sophie Onken

2012

AUS DER KLINIK UND POLIKLINIK FÜR NEUROLOGIE
PROF. DR. ULRICH BOGDAHN
DER FAKULTÄT FÜR MEDIZIN
DER UNIVERSITÄT REGENSBURG

THE ROLE OF THE PROTEOGLYCAN VERSICAN IN HIGH-GRADE GLIOMAS

Inaugural – Dissertation
zur Erlangung des Doktorgrades
der Medizin

der
Fakultät für Medizin
der Universität Regensburg

vorgelegt von
Julia Sophie Onken

2012

Dekan:	Prof. Dr. Dr. Torsten E. Reichert
1. Berichterstatter:	Prof. Dr. Peter Hau
2. Berichterstatter:	Prof. Dr. Markus Riemenschneider

Tag der mündlichen Prüfung: 08.02.2013

Contents

Abbreviations

ADAMTS	A disintegrin and metalloproteinase domain with thrompospondin motifs
APS	Ammonium persulphate
Aqua dest.	Aqua destillata
AS	Amino acid
BCA	Bicinchoninic acid
Bp	Base pair
BSA	Bovine serum albumin
C	Cytosine
CC	Cell count
cDNA	Complementary DNA
Ch	Chamber volume
CIP	Calf intestinal phosphatase
CM	Culture medium
CNS	Central nervous system
CS	Chondroitin sulphate
CS	Cell suspension
Ct	Cycle threshold
DF	Dilution factor
DMEM	Dulbecco’s modified eagle medium
DMSO	Dimethyl sulfoxide
DNA	Deoxyribonucleic acid
dNTP	Desoxyribonucleotide triphosphate
DOXY	Doxycycline
dsRNA	Double-stranded RNA
ECM	Extracellular matrix
EDTA	Ethylendiamine-tetraacetic acid
EGFR	Epidermal growth factor receptor

ELISA	Enzyme-linked immunosorbent assay
FACS	Fluorescence-activated cell sorting
FCM	Fibroblast-conditioned medium
FCS	Foetal calf serum
FIGO	Fédération Internationale de Gynécologie et d'Obstétrique
G	Guanine
GAG	Glycosaminoglycan
GBM	Glioblastoma multiforme
GFP	Green fluorescent protein
HA	Hyaluronican acid
HRP	Horseradish peroxidase
IB	Immunoblot
IF	Immunefluorescence
kDa	Kilodalton
LB-amp	Lysogeny broth - ampicillin
LB	Lysogeny broth
LTR	Long terminal repeat
miRNA	MicroRNA
mRNA	Messenger RNA
MV	Mean value
nt	Nucleotide
ON	Oligonucleotide
p	Probability of obtaining a test statistic
PAGE	Polyacrylamide gel electrophoresis
PBS	Phosphate-buffered saline
PCR	Polymerase chain reaction
qPCR	Quantitative PCR
RIPA	Radioimmunoprecipitation assay
RISC	RNA-induced silencing complex
RNAi	RNA interference
RPM	Rounds per minute

RT	Room temperature
RT-PCR	Reverse transcriptase PCR
SD	Standard deviation
SDS	Sodium dodecyl sulphate
shRNA	Short hairpin RNA
siRNA	Small interfering RNA
SOB	Super optimal broth
T	Thymidine
T_m	Temperature of melting
Taq	Thermophilus aquaticus
Taq DNA Pol	Taq DNA polymerase
TBS	Tris-buffered saline
TGF-ß2	Transforming growth factor ß2
TLR	Toll-like receptor
Tm	Melting temperature
Tris	Hydroxymethyl aminomethane
WHO	World Health Organization

Introduction

I.1 Glioblastoma multiforme

Gliomas include all primary central nervous system (CNS) tumours of glial origin. They account for more than 50% of all brain tumours and are by far the most common primary brain tumours in adults.[1] Gliomas have their origin in different glial cell types, mainly astrocytes and oligodendrocytes. They can be divided into four grades according to different levels of aggressiveness and malignancy that are reflected in the World Health Organization (WHO) classification system. Ependymomas account for 10% of all gliomas and are mainly benign.[2] Oligodendrogliomas account for 10–30% of all gliomas and are mainly low-grade, partly transitioning to high-grade. Astrocytomas account for 60–70% of gliomas.[3] Pilocytic astrocytomas are classified as WHO grade I; low-grade astrocytomas are listed as WHO grade II; anaplastic astrocytomas are classified as WHO grade III and glioblastomas as WHO grade IV. Glioblastoma multiforme (GBM), the most aggressive subtype, may develop *de novo* (primary GBMs) or by progressing from low-grade or anaplastic astrocytomas (secondary GBMs).[4] GBM is associated with the worst prognoses, with a median survival rate of 12–18 months post diagnosis, even under the best available therapy.[5] GBMs account for approximately 50% of all glial tumour types.[6]

Malignant astrocytic gliomas are associated with a dismal prognosis because of their ability to infiltrate diffusely into the normal brain parenchyma.[7] The invasive nature of cells plays an important role in the ineffectiveness of current treatment modalities. The cancer cells that remain after surgical therapy inevitably infiltrate the surrounding normal brain tissue and lead to tumour recurrence. The diffuse nature of GBMs is illustrated by the fact that after surgical resection, the residual pool of invasive cells gives rise to a recurrent tumour, which in more than 90% of cases develops immediately adjacent to the resection margin.[8] Satellite lesions may also occur at a distance from the resection cavity and even in the contralateral hemisphere.[9,10] The above-described aggressiveness and invasiveness, our poor understanding of molecular mechanisms and genetic heterogeneity lead to the poor outcome of GBM treatment. Standard therapy currently consists of surgery, radiation and

chemotherapy.[11] As stated in the above, prognosis is dismal and, consequently, novel therapeutic targets are desperately needed.

I.1.1 Malignancy criteria in GBM

The ability of glioblastoma multiforme cells to infiltrate the sourrounding tissue is influenced by a number of factors accounting complex intracelluar and extracellular pathways, extracellular components and enzyme activity. The process of invasion includes increased synthesis and secretion of several proteases, which selectively degrade extracellular matrix (ECM) components. These proteases also play a role in establishing and maintaining a microenvironment that facilitates tumour-cell survival.[12]

Glioma cell invasion is a complex and multistep mechanism involving a large array of molecules mediating cell-cell and cell–extracellular matrix interactions. These processes allow individual tumour cells to migrate into and invade healthy brain tissue even after macroscopic radical surgical resection of the tumour.[13]

Tumour cells at the invasive front detach from the growing primary tumour mass, adhere to the ECM via specific receptors and locally degrade ECM components, creating a pathway for neoplastic cells to migrate into adjacent tissue. However, the unique histological pattern of invasion shown by primary brain tumours together with the unique composition of the brain ECM suggest that glioma-specific mechanisms might also be involved.[14,15]

In primary brain tumours, many ECM components are up-regulated within both the tumour stoma and at the advancing edge of the tumour. Changes in these ECM components are belived to modulate brain tumour growth, proliferation and invasion, although in many cases little is known about specific interactions and detailed mechanisms.[16] Glioma cells also disseminate along the myelinated fibre tracts of white matter, which results in the distant spread of tumour cells through the corpus callosum to the contralateral hemisphere.[17]

I.2 Extracellular matrix

I.2.1 Structure and function of extracellular matrix

Extracellular matrix (ECM) not only acts as a physical framework, but also exerts a profound effect on cell shape and behaviour, including cell adhesion, spreading, migration, proliferation and differentiation.[18] ECM is involved in normal reparative processes, as well as in primary brain neoplasia.

Cells stay in contact with the ECM via surface receptors.[19] Signal transduction leads to the remodelling of the ECM, which influences changes in motility, the ability to migrate and proliferate, and the expression patterns of a number of proteins (e.g. integrins). This mechanism results in a very dynamic process of composition and decomposition of the ECM. The composition of ECM components varies in different tissue types, especially in comparison to normal brain and brain tumour tissue.[20]

I.2.2 Extracellular matrix in normal brain tissue

Neuronal cell populations are surrounded by various types of ECM molecules. The microenvironment is responsible for the tumour cells' adhesive ability, which has a major influence on neuronal growth and development.[21] The ECM influences numerous functions and processes in the brain. During development of the brain, the ECM plays an important role in the migration of glial and neuronal precursor cells, in cell proliferation, directional axonal growth and expression of synaptic structures.[22]

A well-defined ECM comprises a true basement membrane, cerebral vascularization and the glial *membrana limitans externa*. The *membrana limitans externa* is a basement membrane that covers the entire cortical surface of the brain and also separates astrocyte foot processes from pial cells and the subarachnoid space.[23] The cerebral vascular basement membrane that surrounds the blood vessels of the brain contains type-IV and type-V collagens, fibronectin, laminin, vitronectin, heparan-sulphate and proteoglycans.

Proteoglycans and glycosaminoglycans are abundant in the brain parenchyma. In the mature brain, chondroitin sulphate is located in the cytoplasm of some neurons and astrocytes and in myelinated and non-myelinated axon fibres.[24,25] Both chondroitin sulphate and heparan sulphate are also present in the basement membrane.[26] Heparan sulphate is found as a membrane protein in synaptic vesicles, in the ECM of

the neuromuscular junction and in the basement membranes of Schwann cells.[27,28] Heparan-sulphate proteoglycans have been found to induce cell motility.[29]

I.2.3 Extracellular matrix in brain tumours

We are gaining an increasing understanding of the decisive role which the ECM plays in repair processes and in the development of neoplasia.[30] Major constituents of the ECM in brain tumours are proteoglycan, glycosaminoglycans and glycoproteins.

Previous studies have already investigated changes in the composition of the ECM in normal brain compared to primary brain tumour tissue. It has been shown that tumour cell matrix has changing expression levels of HA and other glycosaminoglycans as well as osteopontin, vitronectin, tenascin-C and thrombospondin, depending on their localization on the blood vessel walls.[31] Glycosaminoglycans are found mainly in brain tumour tissue. Their hyaluronic acid content is shown to increase transiently during tumour-cell migration and is usually found at the interface between the tumour mass and host tissues.[32] Apart from its important role in tumour-cell invasion, hyaluronic acid is implicated in many normal cell functions, including neural-crest migration.[33] Akiyama *et al* succeeded in showing that tumour-cell invasion and migration of primary brain tumours is mediated by the interaction of hyaluronan and cellular receptors called CD44 and RHAMM.[34]

Fibronectin is found at the glioma–mesenchymal junction between tumours and in tumour-associated blood vessels, and it is expressed by glioblastoma cell lines *in vitro*.[35,36] Advanced stages of glioblastoma have been shown to express vitronectin, a component of the ECM that is usually absent from normal brain and in early-stage gliomas.[37] In comparison with fibronectin, laminin and collagen IV, vitronectin is a poor adhesive and migratory protein for U251 and SF767 glioblastoma cells.[38]

Laminin describes a large group of adhesion glycoproteins that are found in all basement membranes and in hyperplastic blood vessels in glioma cells; it is an integral part of the *glial limitans externa*.[39] Laminin 5 in particular has recently been found to be a promoter of glioma adhesion, invasion and migration, which is mediated by integrin α3β2.[40]

Besides glycosaminoglycans and glycoproteins, it has been suggested that proteoglycans play a key role in brain tumours such as, for instance, tenascin-C,

brain-enriched hyaluronic binding (BEHAB, brevican) and versican. Tenascin-C is synthesized by glial and neural-crest cells,[41] as well as by satellite cells of the peripheral nervous system.[42] Its expression pattern increases with higher stages of tumour malignancy in the area of the surrounding vessel walls.

The regulation of these important adhesion and migration factors is currently only partly understood. It has been shown that transforming growth factor-ß (TGF-ß, a member of the cytokine family that comprises homodimeric polypeptides) exerts multiple functions that include regulation of cell growth and differentiation, immunosuppression, induction of angiogenesis and apoptosis, and promotion of ECM production. An effect of TGF-ß2 on invasion has been described in gliomas and other model systems, but no conclusive model yet exists. It is only known that these effects are very complex, consisting of a step-like process of attachment and migration, which involves the components of ECM as well as tumour cells.[43]

I.3 Versican

Versican is a proteoglycan of the lectin family. It was initially identified in the culture medium of human IMR-90 lung fibroblasts.[44] In 1996, versican was identified in human brain and brain tumours.[45] Versican is encoded by a single gene and is located on chromosome 5a 12-14 on the human genome and is called the VACAN-gene. The gene is divided into 15 exons and has a molecular mass of 500 kDa. Versican exists of an N-terminal G1-domain, a glycosaminoglycan-domain (GAG-domain) and a C-terminal G3-domain. Four isoforms of versican – V0, V1, V2, V3 – are generated by means of alternate splicing in the exons of the GAG-domain (Figure 1).

V0 contains a GAG-α exon and a GAG-β exon. V1 contains the GAG-β exon. V2 contains the GAG-α exon and represents the CS-proteoglycan in the brain. V3 contains only both globular domains.[46] Consequently, this isoform exists as a glycoprotein and not as a proteoglycan.

All versican isoforms contain globular domains at the amino terminus (G1) and carboxyl terminus (G3).[47] The G1-domain is composed of an immunoglobulin-like motif, followed by two proteoglycan tandem repeats that bind hyaluronic acid. A linker protein mediates the association of versican with hyaluronic acid. Both hyaluronic acid and the isolated linker protein have the ability to bind to versican's G1-domain.[48]

The G3-domain contains two epidermal growth factor-like repeats, a carbohydrate recognition domain (a lectine-like repeat) and complement binding protein-like subdomains with structural similarity to the selectin family.[49] The difference in sizes of the chondroitin sulphate attachment regions in between the isoforms suggests that the actual number and size of attached chondroitin sulphate chains varies, indicating that the possibility of heterogeneity in number, length and molecular structure of chondroitin sulphate GAG may lead to different structural and functional diversity outcomes.

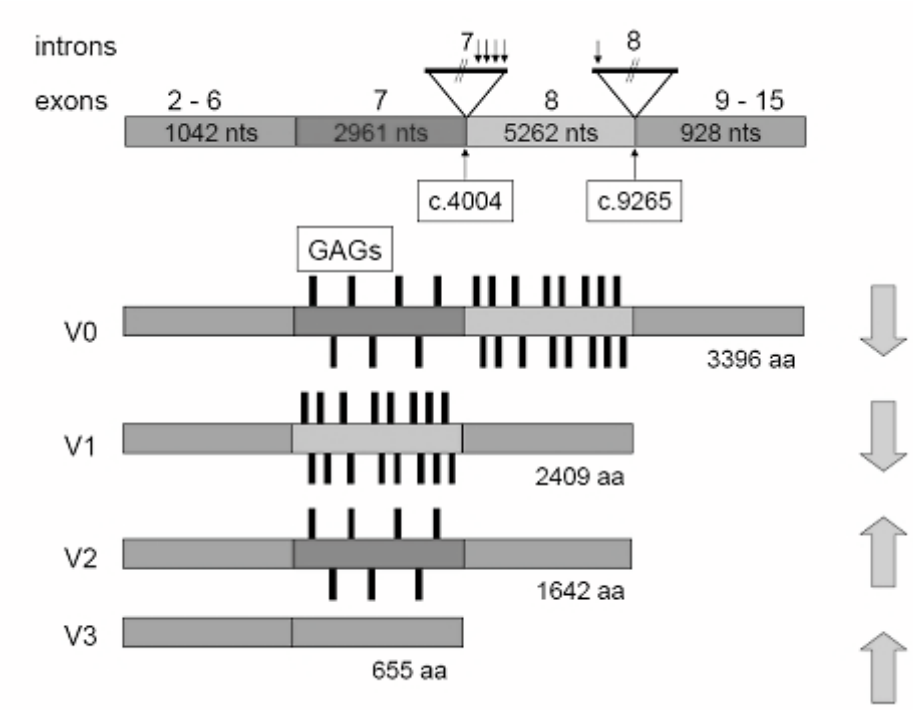

Figure 1: Structure of versican isoforms V0, V1, V2 and V3.[50]

Versican is able to regulate many cellular processes, including adhesion, proliferation, apoptosis, migration and invasion via the highly negatively-charged chondroitin/dermatan sulphate side chains and by means of interaction between the G1- and G3-domains with other proteins.[51,52] The wide range of molecules that have the ability to interact with versican via its G1- and G3-domain and chondroitin sulphate side chains have recently been reviewed.[53] In addition to hyaluronic acid, versican binds to ECM components, including tenascin-R, type I collagen, fibulin-1 and fibulin-2, fibrillin-1 and fibronectin.[54] Versican also binds to cell surface molecules P- and L-selectin, chemokines, CD44, integrin β1 and epidermal growth factor

receptor.[55] Studies have also shown that versican can bind to specific chemokines through its chondroitin sulphate chains and down-regulate chemokine function.[56]

I.3.1 The role of versican isoforms in normal tissue and in cancer

There is little information that attributes distinct functions to the individual versican isoforms in normal tissue and in cancer.[57] Versican isoforms V0 and V1 are mainly expressed in the later stages of embryonic evolution. V0 isoform is particularly prevalent during early embryonic development, but less well represented in adult tissues. Data is now emerging that the V1 isoform may have different functions in cells than in isoform V2. Versican isoform V1 has been shown to enhance cell proliferation and to protect NIH-3T3 fibroblasts from apoptosis.[58] In contrast, isoform V2 exhibits opposing biological activities by inhibiting cell proliferation, although it lacks any association with apoptotic resistance.[59] It has been shown that versican isoforms V1 and V2 may also have distinct functions in normal brain tissue.[60] In the work of Wu *et al*, V1 has been shown to promote neuronal differentiation of neural stem cells and neurite outgrowth of primary hippocampal neurons.[61] However, their experiments were not able to prove these effects for V2. Further studies have proposed an inhibitory effect of versican V2 on axon growth.[62]

It has been proven that the expression of versican is elevated in many cancer cells. Elevated levels of versican are reported in melanomas, osteosarcomas, lymphomas, breast, prostate, colon, lung, pancreas, endometrial and ovarian cancers and in brain tumours.[63,64] Even non-solid cancers, such as human acute monocytic leukemia cells, express V0 and V1.[65] Versican appears to be most commonly secreted by the peritumoural stromal cells in adenocarcinomas, although human pancreatic cancer cells are shown to secrete versican. The expression of versican has also been described in endometrial cancer cells and ovarian cancer tissue.[66] In ovarian cancer, high stromal versican levels correlate with serous cancers and are associated with reduced overall survival, whilst high versican levels in epithelial cancer cells are correlated with clear cell histology (early FIGO stage) and increased recurrence-free survival. Elevated levels of versican in early-stage prostate cancer also predict tumour progression.[67] Elevated versican levels are associated with cancer relapse and poor patient outcome in breast, prostate and many other cancer types.

V0 and V1 are the predominant isoforms present in gliomas.[68] There are no studies to date that have investigated whether V0 and V1 versican have different functions in astrocytic brain tumours. The smallest splice variant, V3, which consists only of the amino- and carboxy-terminal G1- and G3-domains and thus a small glycoprotein lacking chondroitin sulphate chains, might be expected to have properties considerably different from the other isoforms. However, there have been no studies that have directly compared the biological activity of V3 with other versican isoforms. The isoform V3 is expressed in primary endothelial cell cultures following activation by pro-inflammatory cytokines or growth factors. The role of V3 in activated endothelium is not known. The over-expression of V3 in arterial smooth muscle cells results in their increased adhesion to the culture flasks but reduced proliferation and slower migration in scratch wound assays.[69] The over-expression of the isoform V3 in melanoma cancer cells, which markedly reduces cell growth *in vitro* and *in vivo*, actually promotes metastasis to the lung. These findings suggest that isoform V3 may have a dual role as an inhibitor of tumour growth and as a stimulator of metastasis.[70,71] Versican is a large chondroitin sulphate proteoglycan produced by several tumour cell types, including high-grade glioma. The increased expression of certain versican isoforms in the ECM plays a role in tumour cell growth, adhesion and migration.[72] Versican is localized in either the peritumoural stromal tissue of many cancers, being secreted into the ECM by host tissue fibroblasts, or is expressed by cancer cells themselves. Studies have revealed that multiple mechanisms are responsible for differentially regulating the level, localization and biological function of versican in cancer.[73] Modulation and remodelling of the ECM mediated by proteases and interaction with ECM components like versican may be one mechanism by which tumour cells control their microenvironment to facilitate metastasis.[74]

Transforming growth factor-ß2 is an important modulator of glioma invasion, partially by remodelling the ECM.[75] However, it is unknown whether it interacts with versican during malignant progression of glioma cells. As previously shown in our lab, the expression of versican V0 and V1 is up-regulated by TGF-ß2 detected by quantitative polymerase chain reaction and immunoprecipitation, whereas the expression of V2 is not induced.[76] Using time-lapse scratch and spheroid migration assays, it has been observed that the glioma migration rate is significantly increased by exogenous TGF-ß2 and inhibited by TGF-ß2-specific antisense oligonucleotides.[77] Interestingly, an antibody specific to the DPEAAE region of the glycosaminoglycan-b domain of

versican is able to reverse the effect of TGF-ß2 on glioma migration in a dose-dependent manner. It has therefore been hypothesized that TGF-ß2 modulates the expression of versican.[78]

I.4 Question and hypothesis

Regarding reported knowledge about the influence of versican in context with cancer cell mirgration and proliferation and the results of previous works in our lab reported above, I investigate which role the different isoforms of versican might play in glioma cell motility, proliferation and invasion in glioma cell lines. I hypothesize that a targeted down-regulation of specific versican isoforms in glioma cells will substantially reverse functional effects such as the propagation of invasion.

I.4.1 Methodological approach

RNA interference (RNAi) is a regulatory mechanism of cells that physiologically allows them to control protein expression and to destroy external RNA material of viruses. Today, RNA interference is widely used in molecular research to induce post-transcriptional regulation of protein expression. Small interfering RNAs (siRNAs) are useful when investigating the function of special proteins on apoptosis, cancer, gene regulation and many other processes. Small interfering RNAs are 21-26 nucleotide long RNAs that are cut out of long double-stranded RNAs using an enzyme called RNase III Dicer. Artificially created single-stranded RNAs are used as RNA interference in molecular research.[79]

These small RNAs reach the inside of the cell via transfection, which can be performed in different ways. Electroporation and transfection with lipoporus are probable ways. Cell walls are permeabilized and the transfectant (siRNA) enters the cell through pores in the cell wall.[80] Once inside the cell, siRNAs build a protein complex with RISC (RNA-induced silencing complex). RISC binds to complementary RNA. This complex functions as an RNA helicase and nuclease. RNA is consecutively separated and wrested, so intracellular nucleases begin to degrade the RNAs and the gene of interest is no longer translated. The resulting gene knock-down is used to find out about the function of respective genes (Figure 2).

A greater understanding of the mechanisms regulating versican expression and the activity of its isoforms will assist in the development of specific inhibitors of versican-mediated cancer cell metastasis. Significant results could lead to the development of therapeutic methods to down-regulate versican expression, decrease its catabolism or to inhibit its function.

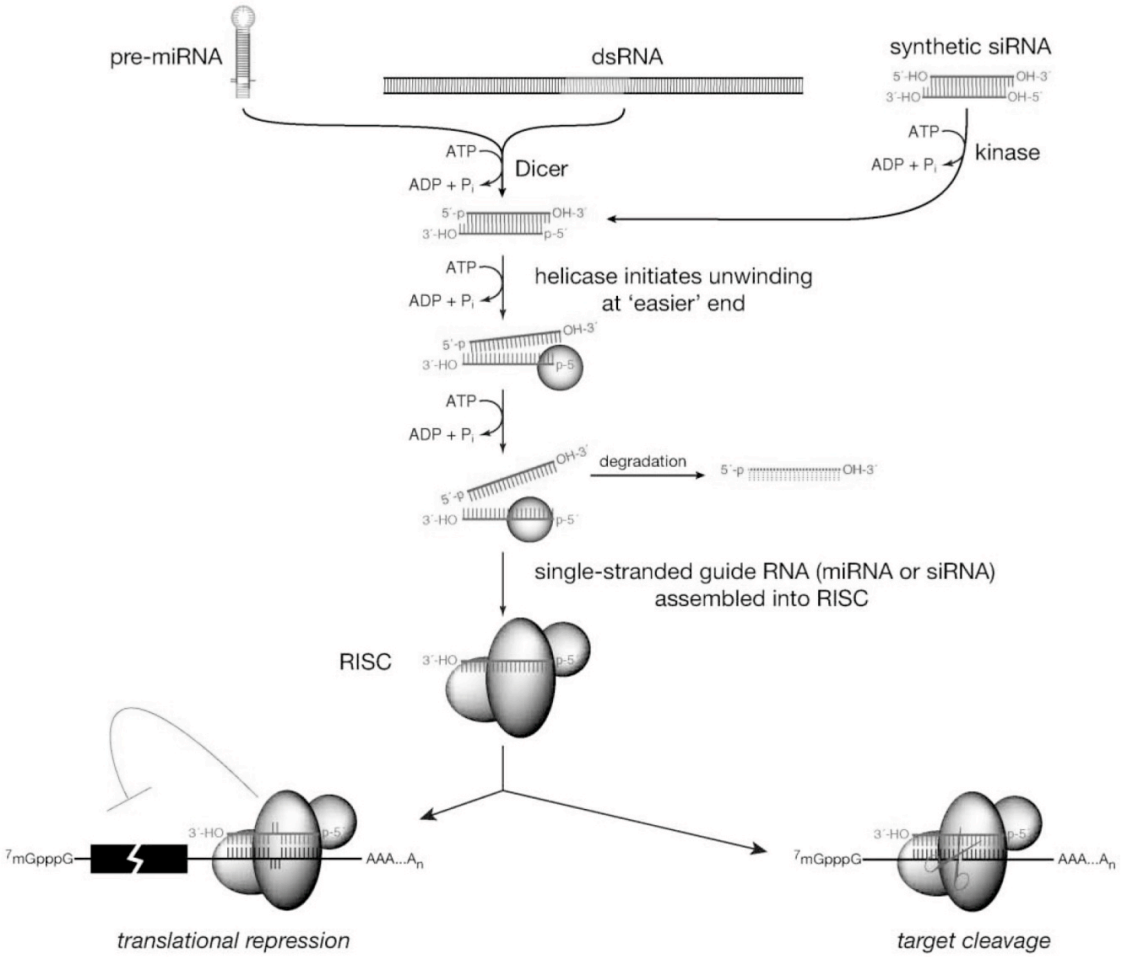

Figure 2: Enzymatic mechanism induced by endogenous and exogenous siRNA in the cell.[81]

Gene silencing via siRNA transfection is a transient effect that lasts a few days, whereas transfection with short hairpin RNA (shRNA) enables a stable and inducible RNAi system. Short hairpin RNA is a DNA molecule that can be cloned into expression vectors. Vectors that express small interfering RNAs within mammalian cells typically use an RNA polymerase III promoter to drive expression of a shRNA

that mimics the structure of a small interfering RNA.[82] The insert that encodes this hairpin structure is designed to have two inverted repeats separated by a short spacer sequence. Once inside the cell, the vector constitutively expresses the hairpin RNA, which induces silencing of the target gene (Figure 3).[83]

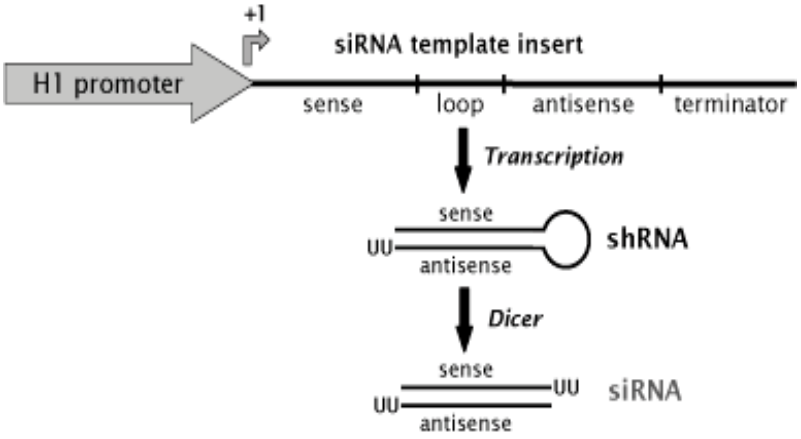

Figure 3: Enzymatic mechanisms in a cell transfected with a short hairpin vector.[75]

I.5 Materials

Chemical	Company
Ampicillin	Sigma
Sodium pyrophosphate	Sigma
10xTris/Glycine/SDS	Bio-Rad
Methanol	Uni.-Lager
2'-Desoxyadenosine-5'-triphosphate Sodium Salt (dATP)	Sigma
2'-Desoxycytidine-5'-triphosphate Sodium Salt (dCTP)	Sigma
2'-Desoxyguanosine-5'-triphosphate Sodium Salt (dGTP)	Sigma
2'-Desoxythymidine-5'-triphosphate Sodium Salt (dTTP)	Sigma
Tween 20	Sigma
30% Acrylamide/Bis Sol. 37% 5:1	BioRad
Bovine Serum Albumin	PAA
LE Agarose	Biozym
70% Propanol a 1l	Braun
99% Alcohol 10l	Uni
Aceton	Uni. Chem.
Acrodisc Syring Filter 0.2um	PALL/VWR
Acrylamide/Bisacrylamide (19:1)	Roth
Adenosine	Sigma
Adenosine-5'-diphosphate Sodium Salt (ADP)	Roth
Adenosine-5'-triphosphate Sodium Salt (ATP)	Roth
AllStars Neg. Control siRNA	Qiagen
Ammonium Persulphate ((NH4)2SO4)	Roth
AMV Reverse Transcriptase	Promega
BCA Protein Standard	KMF
Betaine	Sigma
Bromphenol Blue	Roth
BZO Seal-Film	Biozym
Calcium Chloride (CaCl2)	Sigma
Calf Phosphatase	Calbiochem
Chondroitinase ABC	Sigma

Complete Cocktail Tablets	Roche
Dithiothreitole (DTT)	Sigma
DMEM High Glucose	PAA
DMEM Low Glucose, à 500ml	PAA
DMSO	Sigma- Aldrich
EDTA-Trypsin	PAA
Ethanol	Roth
Ethidium Bromide	Roth
Formamide	Sigma
Glucose	Sigma
Glucosamin-HCl	Fluka
Glycerin	Sigma
Glycerol-2-Phosphate	Sigma
HCL	Uni. Chem.
Hemacolor 2, blue	Merck
Hemacolor 2, red	Merck
HiPerfect Transfection Reagent 1ml	Qiagen
HP Flexible siRNA Design, V3	Qiagen
Hyperfilm ECL 25 sheets 18x24cm	Amersham
Immobilon Western HRP Substrate 250ml	Millipore
Laemmli Sample Buffer 30ml	BioRad
L-Glutamine	PAA
Lipofectamine 2000	Invirtogen
Lipofectamine Transfection Reagent	Invitrogen
Magnesium Chloride (MgCl2)	Roth
MAPK-1 AK Taq 100	Qiagen
MAPK1 Ko. siRNA	Qiagen
Matrigel 20ml	Dianova
MEM Vitamins	PAA
Methanol	Roth
Methylen Blue	Merck
Millipore-Q-Kit-Pack	Millipore
N,N,N’,N’-Tetramethylethylendiamine (TEMED)	Roth
NaCl	Roth

NaHCO3	Merck
NaOH	Roth
Sodium Acetate	Roth
Sodium Citrate	Sigma
Sodium	Roth
Neg. Control siRNA	Qiagen
NEM Non. Essential Amino Acids a 100ml	PAA
PBS-MgCl/-CaCl	PAA
Phosphatse Inhibitor Cocktail	Sigma
Plus Reagent (3mg/ml) 0.85ml	Invitrogen
Polyethylen Glycol	Roth
Potassium Chloride	Roth
Precision Plus Protein Standards 500ul	Biorad
Reblot-Plus Strong Solution	Chemicon
Sodium dodecyl sulphate	Lauryl Sulfat
Substrate Reagent	R&D
Sucofin Skimmed Milk	Real
Supersignal West Piro ECL Subst. 100ml	Pierce
Tris(Hydroxylmethyl)-Aminoethan (Tris)	Sigma
Triton-X 100	Sigma
Trizma Hydrochloride	Sigma-Aldrich
Trypanblue 0.5%	Biochrom
Trypsin-EDTA, a 100ml	PAA
Uridine-5'-triphosphate (UTP)	

Buffers

Easy lysis buffer	10mM TrisHCl pH 8.0
	1mM EDTA
	15% Saccharose
	0.2mg/ml RNAseA
	2mg/ml Lysozym
	0.1mg/ml BSA
TBS Buffer	8g NaCl

	0.2g KCl
	3g Tris- Base pH 7.4
	ad 1000 ml H_2O
SDS-Running Buffer	288.4g Glycin
	10g SDS
	60.6g Tris
	ad 100ml H_2O
DEPEC water	1ml Diethylpyrocarbonate
	ad 1000ml H_2O
PBS	8g NaCl
	1.15g Na2HPO4
	0.2g KCl
	0.2g KH2PO4
	ad 1000ml H2O
Ponceau red dye solution	0.5g Ponceau
	1% Ice acid
	ad 500ml H_2O
RIPA buffer	50mM Tris/HCl pH 7.5
	150mM NaCl
	0.5% Na-desoxycholate
	Protease inhibitor
	0.1% SDS
	1% NP-40
TBE buffer	45mM Tris-Borat pH 8.3
	1mM EDTA
TBST buffer	10mM Tris-HCl pH 8.0
	150mM NaCl
	0.05% Tween
Transfer buffer	39mM glycerin
	48mM Tris
	0.03% SDS
	20% methanol
APS 25%	25g NH_4-Persulphate
	ad 100 ml H_2O

Blot buffer	25nM Tris pH 8.5
	10% Ethanol
	190nM Glycine
Freezing medium	90% FCS
	10% DMSO
Stripping solution	1ml Reblot Strong Solution
	19ml H_2O
Lämmli buffer	1.25ml 1M Tris pH 6.8
	0.7ml 87% Glycerine
	2ml 10% SDS
	2.5mg Bromphenoleblue
	ad 10ml H_2O
Ethidiumbromide stock solution	1g Ethidiumbromide
	ad 100 ml H_2O

Consumables

Biofreeze tubes PP 2ml	Corning
Cover slips 24x60cm	Roth
Nitrocellulose membrane	Schleicher und Schuell
Plastic requirements	Corning Costar
PVDF membrane, 13mm, 8µm	Schleicher und Schuell
Super frost glass slides	Roth
Whatman paper 3MM Whatman	VWR

Vector system

pENTER-THT (KAN)	Invitrogen

Cell lines

	Glioblastoma multiforme
A172	(WHO grade IV)
U87	Anaplastic astrocytoma

	(WHO grade III)
	Glioblastoma multiforme
HTZ349	(WHO grade IV)
	Glioblastoma multiforme
HTZ417	(WHO grade IV)
DH5α	*E. coli* stem

Cell culture medium

Full medium	500ml Dulbecco's MEM
	5ml non-essential amino acids
	5ml vitamins
	25ml FCS
LB-O medium	10g Tryptone
	5g yeast extract
	10g NaCl
SOB medium	20g Tryptone
	5g yeast extract
	0.6g NaCl
	0.2g KCl
	2g MgCl2
	2.5g MgSO4
Transfection medium	Optimem

Enzymes

HinD III	Promega
Alkaline phosphatase	Böhringer Mannheim
BGL II	Roche
DNaseI	Böhringer Mannheim
Restriction endonuclease	Fermentas
Taq DNA Polymerase	Roche

RNase/protease inhibitors

RNasin (RNase inhibitor)	Promega
Trypsin inhibitor	Roche

Size/lengthe standards

(2x250µl) Page Ruler Plus Pertained Protein Ladder	Fermentas
(2x250µl) Spectra Multicolor Broad Range Protein Ladder	Fermentas
1kb RNA-ladder (RNA-Standard)	Gibco BRL
Gene Ruler DNA-ladder Mix (DNA-Standard)	Fermentas
SDS-PAGE Broad Range (Protein-Standard)	Bio-Rad

Antibodies

Anti Versican V0/V1 Neo Antiboy, Rabbit Polyklonal IgG	Biosource
Ap 124P Gt x Ms IgG	Chemicon
Goat F(ab')2 Anti Rabbit Ig's, HRP Conjugate; LDH a	Biosource
Rabbit Anti-Actin	Sigma
Rabbit Anti-Goat IgG, HRP Conjugat	Millipore
Rabbit Anti-Versican V0/V1 Neo Polyclonal AB	BioReagent
ß-Actin mouse polyklonal 0.2ml	Sigma
TGFß2 rec. human 5µg	Tebu.Bio

Kits

Quanti Tec SYBER Green PCR Kit	Qiagen
Reverse Transcription Kit	Promega
RNAeasy Kit	Qiagen
RNase-free DNase Kit	Qiagen
siRNA Starter Kit, QuantiTect Assay, SiRNA Design	Qiagen
Taq PCR Master Mix Kit	Qiagen

Hardware

Bx51	Olympus
Centrifuge 3K 30	Sigma
EC 4000P	Apparatus Corporation
ELISA-Reader	Biotrend
Incubator	Heraeus
Megafuge 1.0 R	Hareaus instruments
Microscope	Leica
Real-time quantitative PCR systems	Stratagene
Thermal Cycler PTC 200	Peltier
Ultrospect 3000 Spectrophotometer	Pharmacia Biotech

Software

Microsoft Excel 2003

Adobe Illustrator 11.0

ImageJ

Adobe Photoshop 8.0

Microsoft Word 2003

MxPro Software

I.6 Methods

I.6.1 Cell culture

I.6.1.1 Glioma cell lines

Different types of glioma cell lines and primary cultures were used for the *in vitro* experiments. Human high-grade glioma cell lines U87MG and A172 were obtained from the American Type Culture Collection (Manassas, VA, USA). The glioma cell lines HTZ349 and HZT417 are primary tumour cell cultures derived from surgical specimens of human high-grade gliomas (WHO grade IV) as described by Bogdahn *et al* (1989).[84] All tumour cells were maintained as standard monolayer cultures in tumour growth medium at 37°C, 5% CO_2, 95% humidity in a standard tissue culture incubator (Heraeus).

I.6.1.2 Cell culture medium

The growth medium comprised Dulbecco's modified Eagle medium (DMEM), low glucose 1g/l (PAA) supplemented with 5% foetal calf serum (FCS), 1% non-essential amino acids (PAA) and 1% MEM-vitamins (PAA). Glioma cells were seeded at an equal density in cell culture flasks containing growth medium. The culture medium was replaced 24 hours after thawing the cells and was then replaced twice a week. Cells were cultivated with 15–20ml of culture medium in a 175cm^2 flask or with 10–15ml of culture medium in a 75cm^2 flask.

I.6.1.3 *E. coli* cell culture

The bacterial colony was gathered using 250ml SOB medium under permanent shaking at 37°C until its concentration reached an optical density of 0.6 at OD_{600}. Bacteria were diluted with 60% LB and 40% glycerin at a dilution of 1:1. The cell suspension was aliquotated in cryo-tubes and stored at -80°C. Plasmid amplification was performed in an *E. coli* strain called DH5α. Non-transformed bacteria were cultivated at 37°C in LBO-medium. Ampicillin-resistant clones were cultivated in an LB-Ampicillin medium.

I.6.1.4 Cell passage

Prior to each experiment or passage of a cell line, cells were detached by trypsination. Cells were flushed with 5–7ml PBS (PAA) for 30 seconds. Then the cell monolayer was coated with 5ml of trypsin (PAA) in a 175cm^2 flask. After 5–10 minutes incubation at 37°C in the tissue culture incubator, trypsin reaction was stopped by adding 5ml of the culture medium to the flask. The bottom of the culture flask was flushed three times using the trypsin/culture medium suspension. The suspension was transferred to a reaction flask (15ml) and centrifuged for 5 minutes at 1,500 RPM at RT (Megafuge, Hareaus instruments). After discharging the supernatant, the cell pellet was dissolved in 1ml of culture medium and the cell concentration was defined.

I.6.1.5 Cryoconservation

Cryoconservation is used to store cells for a long period at -130°C. At these low temperatures, any biological activity, including the biochemical reactions that would lead to cell death, are effectively stopped.

Cells were kept in a special medium consisting of DMSO, FCS and culture medium (dilution 10:40:50) to avoid damage to cells during freezing or warming up. The cells were put in a Biofreeze tube and slowly frozen to -80°C and then stored in liquid nitrogen.

I.6.2 Cell count

For cell culture and many other applications the exact cell concentration of a sample needs to be determined. Determining cellular proliferation, viability and activation are key to a wide variety of cell biological approaches. The need for sensitive, quantitative, reliable and automated methods has led to the development of standard assays.

I.6.2.1 Direct cell count

A Neubauer counting chamber device was used to determine the number of cells (Figure 4).

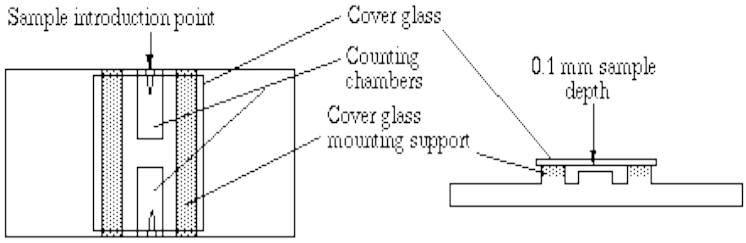

Figure 4: Counting chamber.[85]

The cell suspension was introduced into one of the V-shaped wells using a pipette. The area under the cover glass was filled by means of capillary action. The loaded counting chamber was then placed under a microscope and the counting grid brought into focus at low power (Figure 5). Cells were counted systematically in selected squares.

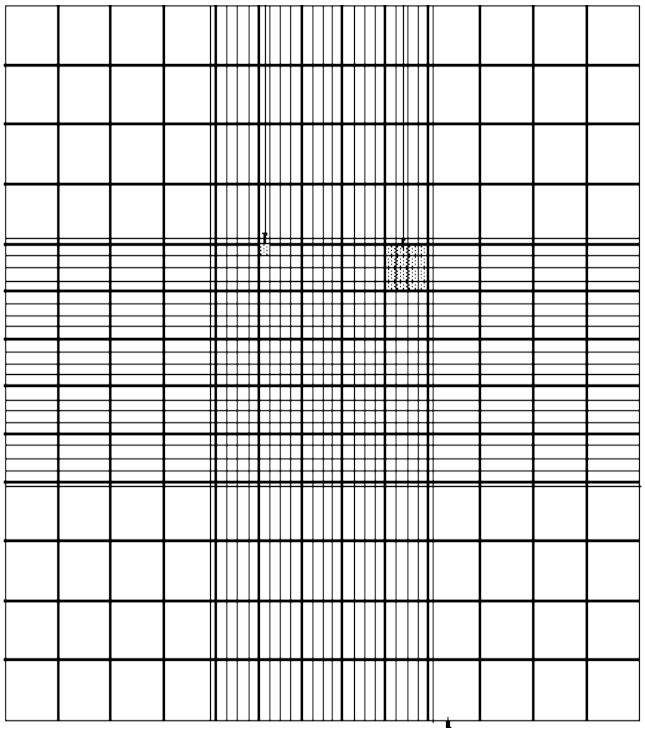

Figure 5: Counting grid.[86] Small square measures 1/400mm^2, 16 small squares measure 1/25mm^2

The total cell count was calculated by multiplying the dilution factor (DF) by cell count (CC), volume of cell suspension (CS) and volume of filled chamber (Ch).

DF x CC x (CS) ml x (Ch) 10000

I.6.2.2 XTT assay

Cells grown in a 96-well tissue culture plate were incubated with 20µl of the yellow XTT solution (final concentration 0.3mg/ml) for 4 hours. After this incubation period, orange formazan solution had formed and was spectrophotometrically quantified using an ELISA plate reader. This assay is based on the cleavage of the yellow tetrazolium salt XTT. Metabolically active cells convert the yellow tetrazolium salt into an orange formazan dye. This conversion only occurs in vital cells. The formazan dye is directly quantified using a scanning multi-well enzyme-linked immunosorbent assay (ELISA). This ensures a high degree of precision and enables computer processing of the data, which allows the rapid and convenient handling of a high number of samples.
An increase in the number of living cells resulted in an increase in the overall activity of mitochondrial dehydrogenases in the samples. This increase directly correlated to the amount of orange formazan formed, which was monitored as the absorbance.[87]

I.7 Preparing RNA

I.7.1 RNA isolation

General requirements when handling RNA are that the endogenous RNases stay inactivates and the samples, solutions and materials are not contaminated with exogenous RNase. All solutions were prepared with 0.1% DEPEC water.[88]
Total RNA was extracted from tumour cells using the RNeasy Mini Kit (Qiagen, Hilden, Germany) RNA purification system following the manufacturer's instructions. All steps were accomplished on ice.
First the RTL-buffer was set up, consisting of 3ml RTL-lysis buffer (Quiagen) and 30ml ß-mercaptoethanol (Sigma). The frozen cell pellets were suspended in 350µl RTL-buffer and vortexed for 1 minute after adding 350µl of ethanol (70%). The 700µl

of cell suspension was transferred to a collection column and centrifuged for 30 seconds at 10,000 RPM. Ethanol and ß-mercaptoethanol were discharged from the lower compartment of the collective column. 700µl RW1-buffer was added to the column and centrifuged for 30 seconds at 10,000 RPM. The lower compartment of the collective column was discharged and the column placed in a 2ml tube. 500µl RPE-buffer was added to the column and centrifuged first for 15 seconds at 10,000 RPM. In a second step, another 500µl of RPE-buffer was added and the column was centrifuged at 10,000 RPM for 2 minutes. Subsequently, the column was placed in a 1.5ml tube and incubated with 30µl RNase-free water for 1 minute and placed in the centrifuge for 1 minute at 10,000 RPM. The 30µl of RNase-free water, which was now in the lower compartment, was again placed in the column and the centrifugation step was repeated. The RNA concentration in the samples was measured and the probes stored at -80°C.

The RNA concentration and purity was determined by measuring the optical density at wavelengths of 260nm and 280nm using the Ultraspect 3000 spectrophotometer (Pharmacia Biotech). The blank value for calibration consisted of 100µl water. 10µl of RNA sample was diluted with 90µl water (1:10). The concentration of RNA in the samples was calculated in µl/ml, taking account of the dilution factor.

I.7.2 Reverse transcriptase polymerase chain reaction (RT-PCR)

First, strand cDNA was generated from 0.5–1µg of total RNA. Gene-specific cDNAs were synthesized using a reverse transcription kit (Promega). Appropriate forward and reverse primers were used in the reverse transcriptase polymerase chain reaction (RT–PCR) for cDNA amplification. A Master mix was prepared for reverse transcriptase-PCR (Table 1).

$MgCl_2$	4µl
10x buffer	2µl
dNTPs	2µl
Oligo dt-primer	1µl
AMV RTase	0.6µl
RNasin	0.5µl
Aqua dest.	0.9µl

Table 1: Mastermix for RT-PCR.

Samples of 1µg RNA were filled up to a volume of 9µl with DEPEC water and mixed with 11µl of Master mix. The RNA was transcribed during 15 minutes of incubation at 42°C. Adding 80µl H_2O, cDNA was dissolved and stored at -20C°. The RT-PCR programme in the light cycler was run at 42°C for 15 minutes, followed by 95°C for 5 minutes and 4°C for 5 minutes.

I.8 DNA synthesis and analysis

I.8.1 Polymerase chain reaction

The polymerase chain reaction (PCR) is a technique used to amplify copies of a piece of DNA that generates millions of copies of a specific DNA sequence. A PCR involves a series of different steps, including denaturation of a DNA double strand, annealing of specific primers to the DNA template and synthesis of the DNA with a polymerase. The method relies on thermal cycling, comprising cycles of repeated heating and cooling that melt DNA double-strands and induce enzymatic replication of the DNA. Primers are short DNA fragments with complementary sequences to the target region. They bind to the 5'end of the DNA template at a certain annealing temperature. After that, a DNA-polymerase is activated and enables amplification of the complementary DNA strand after adding dNTPs. The generated DNA is used as a template for the next replication.
Prior to starting the PCR, a reaction mix was prepared containing the following components (Table 2).

cDNA	1µl
Primer forward	0.5µl
Primer reverse	0.5µl
Taq-polymerase	25µl
Aqua dest.	23µl

Table 2: Reaction mix in PCR.

When preparing the reaction mix all the components were stored on ice. The samples were placed in a master cycler (Eppendorf AG) using an individual programme for each primer pair. Initially, the DNA polymerase was activated at 95°C

for 5 minutes, followed by a DNA amplification step for 30 cycles (95°C for 45 s, 57–60°C for 1 min, 72°C for 45 s), which was extended by 5 minutes at 72°C.

I.8.1.1 Primer design

Primer design is done with help of a *NCBI* primer-designing tool.[89] The following criteria are taken into account: after defining the accession of the mRNA template, the position ranges for forward and reverse primers are entered so that primers are located on specific sites of the target genes. PCR product size and melting temperatures (T_m) are determined. Further primers used to transcribe RNA to cDNA need to span an exon–exon junction in mRNA.

Primer length was chosen in between 17–28 bases. The tool takes account of the base composition, which should consist of 50–60% G+C and includes a 3'-end of a G or C, or CG or GC. T_m was calculated between 55–80^{o}C. Further it was checked that the 3'-ends of primers were not complementary. Runs of three or more Cs or Gs at the 3'-ends of primers were avoided, as were G or C-rich sequences.[90] Any additional homology was excluded by blasting primer sequences through the *NCBI* gene pool database.[91] Table 3 shows all primer sequences used.

V0	Sense	5'GAC AGG TCG AAT GAG TGA TTT GAG 3'
	Antisense	5'GCC ATT AGA TCA TGC ACT GGA TCT G 3'
V1	Sense	5'GAT GCC TAC TGC TTT AAA CGT CG3'
	Antisense	5'GGT TGT CAC ATC AGT AGC ATT TGC3'
V2	Sense	5'-TCACGACTTCAAGTCCTCCTGC-3'
	Antisense	5'- GGTGCCTCCGTTAAGGCACG -3'
V3	Sense	5'- GTGTGGAGGTGGTCTACTTGG-3'
	Antisense	5'- GGTGCCTCCGTTAAGGCACG -3'

Table 3: Primers targeting versican isoforms V0, V1, V2 and V3 and their sequences.

I.8.2 Plasmid amplification in DH5α

I.8.2.1 Generation of competent DHα bacteria

Free DNA was transformed in competent cells, called *E.coli* strain DH5α. DH5α was cultivated in an LB-O medium. Ampicillin-resistant bacteria were cultivated in an LB-Ampicillin medium. DH5α *E.coli* bacteria were scratched out onto an LB-agar plate. The bacterial colony was gathered using 250ml SOB at a concentration of OD_{600}= 0.6. Bacteria were placed on ice for 10 minutes, then centrifuged at 2,500 RPM for 10 minutes at 4°C and suspended in 20ml transformation buffer. After incubation for another 10 minutes, competent bacteria were aliquotated and stored at -80°C.

I.8.2.2 Heat-shock transformation of chemo-competent DH5α

10–100ng of plasmid were added to 50µl of competent DH5α and incubated for 15–30 minutes on ice. Heat shock was performed for 90 seconds at 42°C. Afterwards, bacteria were cooled down on ice and cultivated with 400µl of SOB-medium in a shaking incubator at 37°C. Finally, the bacteria were placed on a resistance medium and stored at 37°C.

I.8.2.3 Mini Prep

Mini Prep is a method that is used to purify plasmid-DNA. Clones were collected from the plate using the tip of a pipette and were given into selection medium containing 3ml LB medium + Ampicillin 100µg/ml for 12–24 hours at 37°C in a shaking incubator. 1.5ml of bacteria suspension was centrifuged at 16,000 RPM for 20 seconds. The cell pellet was suspended in 50µl of *easy lysis* buffer and incubated for 5 minutes at RT. Then cells were cooked for 2 minutes and cooled down on ice. During this procedure the bacteria cell walls rupture, allowing DNA to be isolated. After centrifuging at 16,000 RPM for 10 minutes at 4°C, bacterial DNA and cell debris were removed and the plasmid dissolved in the supernatant.

I.8.2.4 Maxi Prep

To gather larger amounts of plasmids, one clone is picked out of the plate using the tip of a pipette. This clone arises from transformed DH5α bacteria, which are incubated overnight at 37°C.

The clone was incubated overnight at 37°C in a shaking incubator with 500ml LB-medium and Ampicillin. The saturated *E. coli* stem was filled into a GSA tube and was then centrifuged at 5,000 RPM for 10 minutes at 4°C. The pellet was then suspended in 10ml of buffer 1. After adding 10ml of buffer 2, the reaction mix was mixed until the solution appeared to be clear. Next, 10ml of buffer 3 was added and incubated for 15 minutes on ice, followed by centrifuging at 10,000 RPM for 10 minutes at RT. The pellet was then briefly washed with 100µl ethanol and suspended in 2ml TE, pH 7.6. Then 8ml of DNA binding solution was added and incubated for 5 minutes at RT. In the next step the pellet, charged with DNA binding solution, was added to a column. This column was attached to a vacuum. The column was washed first with 30ml washing solution and then with 5ml 80% EtOH. Then the column was dried in a 50ml tube at 3,000 RPM for 10 minutes. After that, the column was attached to a vacuum for another 5 minutes. Finally, DNA was eluted from the column, after1.5ml TEs (75°C) was added at 3,000 RPM for 10 minutes.

I.8.2.5 DNA purification

The first step in DNA purification involves phenol extraction. The plasmid is mixed with phenol/chloroform/isoamylalcohol at a ratio 1:1, after which it is vortexed for 1 minute and then centrifuged for 5 minutes at 14,000 RPM. The supernatant is transferred into a new Eppendorf tube and is mixed with chloroform/isoamylacohol at a ratio 1:1. After brief vortexing and centrifugation for 5 minutes at 14,000 RPM, the supernatant is transferred into a new tube ready for DNA precipitation.

DNA precipitation was done using sodium acetate. 1/10 volume of 3M sodium acetate (pH 5.2) and 2.5 volume 100% ethanol were added to phenol-extracted DNA; the solution was incubated at -20°C for 20 minutes. A pellet of DNA formed after 20 minutes of centrifugation at 4°C and 14,000 RPM. The pellet was washed with 70% ethanol and dried at RT. The pellet was then dissolved in 20µl TE buffer. To check the integrity of purified DNA a gel electrophoresis was performed and the DNA content of the samples was measured photometrically.

I.8.2.6 HIRT-DNA extraction

The HIRT protocol serves to isolate plasmids from human cells.
A 6-well plate was harvested, one third of the cells were centrifuged for 5 minutes at 14,000 RPM, then washed in 100µl PBS and suspended in 100µl HIRT-reagent consisting of 400mM NaCl, 10mM EDTA, 10mM Tris 7.5 and 50µg/ml ProteinaseK 0.2% SDS. The lysate was incubated for 3 hours at 55°C. Adding 30µl 5M NaCl, the cell lysate was incubated overnight at 4°C. After centrifugation for 1 hour at 14,000 RPM at 4°C, phenol/chloroform/isoamylalcohol extraction and DNA precipitation was performed as described in the above. The pellet was then suspended in 5µl of TE buffer. Subsequently, 2.5µl of the solution was transformed into DH5α via heat-shock transformation.

I.8.3 Electrophoresis

Electrophoresis describes the migration of negatively charged molecules under the influence of an electrical field. Migration time in the electrical field varies and is dependent on the molecular weight of the samples.

I.8.3.1 Agarose gel electrophoresis

PCR products were analyzed on 1% agarose gels. 100ml H_2O was heated together with 1mg agarose (Biozym) for 2–5 minutes in a microwave at 500W. The gel was cooled down to 60°C and then filled onto the slide in the electrophoresis chamber. The gel was stacked in the electrophoresis chamber. Slots for samples were generated using the inserted comb. After the gel had hardened, the comb was carefully removed and the chamber was filled up with DEPEC-water to the sea marker. Samples were then loaded onto the gel slots, adding 1µl of ethidium bromide to 10µl of each sample. 5µl of a 500bp ladder was used as the size marker. Gel electrophoresis was performed at 120mA for 30 minutes. PCR products were visualized in a Vilbert Lourmat chamber.

I.8.4 Gradient PCR

Gradient PCR offers the opportunity to investigate primer-binding behaviour at different annealing temperatures at the same time, in one run. Based on the primer sequences, primer pairs show varying binding behaviour at different annealing temperatures.[92] Optimal conditions for each primer pair are defined in a gradient PCR. The gradient cycler (Mastercycler Gradient, Eppendorf) is able to generate up to 12 different temperatures in one run.

The range of temperatures was chosen between 54°C and –65°C (54°C, 54.3°C, 54.9°C, 55.8°C, 57.1°C, 58.7°C, 60.6°C, 62.2°C, 63.3°C, 64.2°C, 64.8°C, 65°C). As the Eppendorf Mastercycler Gradient also provides a gradient function for elongation or denaturation temperatures, the duration of the annealing temperature was tested for 30 seconds and 1 minute. The concentration of cDNA varied between 0.5 and 1µg. The volume of primers was examined from 0.5–1µl. All other components of the reaction mix are fixed. Samples were analyzed in agarose gel electrophoresis.

I.8.5 Quantitative PCR

Quantitative mRNA expression levels were analyzed in a real-time PCR system (ABI PRISM 7000 Sequence Detection System, CA, USA) using SYBR Green dye I. A positive reaction was detected through the accumulation of a fluorescent signal measured using MxPro-Mx3005P software. A mitochondrial 18s housekeeping gene was used as a reference gene in the cells. It was present in all nucleated cell types, since it is indispensable for cell survival. The mRNA synthesis of these genes is considered to be stable and secure in various tissues, even under experimental treatment.[93]

First, two master mixes were prepared, one with the primer pair targeting the gene of interest and the other with the primer pair targeting the housekeeping gene (18s). Prior to preparing the reaction mix, Syber Green was melted on ice and carefully vortexed before use. All components and the master mix were stored on ice during preparation. Table 4 shows the composition of Master mix in qPCR.

cDNA	1µl
Primer forward	0.5µl
Primer reverse	0.5µl
Syber Green	12.5µl
Aqua dest.	10.5µl

Table 4: Master mix for quantitative PCR with a final volume of 25µl.

PCR results were interpreted based on the standard curve. The standard curve consisted of a dilution series containing five values up to a 1:16 dilution. The stock for a standard dilution series contained 1.5µl of each cDNA sample. In the first standard, 6µl of the cDNA stock and 6µl H_2O were mixed; the second standard contained 6µl of the first standard and 6µl H_2O and so on. The volume of the samples was adjusted using aqua dest. to achieve a final volume of 25µl.

Samples were analyzed in a 96-well plate. Each sample was loaded in duplicate. 24µl of the Master mix was loaded into each well using a multi-pipette. 2µl of cDNA standard series was filled into each well dedicated to standard curve and 2µl of cDNA was filled into the respective well of each sample. Standard samples of cDNA were amplified in duplicate with the primers of the housekeeping gene and primers of the target gene. Samples were loaded in triplicate for each primer pair. Figure 6 shows the assignment.

PHKg	Neg.	St1	St1	St2	St2	St3	St3	St4	St4	St5	St5
PTg	Neg.	St1	St1	St2	St2	St3	St3	St4	St4	St5	St5
PHKg	S1	S1	S1	S2	S2	S2					
PHKg	S3	S3	S3	S4	S4	S4					
PTg	S1	S1	S1	S2	S2	S2					
PTg	S3	S3	S3	S4	S4	S4					

Figure 6: 96-well plate with samples: PHKG = Primer housekeeping gene, PTg = Primer target gene, St1-St5 = standard values of dilution series, S1-S4 = samples 1–4.

After loading the Master mix and cDNA onto the 96-well plate, the plate was closed using a bonding sheet and centrifuged for 30 seconds at 6,000 RPM. The plate was then placed in a real-time cycler (Stratagene) and the data were recorded using the MxPro software. Before the run was started, a thermal profile needed to be defined (Figure 13). The plate set-up was done and standard dilution samples were defined. Agarose gel electrophoresis was used to verify the identity of the amplification products and was performed as described in the above.

I.9 Stable and transient transfection

I.9.1 Design of siRNAs

The siRNAs were designed in line with general guidelines and according to the work and findings of Elbashir SM *et al* (2001).[94] Table 5 shows the siRNA sequences.

V1	Target	5`-GGG AGU UCU UCG AUU CCA ATT-3`
	Sense	5`-r(GGG AGU UCU UCG AUU CCA A)dTdT
	Antisense	5`-r(UUG GAA UCG AAG AAC UCC C)dTdT
V2	Target	5´- AGA AAA TAA GAC AGG ACC TGA- 3`
	Sense	5`-r(AAA AUA AGA CAG GAC CUG A)dTdT
	Antisense	5`-r(UCA GGU CCU GUC UUA UUU U)dCdT
V3	Target	5`-TAC TGC TTT AAA CGA CCT GAT-3`
	Sense	5´-r(CUG CUU UAA ACG ACC UGA U)dTdT
	Antisense	5`-r(AUC AGG UCG UUU AAA GCA G)dTdA

Table 5: Sense-, antisense-siRNA sequences and target sequences of versican isoforms V1, V2 and V3.

I.9.2 Calculating the siRNA amount

Initially, the siRNA was delivered lyophilized and was suspended in 250µl of the suspension buffer provided prior to the transfection procedure. The suspension buffer was added to a 1ml tube containing 5nmol of lyophilized siRNA to obtain a 20µM solution. Tubes were heated to 90°C for 1 minute and then incubated at 37°C for 60

minutes. The incubation steps were only needed the first time the siRNA was used. The siRNA solution was stored at -20°C.

I.9.3 Optimizing siRNA transfection

Table 6 summarizes the manufacturer's recommendations regarding the amount of siRNA, volumes of medium and concentrations of siRNAs in different experimental settings (Table 6).

Culture format	Vol. of medium on cells (/ml)	SiRNA amount (/ng)	Final volume of diluted siRNA (/µl)	Final siRNA concentration (/nM)
48-well plate	250	19	50	5
24-well plate	500	37.5	100	5
12-well plate	1100	75	100	5
6-well plate	2300	150	100	5

Table 6: Instructions regarding siRNA transfection with calculated amounts of siRNA and medium in different culture formats

I.9.4 Sh-RNA

I.9.4.1 Insert design

The shRNA-insert consisted of a 19bp-long stem and a loop 9bp in length. The elements were arranged in a sens- loop-antisense direction. The insert was initiated with the sense-sequence at the 5'´end, which is homologous to the sequence of target mRNA, followed by the loop sequence: UUCAAGAGA. The loop sequence was followed by a reverse complementary sequence of the sense strand. A string of 5 thymidines was added to the antisense strand as the termination site for the polymerase III.

I.9.4.2 Transforming specific siRNA into vector

The sense sequence in our siRNA template insert corresponded to the siV1-target sequence (Table 5). The shRNA insert was formed by means of the kinasation of the oligonucleotides, which adhere to the reaction mix. All ingredients were stored on ice when preparing the reaction mix (Table 7). Oligonucleotides were synthesized and annealed containing 1µg of a sense and an antisense strand of the siRNA at 37°C for 1 hour.

Oligo B (10 µM)	1µl
ATP (10mM)	1µl
10x PNK Buffer	1µl
Aqua dest.	5µl
T4 Polynucleotide kinase	1µl

Table 7: Reaction mix for kinasation of oligonucleotides

The annealing step was performed at 95°C for 2 minutes. After brief centrifugation, the reaction mix was incubated for 1 hour at 37°C and then diluted at 1:10 with aqua dest. For ligation of the oligonucleotides and the vector, a reaction mix consisting of the following adjuvants was incubated for 10 minutes at RT (Table 8).

Vector (100ng)	1µl
Kinase mix (1:100 dilution)	1µl
Aqua dest.	1µl
2x Buffer	5µl
5x Buffer	2µl
T4 DNA Ligase	0.5µl

Table 8: Reaction mix for kinasation of oligonucleotides and vector

The vector pENTER-THT (KAN) was used. The vector was transformed into competent cells of an *E.coli* strain. 20µg of the vector was cut using the restriction enzymes Bgl II/HinDIII within an incubation time of 1–2 hours at 37°C. Transformation was done in DH5 α as described in the above. On PCR level the identification of positive clones was done using specific primers. Table 9 shows the Master mix used for PCR.

ON x 20 pmol/µl	1µl
ON y 10 pmol/µ	2µl
10x Taq Buffer	5µl
dNTPs (2 mM)	5µl
Aqua dest.	36µl
Taq DNA Pol	1µl

Table 9: PCR mix

I.9.5 Transfection of adherent cells

I.9.5.1 SiRNA transfection of adherent cells

Cells were transfected according to the manufacturer's instructions (Invitrogen). For transfection of adherent cells, cells were harvested and counted as described in the above. Experiments were run with 200,000 cells per well in a 6-well plate. When preparing the transfection mixture, Lipofectamine 2000 (Invitrogen) and the calculated amount of siRNA (Table 6) were diluted in 250µl Optimem medium (Invitrogen) and incubated separately for 5 minutes at RT while being stored on ice. Afterwards, the two collection tubes were mixed and incubated for another 20 minutes in a 2ml tube. The transfection reagent was then added to the cells. Fifteen minutes prior to adding the transfection reaction mixture to the cells, they were disseminated in 500µl of culture medium in the 6-well plates. After adding transfection mixture to the cell suspension the , 6-well plates were shaken for about 10 minutes to spread the cells evenly and to gain a consistent cell monolayer. The cells were incubated together with the transfection medium for 4 hours in the incubator at 37°C. During that time, the cells became adherent, permeabilized and absorbed the transfection reagent. After four hours of incubation the remaining transfection reagent was removed and replaced with normal culture medium.

I.9.5.2 ShRNA transfection of adherent cells

In accordance with the manufacturer's protocol (Invitrogen), cells were seeded to a 6-well plate the day before the transfection procedure. The experiment was performed in a 6-well plate. Each well consisted of 200,000 cells. 3µg of the shRNA plasmid was used. Lipofectamine 2000 (Invitrogen) and the calculated amount of shRNA

were diluted in 250µl Optimem medium (Invitrogen) and incubated separately for 5 minutes at RT while being stored on ice. Afterwards, the content of the two collection tubes was mixed and incubated for another 20 minutes in a 2ml tube. The transfection reagent was then added to the cells and left for 4 hours. The transfection reagent was then discharged and the wells filled up with the culture medium.

I.9.5.3 Monitoring transfection efficiency using florescence

Alexa Fluor-labelled siRNA was used to check transfection efficiency. Transfection was performed as describe in the above. The amount of Alexa Fluor-labelled siRNA was adapted to the protocol. 1–100nM of Alexa Fluor-labelled siRNA was used for transfection in a 6-well plat containing 50,000 cells. Analysis was performed under the fluorescence microscope (Leica). Experiments were run using cells on day 2 after transfection.

Efficient transfection in shRNA-transfected cells was monitored using a co-transfection with a GFP-linked vector and the shRNA-expressing vector at a dilution of 1:4. Transfection was verified 2 hours after transfection under a fluorescent microscope (Leica). Transfection efficiency was determined by counting all cells in one visual field under bright field microscopy. The number counted was correlated to the number of cells counted in the same visual field under fluorescent microscopy. The transfection rate was quoted as a percentage.

I.10 Protein

I.10.1 Protein isolation techniques

Different methods of protein isolation were tested to detect protein in western blot. First, RIPA buffer, one of the most reliable buffers, was used to lyse cultured mammalian cells, which enables protein to be extracted from cytoplasmic components, membrane and nuclear proteins. Before use, culture medium was removed from the cells, which were plated in a 6-well plate. Cells were washed twice with 5–7µl of PBS. Then 200µl of ice-cold RIPA buffer was added to each well. Cells detach from the bottom of the culture with slight pivoting. The suspension of RIPA and cells was transferred into a 2ml tube. The tubes with harvested cells were incubated for 15 minutes at 4°C in a shaking incubator. Then the tubes were

centrifuged for 10 minutes at 10,000 RPM and 4°C. The supernatant was stored in a new tube at -20°C or was analyzed in a BCA assay.

The second protein isolation technique was performed using enzymatic digestion with Chondroitinase ABC. The enzyme Chondroitinase ABC digests GAG chains at 37°C over a period of 2 hours. Chondroitinase ABC wass stored at -20°C and was slowly melted at RT before use. The enzyme solution was prepared based on SIGMA's instructions. The product was reconstituted in a 0.01% bovine serum albumin aqueous solution. Subsequent dilutions were made into a buffer containing 50mM Tris, pH 8.0, 60mM sodium acetate and 0.02% bovine serum albumin. All solutions were freshly prepared. Then 0.25 units of Chondroitinase ABC were incubated with the cell pellet of 20,000 cells. The cell lysates were incubated with Chondroitinase ABC with equal amounts 50µg of protein solution overnight at 37°C prior to loading onto western blot. Probes were analyzed in western blot.

Thirdly, cells were harvested out of a 175m^2 culture flask using the cell scraper. The cell monolayer was washed with 5–7ml of PBS. Subsequently, 2ml of PBS was added to the flask and cells were scraped off the bottom of the culture flask. The content of the culture flask was transferred into a tube and vortexed for 1 minute at 10,000 RPM. The supernatant was then used for protein analysis.

I.10.2 Immunprecipitation

Immunprecipitation was performed to augment and enrich the content of the protein of interest in a sample. To that end, 200µl of G Sepharose was added to the supernatant of a 10ml culture flask and incubated at 4°C for 6 hours for pre-clearing in the overhead shaker. After centrifugation, the non-specifically bound G beads were discarded and the supernatant was incubated with the required antibody (e.g. 2 mg/ml versican V0/V1 Neo-polyclonal antibody) at 4°C overnight. After washing, the beads were boiled in the protein loading dye for 5 minutes and loaded directly into the pre-poured Tris-HCl-glycine SDS–polyacrylamide gel electrophoresis (PAGE) gels (10%) along with pre-stained molecular weight standards (Bio-rad Laboratories, Palo Alto, CA, USA). Electrophoresis, blotting and blocking were performed as described below. The blocking was performed for 1 hour at RT with 5% non-fat freeze-dried milk and then incubated with 1mg/ml of the versican V0/V1 Neo-antibody at 4°C overnight. Immune complexes were visualized using a horsedish

peroxidase-conjugated antibody followed by chemoluminescence reagent (Pierce Biotechnology). Manual film development was performed as described below.

I.10.3 BCA assay

The BCA protein assay was used to determine the concentration of proteins in samples. It was performed according to Uptima's protocol using a BCA protein assay kit (Pierce/Uptima 23225) in a 96-well plate. The standard ranges between 0µg/ml and 2mg/ml of protein concentration. The samples were loaded in duplicate, diluted in aqua dest. at a ration of 1:4 and undiluted (Figure 7). Subsequently, a mixture of 10µl reagent A and 200µl reagent B was added to each well. The plate was incubated for 30 minutes at 37°C. The absorbance of the formed BCA-copper-chelate complex was detected using an ELISA-Reader at a wavelength of 540nm. The standard curve and sample values were analyzed using the Standard BCA software program called Softmax.

A 200 ug/ml	A	blank Puffer A	Blank	S1	S1	etc.
B 1000 ug/ml	B	-	-	S2	S2	
C 750 ug/ml	C	-	-	S3	S3	
D 500 ug/ml	D	-	-	S4	S4	
E 250 ug/ml	E	-	-	S5	S5	
F 100 ug/ml	F	-	--	S6	S6	
G 20 ug/ml	G	-	-	S7	S7	
H 0 ug/ml	H	-	-	S8	S8	

Figure 7: Distribution of standard A-H and samples (S) in duplicate

I.10.4 Polyacrylamid gel electrophoresis

SDS-PAGE stands for Sodium dodecyl sulphate (SDS) polyacrylamide gel electrophoresis (PAGE) and is a method used to separate proteins according to their size. After assembly of the gel apparatus (Biometra), the running and stacking gels were prepared. Solution components and percentages of gels consist of specific quantities of ingredients (Table 10). Water hoses were attached to the electrophoresis chamber to cool the apparatus.

The running gel was filled into the gel apparatus and is immediately covered with 1ml of isopropanol for 30 seconds to burnish the surface of the gel. Next, isopropanol was discharged and the stacking gel poured on top of the running gel. A comb was placed adjacently. The comb was removed once the gel had hardened after approximately 20 minutes. The gel apparatus was fixed in an electrophoresis chamber and the chamber was filled with Tris/glycine/SDS running buffer (Biorad Laboratories) at a dilution of 1:10 with aqua dest.

Samples were denaturized at 95°C for 5 minutes after adding Laemmli sample buffer (dilution 1:1) before loading. 10–30µg of a sample and 5µl of the molecular weight marker were loaded onto the gel. The electrophoresis was run at 160V until probes passed the stacking gel, then power was turned up to 180V. The run was stopped once the dye molecules reached the bottom of the gel.

Solution components	**Running gel**		
	6%	**8%**	**10%**
H_2O	7.9	6.9	5.9
30% acrylamide mix	3	4	5
1.5M Tris (pH 7.8)	3.8	3.8	3.8
10% SDS	0.15	0.15	0.15
10% ammonium persulfate	0.15	0.15	0.15
TEMED	0.012	0.009	0.006

Solution components	**Stacking gel**
	5%
H_2O	6.8
30% acrylamide mix	1.7
1.0 M Tris (pH 7.5)	1.25
10% SDS	0.1
10% ammonium persulphate	0.1
TEMED	0.001

Table 10: Recipe for running gel and stacking gel

I.10.5 Transferring and visualizing the protein

A semi-dry blot was performed to transfer and visualize the protein. A nitrocellulose membrane and 6 Whatman papers were cut to the estimated size of gel. Next, a nitrocellulose membrane and 6 Whatman papers were wetted in ice-cold transfer buffer for 5 minutes. Figure 8 shows the experimental set-up. Three Whatman papers were placed at the bottom of the blotting apparatus, followed by nitrocellulose membrane, gel and were covered with three Whatman papers. The cathode is placed on top and the blotting was started for 90 minutes at 80mA.

The nitrocellulose membrane was stained with Ponceau red to check for sufficient and consistent protein transfer. The incubation time with Ponceau red lastes 5 minutes on an agitator. Subsequently, the membrane was washed with aqua dest. until clear protein bands became visible. A colour photocopy was done for documentation purposes.

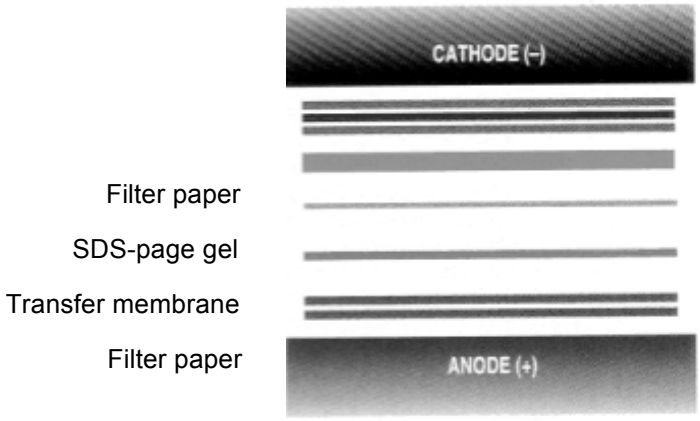

Figure 8: Experimental set-up for blotting[95]

I.10.5.1 Blocking and incubation with antibody

In the next step, the membrane was blocked to avoid unspecific binding of the antibody. The blot membrane was therefore incubated on an agitator with 1.5% BSA in TBS-Tween for at least 30 minutes at RT. The blocking solution was discharged and the membrane shrink-wrapped with the antibody dissolved in TBS-Tween washing-buffer and incubated overnight at 4°C on an agitator. The antibodies were used in specific concentrations (Table 11).

Rabbit Anti-Versican $V_{0/1}$	2µg/ml
Rabbit Anti-Versican $V_{0/2}$	2µg/ml
ß-Actin mouse polyclonal	1µg/ml
Horsedish peroxidase-conjugated antibody	1µg/ml

Table 11: Concentrations of used antibodies

After discharging the first antibody, the blot membrane was washed six times for 5 minutes with TBS-Tween, followed by incubation with the second antibody at a dilution of 1:1000 in TBS-Tween for 1 hour. After that step, the blot membrane was again washed six times for 5 minutes with TBS-Tween. The antibody Rabbit Anti-Versican V0/V1 Neo Polyclonal (BioReagent) and Antibody Rabbit Anti-Versican V0/V2 Neo Polyclonal (BioReagent) were used for western blotting.

The Antibody Rabbit Anti-Versican V0/1 detects a ~70kDa protein representing versican from mouse cumulus oocyte complexes. The PA1-1748A immunogene is a synthetic peptide corresponding to residues CGGD(436) PEAAE(441) of human Versican V0/V1 Neo. The Antibody Rabbit Anti-Versican V0/V2 detects a 64kDa protein representing Versican V0/V2 Neo in human samples. The PA3-119 immunogene is a synthetic peptide corresponding to residues CGGN(400), IVSFE(405) of human versican.[96]

The tissue samples from mouse brain and cell pellets of glioma cell lines HTZ349, HTZ417, U87 and A172 were evaluated. Different isolation techniques were tested as described in the following. Western blot was performed using 20–50µg of the generated protein sample. The samples were loaded onto the gel mixed with sample buffer (Lammli) with or without beta-mercaptoethanol. The sample buffer was used at a dilution of 1:1. Samples were then denatured at 90°C for 5 minutes before loading. The samples were vortexed before and after heating. The protein was separated using SDS-PAGE and then transferred to nitrocellulose membrane for protein detection.

I.10.5.2 Manual film development

The ECL Kit (Sigma) was used as a substrate for colour development. The membrane was coated for 30–60 seconds with a mixture of 1ml of each solution. The

membrane was then placed in a developing chamber and covered with a film. Each film was exposed at three time points. The exposure time of a film varies between 3 seconds, 1 minute and 5 minutes. As soon as the film was developed, the film was placed over the blot membrane and the marks of the size marker were transferred onto each film.

I.10.5.3 Stripping

The stripping solution was diluted at 1:20 in aqua dest. and incubated with the blot membrane for 20 minutes at RT. Next, the membrane was washed three times using TBS-Tween, each time for 10 minutes. Subsequently, the membrane was again blocked and incubated with another antibody or stored at -80°C for future experiments.

I.10.6 Immunocytochemistry

Immunocytochemistry is a method that helps to prove the expression of and to discover the localization of a protein/antigen of interest. Immunocytochemistry is especially used to determine the exact localization and place of progression of ECM molecules with specific antibodies.

Immunocytochemistry was used in order to visualize the exact location of versican and its isoforms in the surrounding of the cell and cell surface. Therefore differing fixation methods were tested. PFA fixation permits cytoplasmic proteins to become visible. Methanol fixation was used to detect proteins on the nuclear side and the cytoplasm.

Cells were seeded in 6-well plates on cover slips at least two days prior to fixation. For methanol fixation, culture medium was drained off and cover slips were rinsed in PBS. PBS was drained off and pre-cooled, and then 100% methanol was added at -20°C for 10 minutes. After the fixation step, cover slips were washed three times for 5 minutes. Cells were then permeabilized with 0.01% Triton X-100 in PBS for 30 seconds and then again washed three times in PBS for 5 minutes. Cover slips were incubated in 1% BSA, PBS pH 7.5 for 30 minutes to block unspecific binding of the antibodies and then incubated with primary antibody in 1% BSA, PBS pH 7.5 for 60 minutes at RT. After the cover slips were washed another three times with PBS, they

were incubated with the second antibody, Alfa-Rb Alexa 488. This fluorescent antibody is used in 1:1000 dilutions. Another washing step was performed. Prior to analyzing under florescence microscope, the cover slips were mounted in PPD-mounting medium (90% glycerol) and sealed with nail polish.

For PFA fixation, the medium consisted of 1.85g PFA, 3.5 ml dH_2 and 10µl of 10M KOH. The fixation buffer was warmed to 37°C and added directly to cells after the culture medium was discharged and then fixed for 5–20 minutes. The washing and incubation steps with antibodies were performed as described in the above.

I.10.7 Functional assays

I.10.7.1 Proliferation assay

In the proliferation assay, cells were harvested and counted 24 hours after transfection as described in the above. Five thousand cells per well were immediately seeded into a 12-well plate. Cell counts of each group (e.g. native cells, siRNA-transfected cells and cells incubated with Lipofectamine) were defined at three to four time points (48 hours, 72 hours and 96 hours after transfection). Cell counting was performed as described in the above. The experiment was performed at least in triplicate and was repeated three times. Untreated cells, cells incubated with Lipofectamine, nonsense-siRNA-transfected cells and target-siRNA-transfected cells were used as control groups. The statistical analysis was performed as described below.

I.10.7.2 Attachment assay

The attachment assay was performed in a 96-well plate. Figure 9 shows the plate setting. Five thousand cells were seeded simultaneously five-fold to analyse three different time points. The first blank value containing 100µl of culture medium and a positive control containing 5,000 cells in 100µl culture medium per well were sown onto the 96-well plate five-fold. Then cell suspensions containing 25,000 cells/500µl of each investigated group were prepared and distributed across five tubes at a volume of 100µl per tube. 5x100µl of each group were seeded into a 96-well plate using a multi-pipette adjusted at 120µl. At predetermined time points (i.e. 10, 25 and 45 minutes after seeding) cells were flushed three times with 100µl PBS. PBS was

discharged after the last washing step and replaced with 100µl of culture medium. Next, the well plate was put back into the incubator for 4 hours. Subsequently, wells were filled with 40µl of the XTT assay solution and incubated for another 2 hours. Quantitative analysis of the cells remaining in the culture plate was done by measuring photospectrometric absorption with an ELISA-Reader. A negative and positive control group served as reference values. The negative control group (BV) consisted of culture medium without cells, the positive control group (PC) comprised a distinct number of cells that dis not undergo flushing during the experiment.

bv	bv	bv	bv	bv	bv
pc	pc	pc	pc	pc	pc
nat	nat	nat	nat	nat	nat
si-c	si-c	si-c	si-c	si-c	si-c
si-t	si-t	si-t	si-t	si-t	si-t
nat	nat	nat	nat	nat	nat
si-c	si-c	si-c	si-c	si-c	si-c
si-t	si-t	si-t	si-t	si-t	si-t
nat	nat	nat	nat	nat	nat
si-c	si-c	si-c	si-c	si-c	si-c
si-t	si-t	si-t	si-t	si-t	si-t

Figure 9: Test arrangement of 96-well plate in attachment assay. Bv = culture medium without cells, pc = culture medium containing 5,000 cells per well, nat = native cells, si-c = control-siRNA-transfected cells, si-t = target-siRNA-transfected cells

I.10.7.3 Scratch assays

The spreading and migration capabilities of cells were assessed using a scratch (wound) assay to measure the expansion of a cell population on a given surface. Cells were seeded into uncoated 6-well tissue culture dishes at a density of 100% confluence and cultured in culture medium containing 5% FCS. The cell monolayer was then scratched using a 100µl sterile pipette tip. The cellular debris was removed by flushing the cell monolayer with 500µl PBS. The wounded monolayer was then

incubated with 5% FCS medium for 48–72 hours. A grid was printed onto the culture dish and the wound area was inspected in marked fields at different time intervals until closure of the wound. The wound areas were photographed under a light microscope in defined rectangles created by the printed grid. The width of the scratch was measured at 6 and 12 hours after treatment. Thus, the cells that invaded the grid rectangle were counted. The number of invaded cells was correlated to the number of migrated cells in untreated control groups by statistical analysis. The experiments were run in triplicate and repeated at least three times.

I.10.7.4 Boyden chamber

The Boyden chamber assay, originally introduced by Boyden for the analysis of leukocyte chemotaxis, is based on a chamber of two medium-filled compartments separated by a microporous membrane measuring 8µm in diameter.

Prior to starting the experiments, each cell population was grown in equal (80%) confluence in culture dishes under normal conditions. Cells were harvested as described in the above. The cell pellet was suspended in 200µl of DMEM and cell count was determined. The experiments were run with 5,000–10,000 cells per chamber.

The Boyden chamber consists of two compartments. The lower chamber is separated from the upper chamber by a porous membrane (Figure 10). The lower chamber was filled with 110µl of fibroblast-conditioned medium (FCM). The 8µm mircoporous membrane was placed on top of the convex FCM fluid level, avoiding air bubbles. The membrane was fixed using the upper chamber's screw cap. Then the cell suspension with a defined cell count was placed into the upper chamber. The experiments were done in triplicate. The chambers were returned to the incubator for 4 four hours at 37°C.

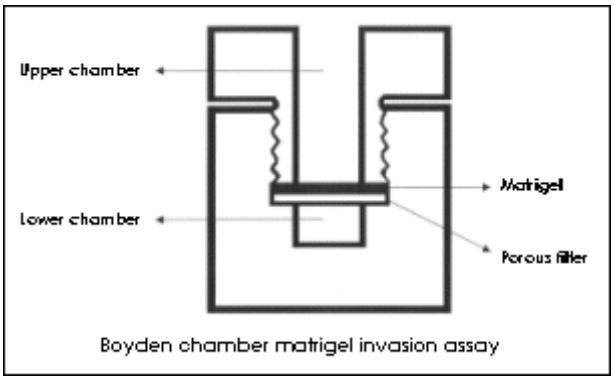

Figure 10: Boyden chamber: Upper chamber filled with cell suspension; lower chamber filled with chemoattractant. Upper and lower chamber are separated by a porous membrane

After the appropriate incubation time (4 hours), the fluid remaining in the upper chamber was discharged and the membrane carefully removed. The cells that were attached to the porous membrane were fixed and then stained with dye solution (Haemacolor). To that end the membranes were raised for 1 minute in a fixation medium and for 1 minute in dye solution 1 and 2. The stained membranes were then put on a glass slide and analyzed under a microscope. The cells were counted on the filter membrane under a microscope in three to five visual fields (Leica) and statistically analyzed using the ImageJ software.

I.10.8 Statistical analysis

Statistical analysis is performed in different experiments to substantiate results and determine their statistical significance and validity. In western blot and semi-quantitative PCR, the results of particular products are visible as bands on blot membrane or under visualization in a Vilbert Lourmat chamber in agarose gel electrophoresis.

To compare signal intensity, bands were scanned and underwent analysis using the ImageJ software. The images were opened using this software and measurements were set. The pictures needed to be inverted for signal intensity to be measured. Subsequently, the mean grey value, standard deviation modal grey value and median were defined. The ImageJ results were transferred to an Excel sheet; analysis involved comparing different treated cells with native and control samples (Microsoft Office Excel 2008).

In real-time PCR, the standard curve-based analysis is used. The standard curve values were generated from the data provided by the MxPro software, based on measured threshold cycle (Ct) values. Ct is defined as the number of cycles required for the fluorescent signal to cross the threshold (i.e. for it to exceed the background level). As Ct levels are inversely proportional to the amount of target nucleic acid in the sample,[97] Ct-levels of a target gene were divided by the Ct levels of the housekeeping gene to obtain a normalized target value. Each of the normalized values was divided by the normalized control (untreated) sample value (Ct) to generate the relative expression levels. Table 12 gives an example of the calculation.

Sample	MV	SD	Calculated 1/18sxsiV1	CT-level 18s	1/18s	CT-level siV1
Native	1.28291	0.348339	0.904771	104.80	0.009541	94.82

Table 12: Extract of an Excel table showing an example of calculated expression levels. MV = mean value, SD = standard deviation, calculated 1/18sxsiV1 = relative expression level in the sample

In Boyden chamber assays, five visual fields per membrane were analyzed using the ImageJ cell counter tool. The experiments were carried out five-fold and repeated at least two times. The attachment assay was performed five-fold and repeated three times. The metabolic activity in compared groups was measured in the Elisa-Reader. The proliferation assay was performed four- to five-fold for each time point and repeated at least three times. The direct cell count provided the values for statistical analysis. In the scratch assay, the cells that invaded the grid were counted. At least four rectangles per well were counted. The experiments were done in triplicate.
The mean value and the standard deviation of all experiments mentioned in the above were calculated with Microsoft Office Excel 2008. Student's T-test was assessed in each experiment to compare values of treated cells with untreated cells or control groups (Figure 11).

=T-test (Matrix1; Matrix2; page; type)

Figure 11: Formula for Student's T-test

Results

I.11 Set up experiments

The aim of this work was to investigate the influence of versican isoforms V1, V2 and V3 on cell motility, migration and proliferation ability. Specific siRNAs were used as a silencing tool. For quantitative analysis of my results and proof of successful transfection procedure, different methods had to be established before these methods could be applied to generate results. The challenges posed by and solutions found in regard to reverse transcriptase PCR (RT-PCR), quantitative real-time PCR (qPCR), western blot and immunostaining will be described in the following.

I.11.1 RT-PCR

The first challenge in the PCR experiments was to design specific primers for versican isoforms V1, V2 and V3. Taking account of guidelines for primer design, primers were created that were capable for analysis in RT-PCR and qPCR. Primer pairs do not show complementary structures and potential to form secondary structures, for example hairpin structures. Runs of three or more Cs or Gs at the 3'-ends of primers were avoided. The transcript of each primer pair matches the exon–exon border sequence in the corresponding mRNA.

Table 13 shows the primer sequences with their sense and antisense strands for each versican isoform.

V0	Sense	5'GAC AGG TCG AAT GAG TGA TTT GAG 3
	Antisense	5GCC ATT AGA TCA TGC ACT GGA TCT G 3'
V1	Sense	5'GAT GCC TAC TGC TTT AAA CGT CG3'
	Antisense	5'GGT TGT CAC ATC AGT AGC ATT TGC3´
V2	Sense	5'-TCACGACTTCAAGTCCTCCTGC-3'
	Antisense	5'- GGTGCCTCCGTTAAGGCACG -3'
V3	Sense	5'- GTGTGGAGGTGGTCTACTTGG-3'
	Antisense	5'- GGTGCCTCCGTTAAGGCACG -3'

Table 13: Primer sequences for versican isoforms V1, V2 and V3

The product length of the designed primers yields the requirements for analysis in quantitative PCR. The cDNA fragment of V1 generates a length of 228bp, the cDNA of V2 has a length of 208bp and the cDNA of V3 has a length of 154bp.

To optimize PCR results, the individual annealing temperature for each primer pair and the amount of RNA was determined by gradient PCR. The following conditions were found to be suitable for primers targeting V1: the DNA polymerase was activated at 95°C for 5 minutes and amplified in 30 cycles at 95°C for 30 seconds, at 66°C for 30 seconds, at 72°C for 30 seconds and was extended at 72°C for 5–7 minutes. The PCR was run with 3µg RNA, with no further adjuvants.

The best results in PCR with primers targeting V3 were achieved with 5µg RNA and an annealing temperature of 55°C. The product of V2 appeared faint or absent in all investigated cell lines. Thus, primer efficiency was enhanced with different adjuvants to the Master mix (e.g. Betaine, DMSO, formamide 5%, glycerol 10–15%, polyethylene glycerol 600 5–15 %). The best results were archived in the presence of 1µl DMSO in 20µl Master mix for V2 and 3µl of RNA (Figure 12). Best results were seen at an annealing temperature of 45°C.

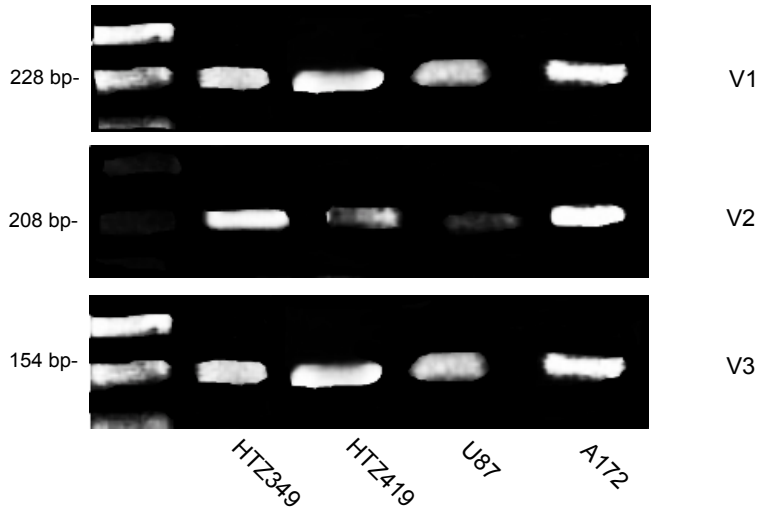

Figure 12: Expression of the different isoforms of versican V1, V2 and V3 in malignant glioma cell lines (HTZ349, HTZ417, U87 and A172). The signal of V2 and V3 shows varying intensity in different glioma cell lines

I.11.2 Quantitative PCR (qPCR)

SYBR Green I, a fluorescent DNA-binding dye and a hot-start mediated Taq-polymerase, was used in qPCR. An adequate thermal profile was established for primers V1 and V3. The hot-start Taq-polymerase was activated for 10 minutes at 95°C in cycle 1, followed by 40 cycles in segment 2, comprising 1 minute at 95°C, 1 minute at 62°C and 1 minute at 72°C. Segment 3 includes one cycle of 1 minute at 95°C, 1 minute at 63°C and 30 seconds at 95°C. Further information on the function of my primers is provided in the analysis of the melting curves (Figure 13). For primers V1 and V3, the respective melting curves show a sharp peak on the estimated number of cycles, whereas the product of primers for V2 is not properly detectable (data not shown).

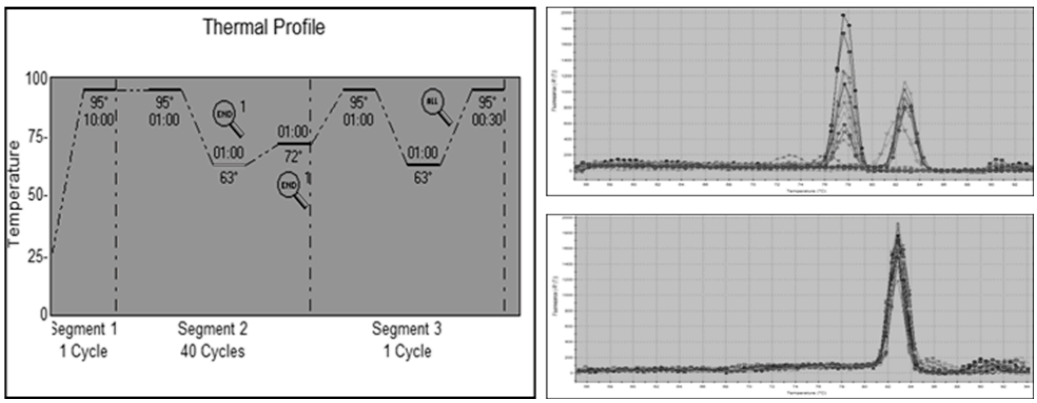

Figure 13: Thermal profiles and melting curves in qPCR. The image on the left shows the thermal profile for primers targeting V1. The images on the right show the melting curve of V1 (above) and 18s (below)

I.11.3 Western Blot

Western blot served the semi-quantitative analysis of specific protein expression in my experiments. Unfortunately, no antibody was available to detect versican isoform V3, which is why the analysis of its expression pattern is only based on the PCR results.

At the beginning several difficulties were encountered in regard to the detection and identification of the protein band in western blotting (Figure 14). Different protein isolation techniques were therefore tested. The isolation of protein out of a cell lysate

using RIPA buffer generated multiple bands on the blot, which could not be assigned to a specific product of the antibody V0/1. Accordingly, different harvesting methods were examined (Figure 14). It became clear that in samples of culture medium containing FCS, antibody did not bind to the protein in a detectable amount, probably due to unspecific coverage of antigen epitopes. In culture medium samples without FCS, a clear protein band was detected, but unfortunately cells are not able to survive in culture medium without FCS for more than 6 hours. Therefore, the most efficient and reproducible method was to discharge the culture medium and carefully scrape off the cell monolayer from the bottom of the culture flask, adding PBS as described in the above. Western blot was run with the supernatant. It was demonstrated in further experiments that it was more efficient to load the protein samples under non-reducing conditions because, otherwise, when adding reducing agent ß-mercaptophenol the antibody V0/1 shows cross-binding.

Further troubleshooting involved determining the blocking reagent. Best results were achieved when membrane blocking was performed using BSA 1.5 % dissolved in TBS-Tween.

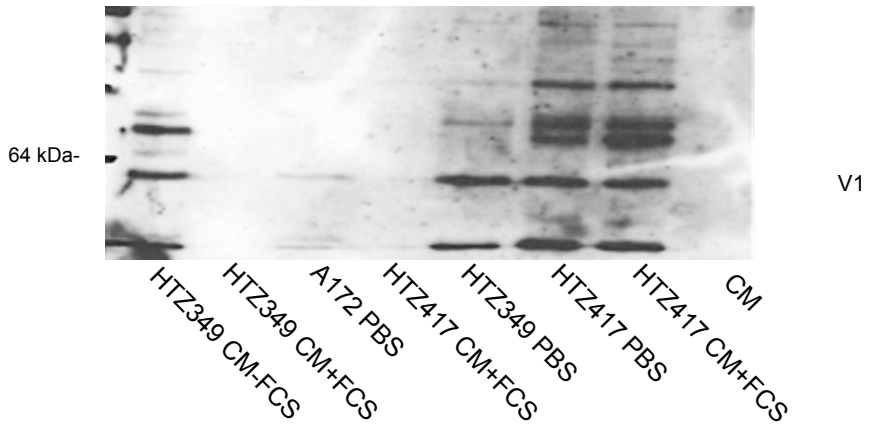

Figure 14: Results of a western blot with samples of 20µg protein of HTZ 349, incubated with antibody V0/1 using different protein isolation techniques. CM = culture medium, FCS = foetal calf serum, CM-FCS = culture medium without FCS, CM+FCS = culture medium with FCS, PBS = cells were harvested after adding PBS

In further experiments, different protein concentrations were tested. The best results were obtained using 20µg of protein (Figure 15).

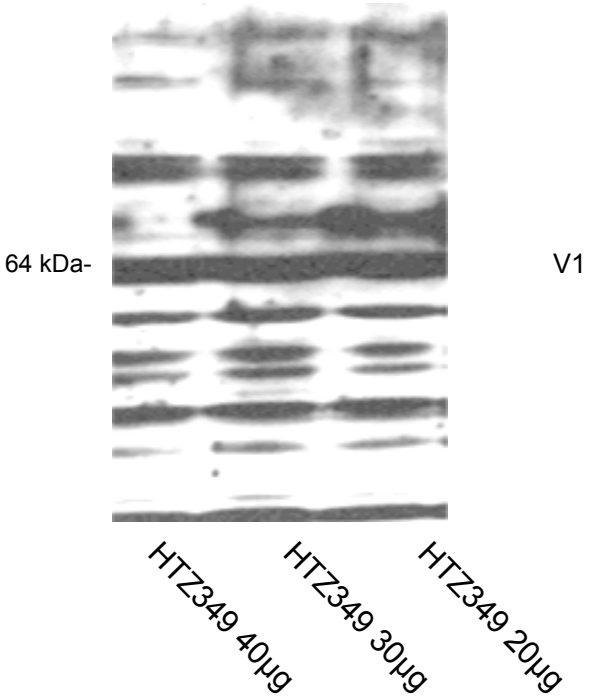

Figure 15: Western blot with HTZ349 and antibody V0/1 with different concentrations of protein (40µg, 30µg, 20µg)

To generate more specific results, the protein concentration in the samples was enriched using immunoprecipitation. As described in the above, cell lysate was prepared to recover proteins in the supernatant. Protein G beads were saturated with the primary antibody V0/1, loaded and analyzed in western blot (Figure 16). The blot membrane showed a broad band at around 75kDa (the product is supposed to appear at around 70kDa) in all investigated samples. Signal intensity corresponded to the protein concentration.

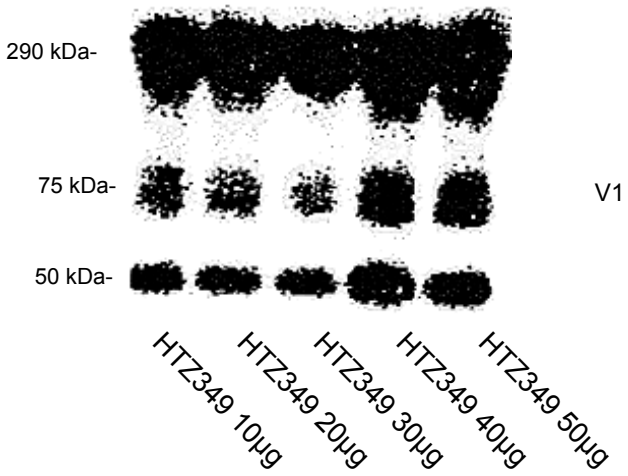

Figure 16: Immunoprecipitation with antibody V0/1 in protein samples of HTZ349 and at different protein concentrations (10µg, 20µg, 30µg, 40µg and 50µg)

I.11.4 Immunocytochemistry

Immunostaining was performed to detect the localization of versican isoforms V1 and V2. The experiments were performed using the cell line HTZ349. The negative control was incubated only with the fluorescent antibody without addition of any targeting antibody. Some fluorescent signal was detected in all groups (Figure 17). The binding of antibody Neo V1/0 appears to capture all parts of the cell, especially the nucleus and extracellular matrix between two cells. The negative control showed strong enhancement of the cytoplasm and the central part of the cell. In the experiment with the antibody Neo V2/0, cells showed broad enhancement in the cytoskeleton with relief of the nucleus.

PFA- fixation in HTZ349

Negative control | Antibody Neo V1/0 | Antibody Neo V2/0

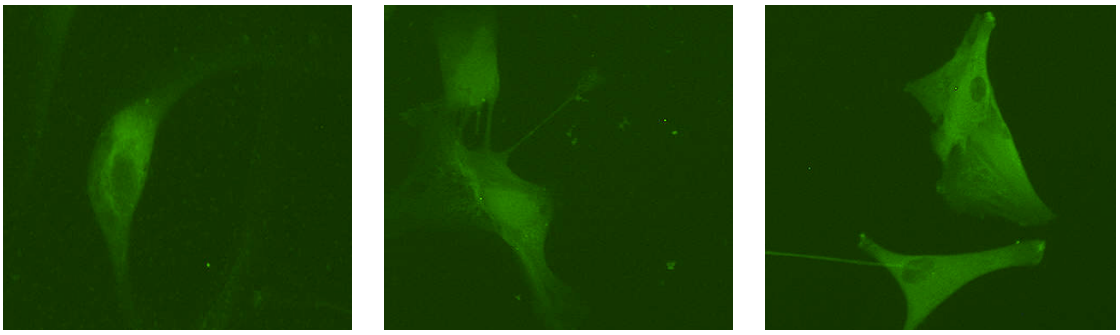

Figure 17: PFA-fixation in HTZ349. Left: Negative control, fixated HTZ349 cells incubated with fluorescent antibody Alfa Rb-Alexa 488. Centre: HTZ349 incubated with florescence antibody Alfa-Rb Alexa 488 and antibody Neo V1/0. Right: HTZ349 incubated with florescence antibody Alfa-Rb Alexa 488 and antibody Neo V2/0

In the cells fixated using methanol, the negative control showed only poor fluorescent emission. By contrast, cells incubated with antibody Neo V1/0 and Neo V2/0 showed rod-shaped enhancement in the cytoplasm and around the nucleus. Whilst antibody Neo V1/0 showed binding in the cytoplasm and nucleus, the antibody Neo V2/0 appeared to accumulate in the area of the nucleus (Figure 18).

Methanol- fixation in HTZ349

Negative control | Antibody Neo V1/0 | Antibody Neo V2/0

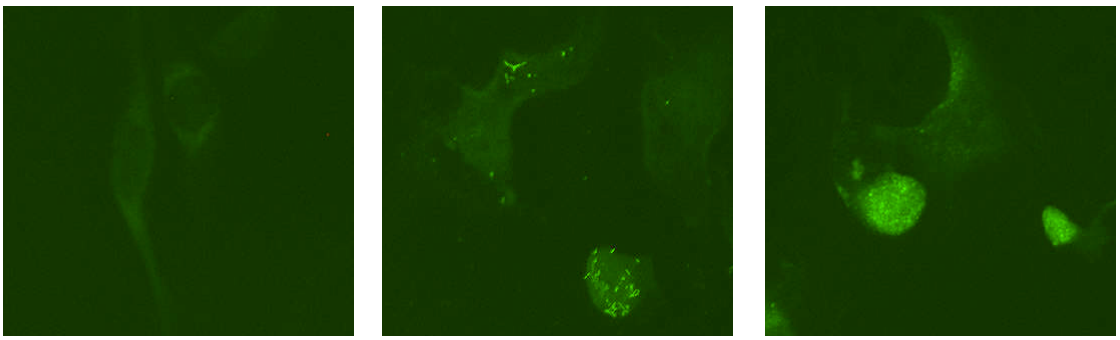

Figure 18: Methanol-fixation in HTZ349. Left: Negative control, fixated HTZ349 cells incubated with fluorescent antibody Alfa-Rb-Alexa 488. Centre: HTZ349 incubated with florescent antibody Alfa-Rb Alexa 488 and antibody Neo V1/0. Right: HTZ349 incubated with florescent antibody Alfa-Rb Alexa 488 and antibody Neo V2/0

I.11.5 SiRNA

I.11.5.1 SiRNA design

The mRNA sequence of the gene of interest was needed to design an siRNA and was retrieved from the NCBI database. In this context, it is important to remember that the structure of versican isoforms is a combination of different elements of V0 (Figure 19).

In V0, the G1- and G3-domain are connected by means of α- and ß-chains. V1 contains G1-domain, ß-chain and G3-domain; V2 contains G1-domain, α-chain and G3-domain; and V3 contains G1- and G3-domain. As regards the structural homologies between V1, V2 and V3, siRNA target regions need to overlap in the bordering regions of the adjoining domains. As regards the mRNA sequence of V1, the crossing between G1-domain and ß-chain region was chosen for a proper target sequence as no other isoform shows a crossing area between the G1-domain and the ß-chain. The specific sequence for siRNA targeting V2 is supposed to be found in the crossing between the G1-domain and the α-chain. The target sequence for siRNA in the mRNA of V3 is localized at the junction between the G1- and the G3-domain.

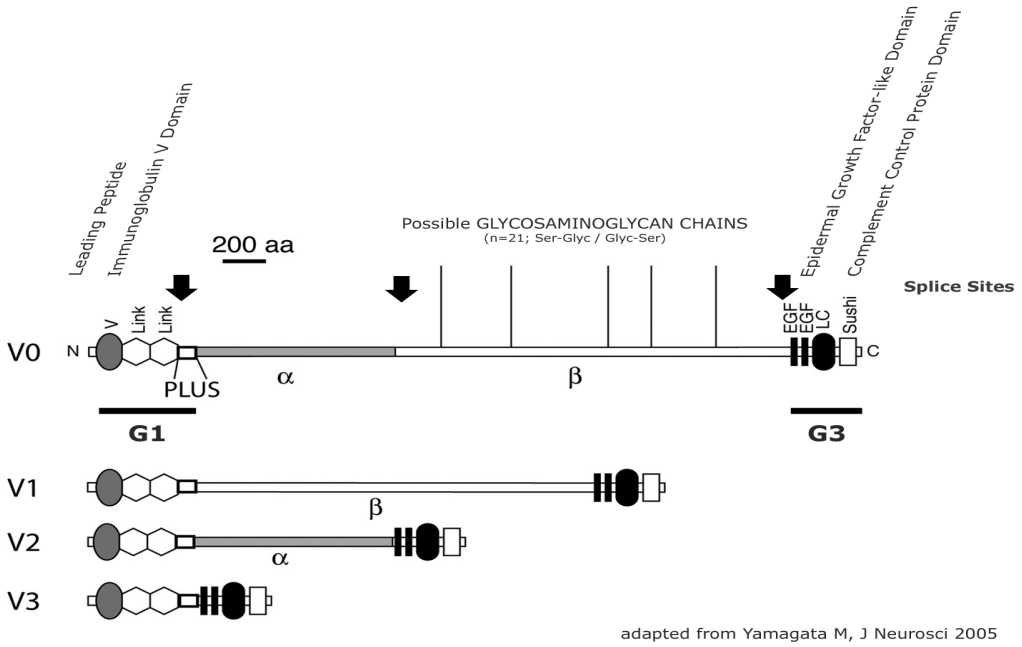

Figure 19: Structure of versican isoforms. Alternative splicing of V0 generates V1, V2 and V3[98]

The above- mentioned guidelines needed to be considered in the siRNA design. Finally, siRNA target sequences have a length of 21nt (Table 14). Regions within 50–100bp of the start codon and the termination codon in mRNA had to be avoided. Even intron regions, stretches of four or more bases such as AAAA, CCCC, regions with GC content <30% or >60% were avoided, as these sequences generate binding problems in the target region.[99] The sequences of the sense- and antisense-strand were blasted through the human genome using the NCBI database. Any homologies of the chosen siRNA sequences to other human gene sequences were ruled out.

	Target	5'-GGG AGU UCU UCG AUU CCA ATT-3'
V1	Sense	5'-r(GGG AGU UCU UCG AUU CCA A)dTdT
	Antisense	5'-r(UUG GAA UCG AAG AAC UCC C)dTdT
	Target	5'- AGA AAA TAA GAC AGG ACC TGA- 3'
V2	Sense	5'-r(AAA AUA AGA CAG GAC CUG A)dTdT
	Antisense	5'-r(UCA GGU CCU GUC UUA UUU U)dCdT
	Target	5'-TAC TGC TTT AAA CGA CCT GAT-3'
V3	Sense	5'-r(CUG CUU UAA ACG ACC UGA U)dTdT
	Antisense	5'-r(AUC AGG UCG UUU AAA GCA G)dTdA

Table 14: Target sequences in mRNA of V1, V2 and V3, including sense- and antisense-strand of siRNAs

The negative control was designed by scrambling the target-siRNA sequence. The control RNA had the same length and nucleotide composition as the siRNA, but had at least four to five bases mismatched to the siRNA. Further, it was ruled out that the scrambled siRNA was able to create new homology to other genes.

I.11.5.2 siRNA transfection

Set up experiments for siRNA transfection in HTZ349, HTZ417, U87 and A172 were started with the transfection reagent Lipofectamine plus (invitrogen) and siRNA targeting MAPK and non-silencing, Alexa Fluor-labelled negative control siRNA. As under Lipofectamine plus, most of the cells looked highly impaired when their cell shape was examined under the microscope and died during the transfection procedure even at lower concentrations (2µg, 1.5µg and 1µg) of Lipofectamine. The

transfection reagent was thus changed to Lipofectamine 2000 and the transfection medium Optimem was used. Under these new conditions, the vitality and survival rate of the cells improved.
The transfection efficiency rate was determined by analyzing Alexa Fluor-labelled negative control siRNA (data not shown).

I.11.5.3 Creating shRNA

As the results of the experiments with siRNA targeting V1 necessitated further long-term investigations, for example in animal assays, a short hairpin transfection system was established. The silencing effect of siRNA transfection is a transient effect lasting several days, which means a limitation of siRNA use in functional assays lasting longer than four days. For that reason I decided to operate a stable and inducible system of RNAi, so-called short hairpin RNA (shRNA). The following sequences for a short hairpin construct were chosen (Table 15).

mRNA sequence	5’ GGG AGU UCU UCG AUU CCA ATT ‘3
Top sequence	5’GATC CCC GGG AGT TCT TCG ATT CCA TTCAAGAGA AAT TGG AAT CGA AGA ACT CCC TTTTT GGAAA ‘3
Bottom sequence	5’AGC TTTCC AAAAA GGG AGT TCT TCG ATT CCA ATT TCTCTTGAA AAAT TGG AAT CGA AGA ACT CCC GGG ‘3
Duplex	3’GATC CCC GGG AGT TCT TCG ATT CCA ATT TTCAACACA AAT TGG AAT CGA AGA ACT CCC TTTTT GGAAA GGG **CCC TCA AGA AGC TAA GGT TAA** AAGTTCTCT TTA ACC TTA GCT TCT TGA GGG AAAAA CCTTTTCGA _5

Table 15: Top sequence: GATC served as the BGL II cutting site in the top sequence, CCC represented the spacer followed by sense-, loop- and antisense sequence, termination signal TTTTT GGAAA and spacer CCC. The Hind III cutting site is located in the palindromic sequence in the reverse and bottom sequence.

The plasmid has a RNA Polymerase III-dependent promoter and a terminator signal for the transcript area (5 Ts one after another). The sequence of siRNA targeting V1 was ligated into the pENTR-THT vector. After transcription of the vector sequence,

the RNA was folded into a hairpin-like structure, which is a substrate for the enzyme Dicer and leads to cellular production of the siRNA.

The experiments were run with co-transfection of fluorescent markers like GFP and PDS Red to analyze transfection efficiency. Figure 20 shows GFP and shV1 co-transfection in HTZ349 under the fluorescence microscope and the same slice under the bright field microscope. The photographs were taken 24 hours after transfection.

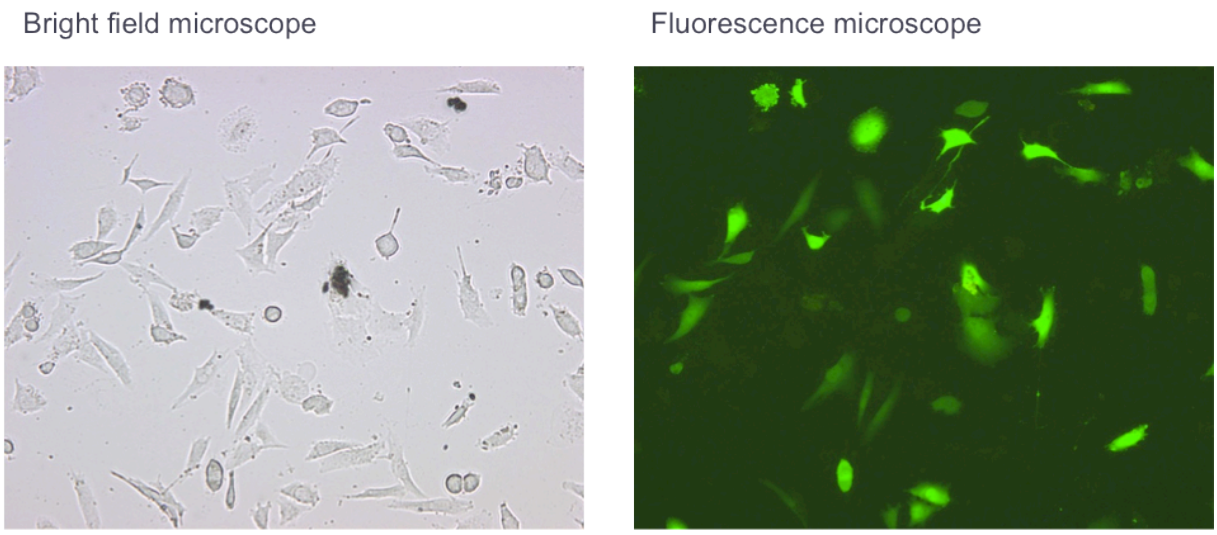

Figure 20: GFP and shV1 co-transfection in HTZ349 under the fluorescence microscope (left) and the same slice under the bright field microscope (right).

Figure 21 shows the transfection efficiency in GFP-transfected cells, cells co-transfected with an empty control GFP-containing vector and cells co-transfected with shRNAV1 and GFP. Subtracting the bright field image and fluorescence image revealed a transfection efficiency of 36% in GFP-transfected cells, 29% cells co-transfected with an empty control vector GFP and 35% in cells co-transfected with shV1 and GFP.

Despite the poor transfection efficiency, the results in western blot showed a clear alleviation of the band of V1 in shV1-transfected cells, although a mild alleviation of control vector transfected cells was observed. In the blot that was incubated with the antibody targeting V0/2, the expression pattern of V2 did not change. Ponceau staining of the blot membrane showed equal protein loading in all samples.

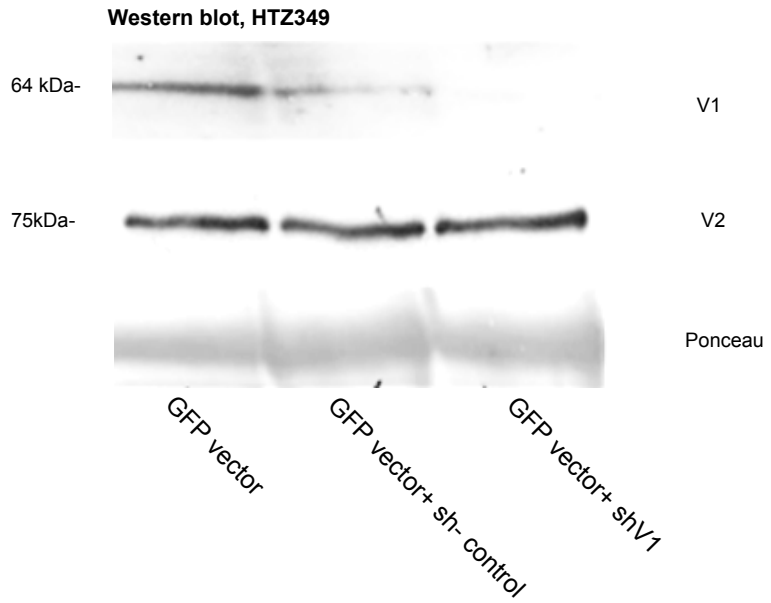

Figure 21: Western blot with GFP-transfected cells (GFP vector), cells co-transfected with an empty control vector GFP (GFP control + sh-control) and cells co-transfected with sh-RNA targeting V1 and GFP (GFP vector + shV1) 24 hours after transfection. Antibody V0/1 and V0/2, Ponceau staining

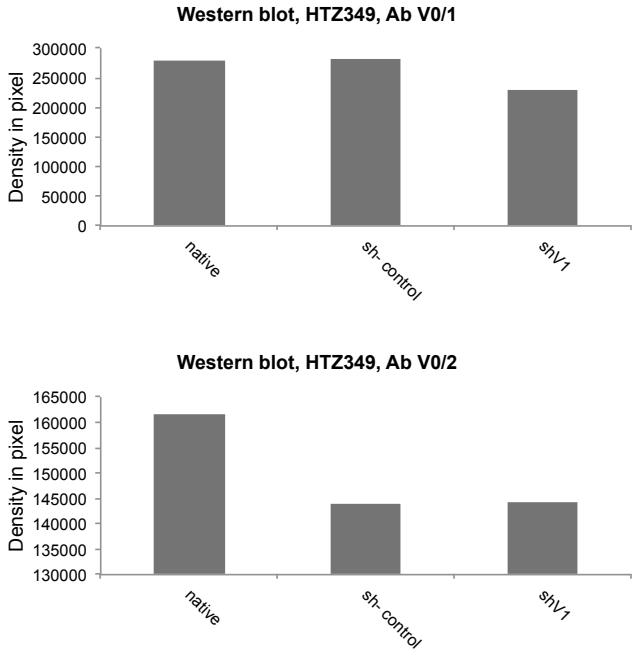

Figure 22: Statistical analysis of western blot results with harvested cells of the same experiment with antibody V0/1 (above) and V0/2 (below) with Ponceau staining as marker

I.12 Transfection with siV1, siV2 and siV3

The transfection efficiency in all experiments was monitored on the protein and PCR level. Control groups in the experiments consisted of cells incubated with Lipofectamine only, nonsense-siRNA transfected cells (si-control) and native cells (native). These control groups helped to assign whether changed cell behaviour, especially in functional assays, was due to side effects of the transfection procedure or could be regarded as a specific effect of the siRNA. Mitochondrial 18s was chosen as the housekeeping gene, as it is present in all nucleated cells types. The mRNA synthesis of these genes was considered to be stable and secure in various tissues, even under experimental treatment.[100]

I.12.1 Semi-quantitative analysis of siv1 transfection in RT-PCR

In real-time PCR, cDNA of different cell lines HTZ349, HTZ417, U87 and A172 were analyzed at different time points after transfection. Assays were repeated at least two times in each cell line. Native cells, nonsense siRNA-transfected cells and siV1-transfected cells were harvested 24 hours and 48 hours after seeding and analyzed in PCR with primers targeting V1.

A strong down-regulation of V1 expression in HTZ349 on days 1 and 2 after transfection was detected. In samples harvested on day 2 after transfection, a slight increase in signal was seen in siV1-transfected cells. Both control groups, nonsense siRNA-transfected cells and native cells, showed strong signal, whereupon a slight regulation of V1 expression was assumed in nonsense siRNA- transfected cells (Figure 23).

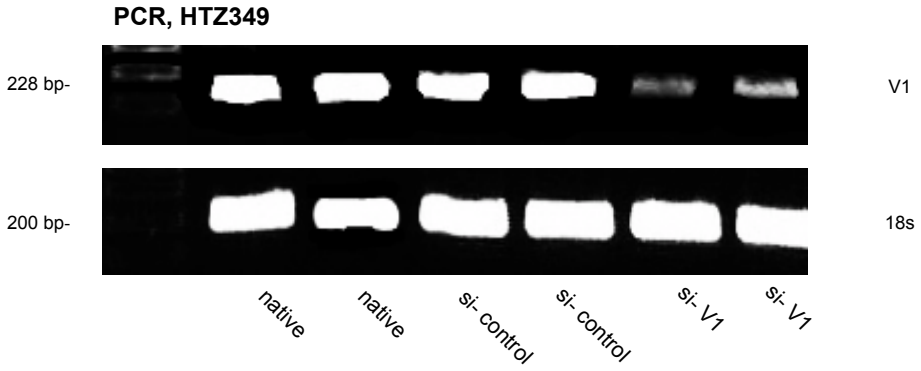

Figure 23: Results of RT-PCR with HTZ349 after transfection with siRNA targeting V1 on day 1 with primers targeting V1 and 18s

Equal loading of RNA in RT-PCR and cDNA in electrophoresis is proven in analysis with primers targeting the housekeeping gene 18s. The housekeeping gene expression showed consistent bands in all samples (Figure 23).

The down-regulation effect of siV1 was visible within the first three days after transfection (Figure 24). On days 4 and 5 the signal of V1 in siV1-transfected cells became nearly as strong as in native cells and control groups. No regulatory effect was seen in the controls groups (Lipofectamine-incubated cells and nonsense siRNA-transfected cells) compared with native cells. Equal signal intensity in the native sample and control groups was maintained on days 3, 4 and 5 after transfection (data not shown).

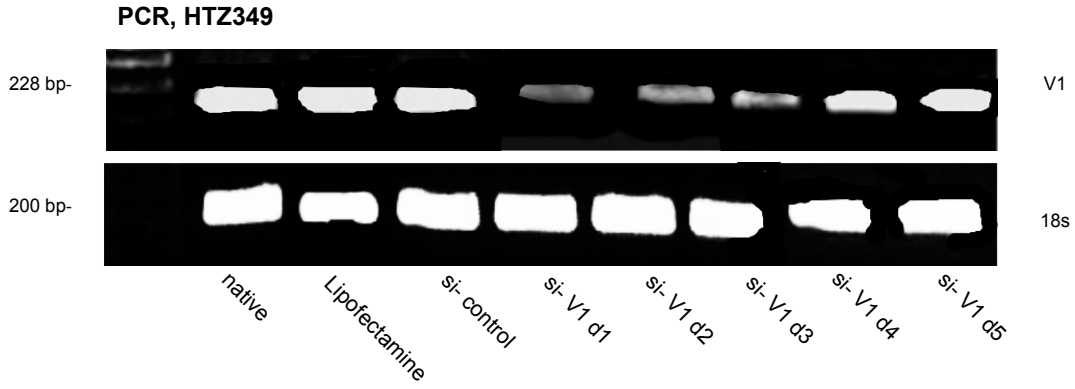

Figure 24: Results of RT-PCR with HTZ349 after transfection with siRNA targeting V1 on days 1, 2, 3, 4 and 5 with primers targeting V1 and 18s. Control groups: native cells, Lipofectamine treated cells and control siRNA transfected cells

As regards the possibility of off-target effects in siRNA transfection, PCR was run with primers targeting V2 and RNA samples of native cells, nonsense siRNA-transfected cells and siV1-transfected cells (Figure 25). The product of versican isoform V2 on estimated length appeared in none of the samples. The bands at the bottom of the gel were interpreted as primer dimers. The same samples were used for a PCR run with primers targeting V3 (Figure 25). The product appeared in the estimated length. No regulatory effect of V3 was seen in any of the samples, especially not in the sample comprisingsiV1-transfected cells.

The results were replicated in cell lines HTZ417 (Figure 26), U87 (Figure 27) and A172 (Figure 28) at two to three different time points (data not shown).

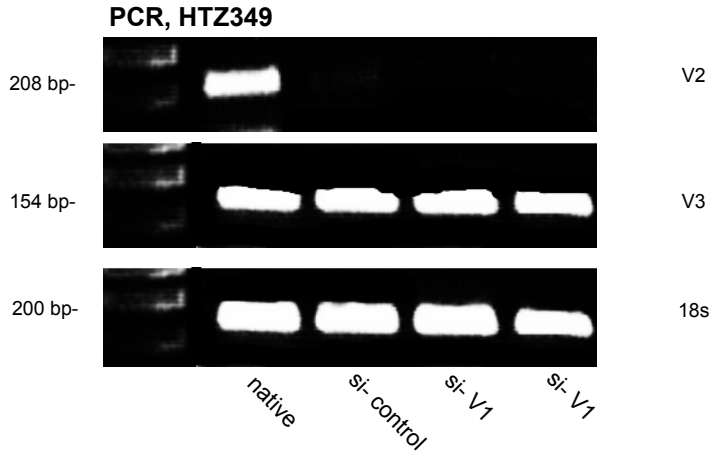

Figure 25: RT-PCR with HTZ349, transfected with siV1 and primer V2, V3 and 18s

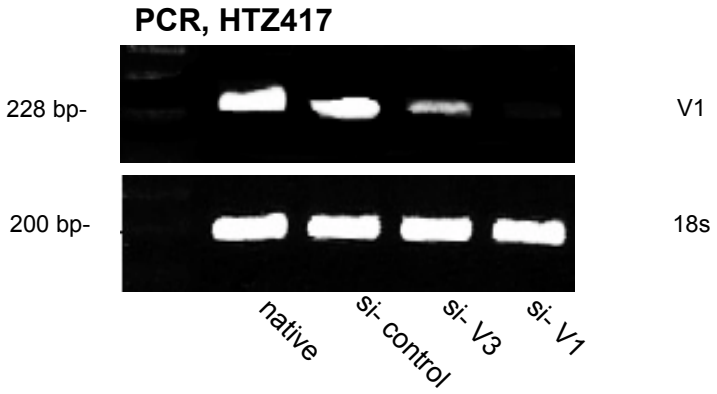

Figure 26: RT-PCR with HTZ417 and primers targeting V1 and 18s. Cells were transfected with si-control, siV1 and siV3

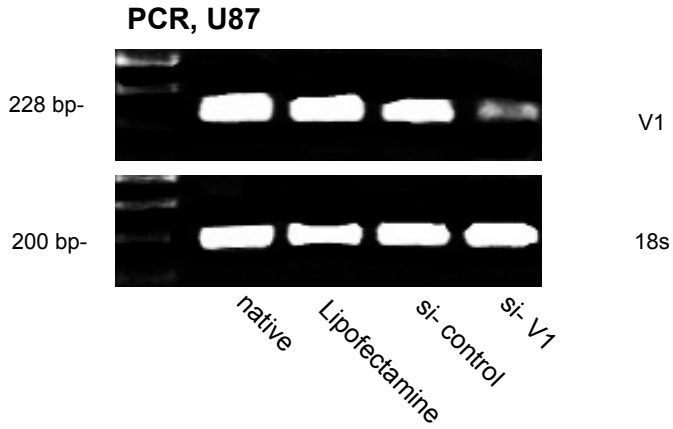

Figure 27: RT-PCR with U87 and primers targeting V1 and 18s. Cells were transfected with siV1, si-control and Lipofectamine

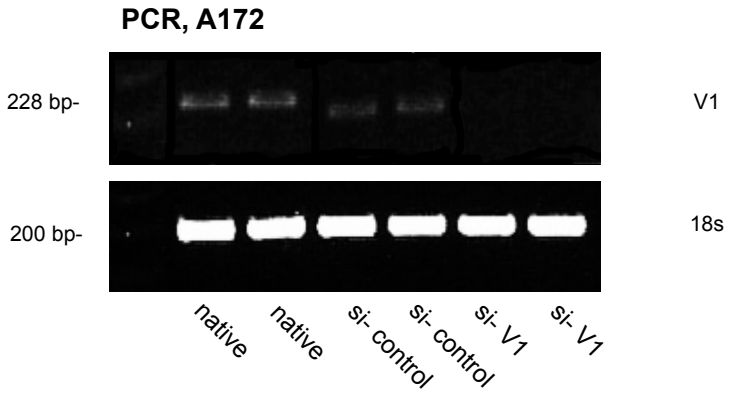

Figure 28: RT-PCR with A172 and primers targeting V1 and 18s. Cells were transfected with siV1 and si-control

I.12.2 Semi-quantitative analysis of siV2 transfection in RT-PCR

Figure 29 shows the results of a PCR with native cells, siV2- and siV3-transfected cells using primers detecting V1, V2, V3 and 18s. The first image confirms equal cDNA loading on the PCR level, as the expression of the housekeeping gene 18s showed consistent signal intensity in all investigated cell populations. The analysis of the product in PCR with primers detecting V1 showed a complete suppression of V1 in siV2- and V3-transfected cells. By contrast, the product V2 appeared on the PCR

level on the estimated length in native cells, siV2- and siV3-transfected cells. Compared with native cells, the expression of V2 appeared to be decreased in siV2-transfected cells, but still detectable. PCR results with primers targeting V3 in the same samples did not show any obvious regulation of V3 expression in siV2-transfected cells.

I.12.3 Semi-quantitative analysis of siV3 transfection in RT-PCR

In the experiment using siV3 transfection, RT-PCR showed a mild regulation of V3 in siV3-transfected cells (Figure 29). Off-target effects were examined in the same samples and with primers targeting V1 and V2. The PCR results showed a complete suppression of product V1 in cells treated with siV3. Control runs with primers targeting V2 also showed regulation of V2 in siV3-transfected samples. The PCR with primers targeting 18s confirmed equal cDNA loading.

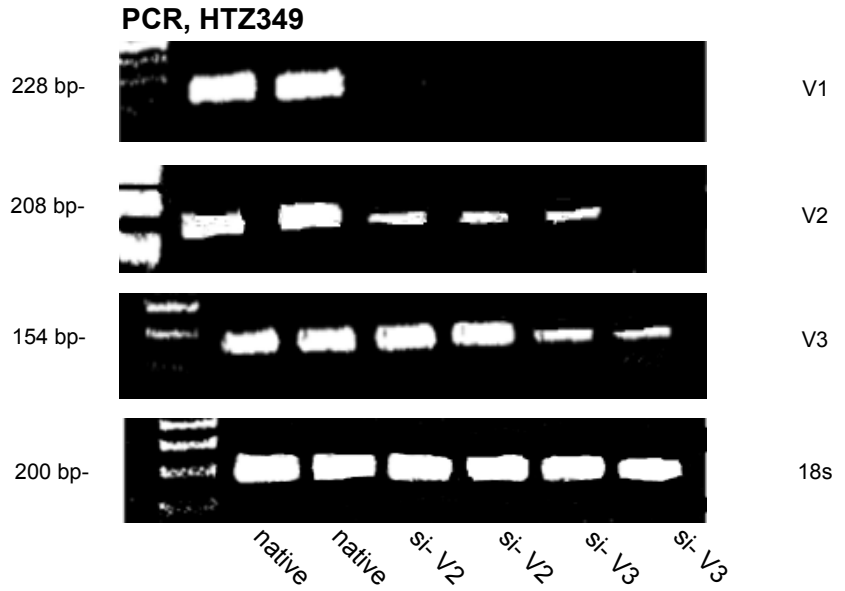

Figure 29: RT-PCR with HTZ349 and two different samples of native cells, siV2- and siV3-transfected cells with primers for 18s, V1, V2 and V3

I.12.4 Quantitative PCR in siV1-transfected cells

In quantitative PCR, versican isoform V1 was amplified and simultaneously quantified. The analysis was based on standard curve method as described in the

above. 18s was again used as the housekeeping gene. Native samples and siV1-transfected cells were compared.

The standard curves contain squares that exposed the range of cDNA dilution series set in duplicate. A triangle symbol marks the concentration of cDNA in the samples, which were analyzed in a dilution of 1:20. The diagram shows the standard curve for the product 18s and for the product V1. All samples needed to lie within the standard dilution series values for valid analysis (data not shown).

For analysis, the target gene value was divided by the reference gene value. The ratio of target gene values was obtained in relation to the control sample and was corrected with the values of our reference gene. According to the findings in RT-RCR, siV1-transfected cells showed a massive decrease in V1 expression in comparison to native cells on the qPCR level (Figure 30). The nearly complete down-regulation of V1 was definitively proven on day 1 ($p = 0.03$) and on day 2 ($p = 0.022$) after transfection, and was less distinctive on day 3 after transfection ($p = 0.28$) according to the results obtained in RT-PCR. Figure 31 shows the down-regulation of V1 in HTZ419 on day 1 ($p = 0.03$) and on day 2 ($p = 0.03$) after transfection, and was less significant on day 3 after transfection ($p = 0.107$).

Subsequently, the same samples were analyzed in RT-PCR with primers targeting V3 to exclude off-target effects. Experiments showed that there was no significant influence on the expression pattern of V3 obtained in siV1-transfected cells on days 1, 2 and 3 after transfection. Unfortunately, primers targeting V3 could not be established in qPCR.

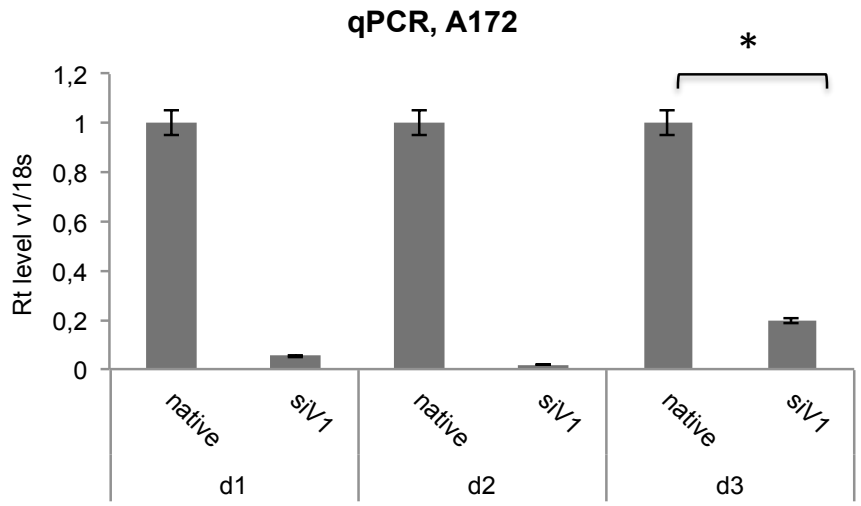

Figure 30: Quantitative PCR results of siV1-transfected in A172. The analysis compared the product of primers targeting V1 in native and siV1-transfected cells. * p = 0.028

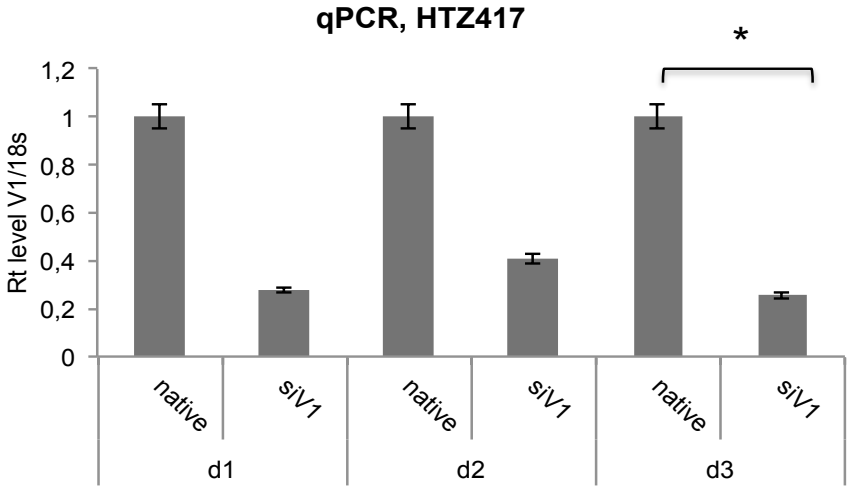

Figure 31: Quantitative PCR results of siV1-transfected in HTZ417. The analysis compared the product of primers targeting V1 in native and siV1 transfected cells. * p = 0.107

I.12.5 Protein regulation

After successful down-regulation of isoform V1 in siV1-transfected cells on the PCR-level, the expression of V1 on protein level was investigated. Protein harvesting was performed as described in the above. The experiments were run with a protein concentration of 20µg for each sample. Ponceau staining was used to control equal

protein loading. A regulatory effect of siRNA-targeting V1 was seen in the decreased expression of protein V1 in western blot (Figure 32, Figure 33). The same samples were analyzed with antibody V0/2. An off- target regulation of V2 in siV1-transfected cells was ruled out (Figure 34). Reference groups again consistened of cells incubated with Lipofectamine and nonsense-siRNA transfected cells (si-control). Interestingly, the expression of V1 in native and Lipofectamine-transfected cells appeared to remain nearly equal, whereas the si-control-transfected cells showed a clear decrease in V1-expression (Figure 33).

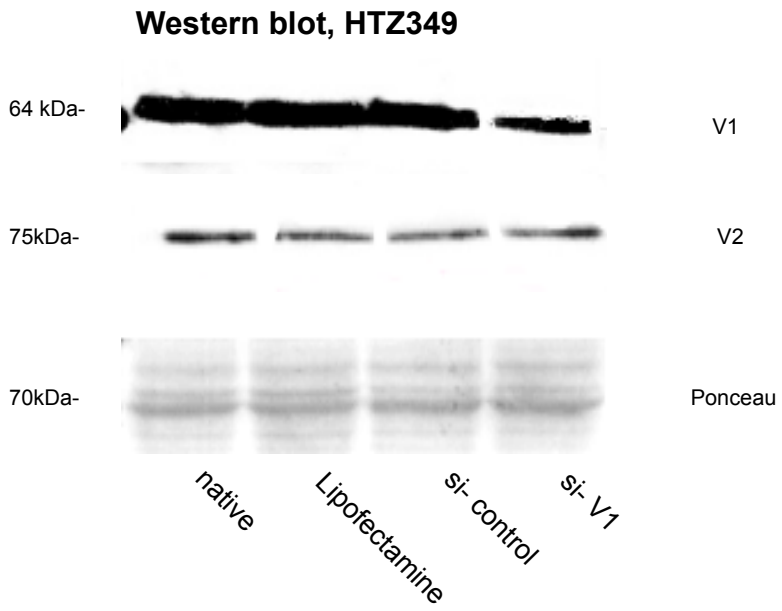

Figure 32: Results of western blot in HTZ349, transfected with siV1. Western blot was performed with antibody V0/1 and V0/2

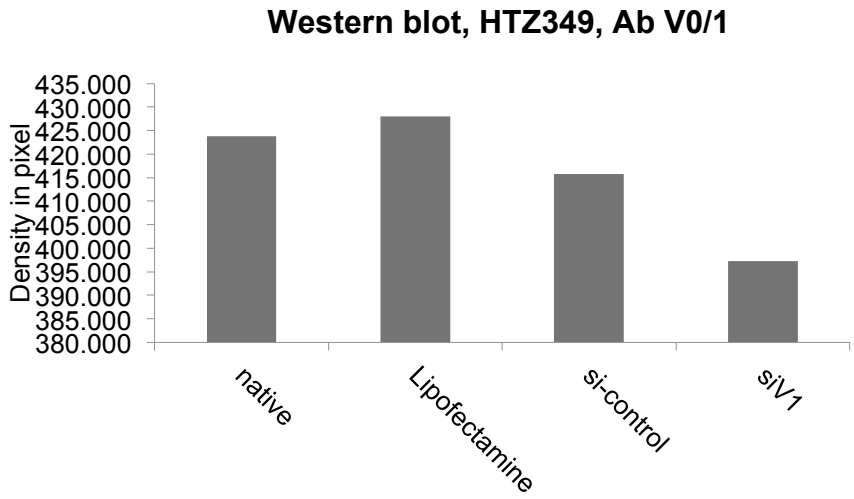

Figure 33: Statistical analysis of western blot results in HTZ417 transfected with siV1. Western blot was performed with antibody V0/1

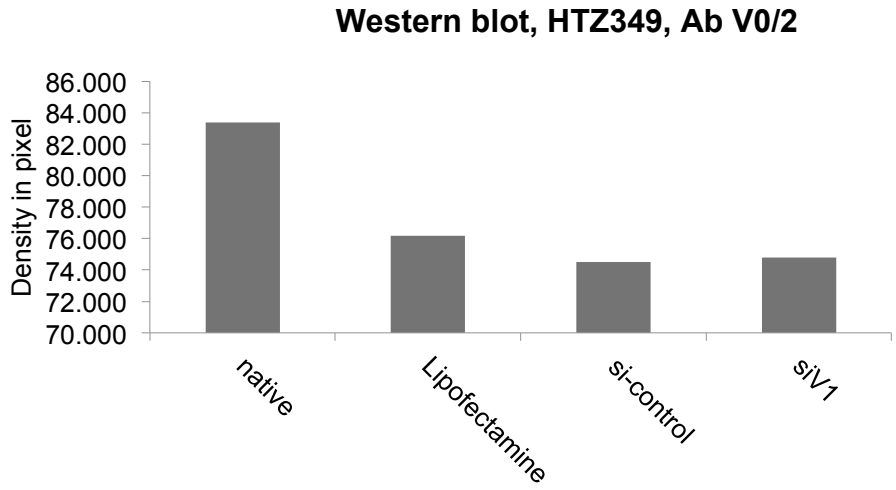

Figure 34: Statistical analysis of western blot results in HTZ417 transfected with siV1. Western blot was performed with antibody V0/2

Further, an analysis of protein expression of V1 and V2 in siV2- and siV3-transfected cells was determined in western blot using antibody V0/1 and V0/2. Figure 35 shows the stable expression of V1 in si-control-transfected cells compared with siV2- and siV3-transfected cells. Findings on the PCR level, which showed a decreased level of cDNA V1 in siV2-transfected cells, could not be confirmed on the protein level. Corresponding to findings in western blot analysis with siV1-transfected cells in

HTZ349 (Figure 33), the expression level of V1 in si-control-transfected cells was decreased compared to native cells (Figure 35).

Analysis of siV2- and siV3-transfected cells with antibody V0/2 showed no visible impairment of V2 and V3 expression on the protein level (Figure 36). These findings confirm observations under the PCR analysis (Figure 29).

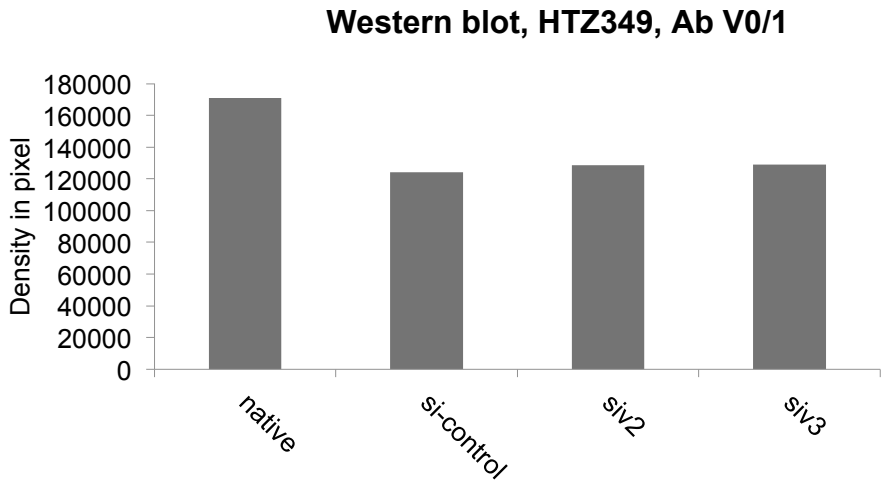

Figure 35: Statistical analysis of western blot results in HTZ349 transfected with siV2 and siV3. Western blot was performed with antibody V0/1

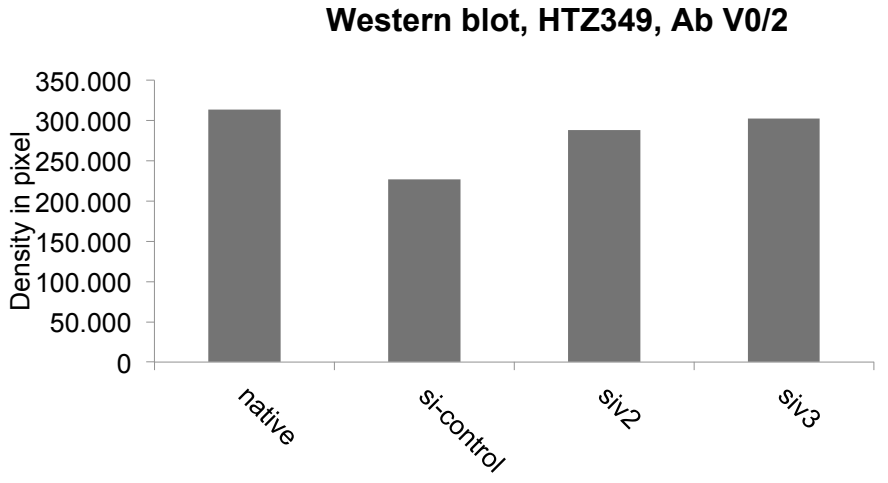

Figure 36: Statistical analysis of western blot results in HTZ349 transfected with siV2 and siV3. Western blot was performed with antibody V0/2

I.12.6 Proliferation assay

I.12.6.1 Proliferation assay for siV1-transfected cells

The cell proliferation assay was performed using native cells, Lipofectamine-incubated cells, control siRNA-transfected cells and siV1-transfected cells. In the experiment, 10,000 cells were seeded per well and counted on days 1, 2, 3, 4, 5, 6 and 7. Cell count on day 1 was halved in all investigated groups (Figure 37, Figure 39). In HTZ349 all cell populations showed a proliferation stop within the first two days of the experiment. On day 3 to 4r, native cells, Lipofectamine-incubated cells and control siRNA-transfected cells started to proliferate nearly in the same manner, whereas the population of si-control-transfected cells seemed a little less active (Figure 37). The proliferation rate of siV1-transfected cells was significantly lower than in si-control-transfected cells on day 5 ($p < 0.001$) and on day 7 ($p = 0.005$) in the experiment. As measured by cell count on days 4 and 7, cell count was increased 7.6-fold in nonsense siRNA-transfected cells and 6.6-fold in siv1-transfected cells. These findings were reconfirmed in an analysis of cell lines HTZ419 and U87. The strongest effect was seen in the cell line U87 on day 3 ($p = 0.002$).

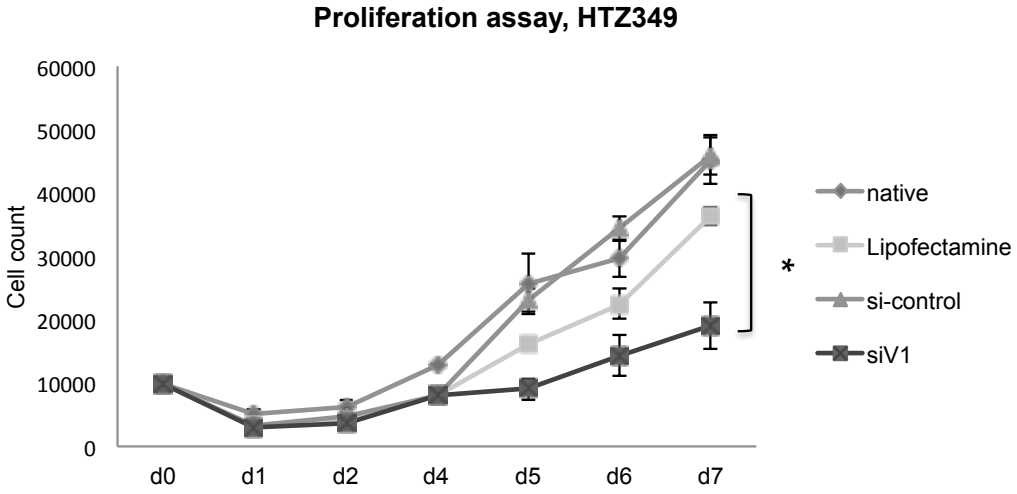

Figure 37: Proliferation assay with HTZ349. Starting point: 24 hours (d0) after transfection. 10,000 cells per group were placed in triplicate in a 12-well plate and harvested and counted on days 1, 2, 4, 5, 6, 7 after transfection. *p = 0.005 (si-control to siV1 on day 7), p < 0.001 (si-control to siV1 on day 5)

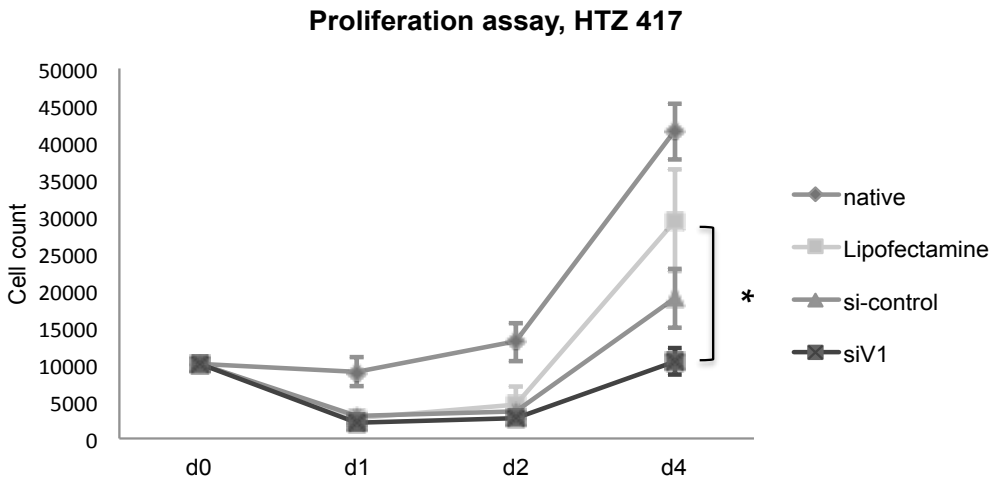

Figure 38: Proliferation assay with HTZ417. Starting point: 24 hours (d0) after transfection. 10,000 cells per group were placed in triplicate in a 12-well plate and harvested and counted on days 1, 2 and 4 after transfection. *p = 0.01 (si-control to siV1 on day 7)

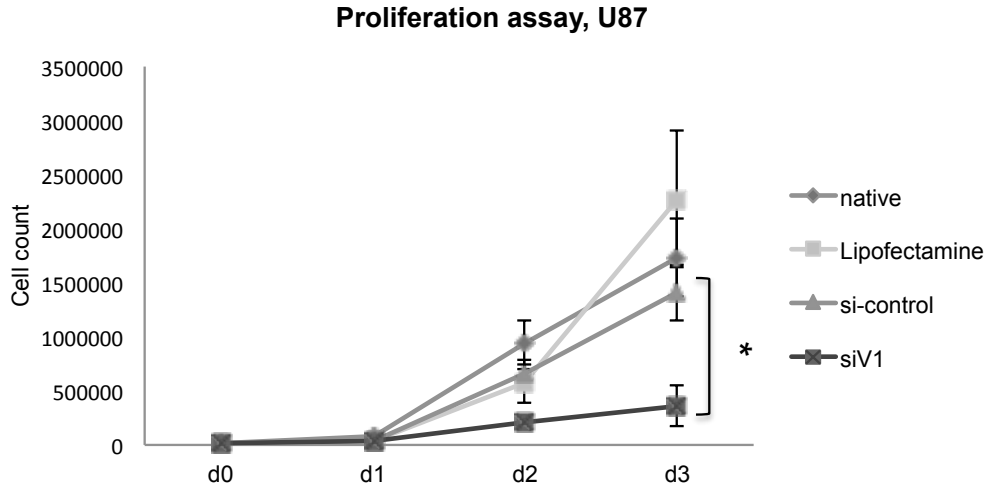

Figure 39: Proliferation assay with U87. Starting point: 24 hours (d0) after transfection. 10,000 cells per group were placed in triplicate in a 12-well plate and harvested and counted on days 1, 2, 3 after transfection. *p = 0.002 (si-control to siV1 on day 7)

The RNA content of harvested cells from these experiments was analyzed in semi-quantitative PCR. The results showed nearly complete suppression of V1 within the first three days. On days 4 to 7 a product of V1 was again visible on the PCR level.

I.12.6.2 Proliferation assay for siV3-transfected cells

Proliferation assays were repeated under the same conditions with cells transfected with siRNA targeting V3. All groups showed the same proliferation ability (Figure 40). After a slight decrease in cell population within the first day, the proliferation rates of all groups including siV3-transfected cells developed normally without significant changes. Cell count increased in all groups about 3.1-fold on day 5. There was no statistically significant change to be seen in the proliferation rate of siV1-transfected cells compared to si-control-transfected cells (p = 0.085).

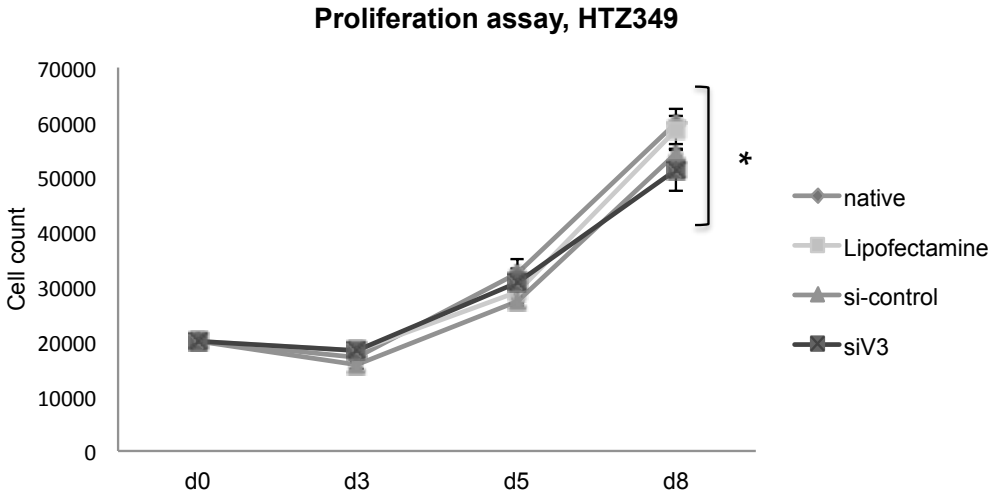

Figure 40: Proliferation assay of HTZ349 in siV3-transfected cells. Cells were harvested and counted on days 3, 5 and 8. *p = 0.085

I.12.7 Attachment assay

In the test run of the attachment assay with all cell lines it was observed that HTZ349, HTZ417, U87 and A172 showed different attachment behaviour in cell culture. Thus, the time to attachment to the culture dish after seeding was determined for each cell line prior to starting with experiments. A172 cells began to attach to the culture plate 15 minutes after seeding. HTZ349 and HTZ417 attached within the first 30 minutes and U87 attached after 20 minutes. The experiments were performed as described in the above. Experiments were run with native cells, Lipofectamine-treated cells, control siRNA-transfected cells and siRNA- transfected cells.

I.12.7.1 Attachment assay for siV1-transfected cell

In the attachment assay with HTZ349, no significant changes were seen in the attachment behaviour of siV1- and si-control-transfected cells compared to the other cell populations. Even the extended observation period up to 60 minutes showed the same results (Figure 41, Figure 42). These findings were confirmed in the attachment assay with cell lines HTZ419 and A172 (Figure 43 – Figure 46).

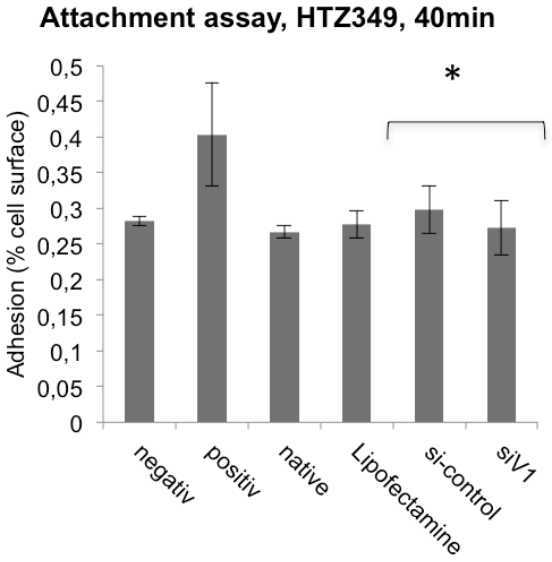

Figure 41: Attachment assay with HTZ349 and siV1-transfected cells. Experiments were run with 5,000 cells per well five-fold for each group. Analysis was performed 40 minutes after seeding. *p = 0.36

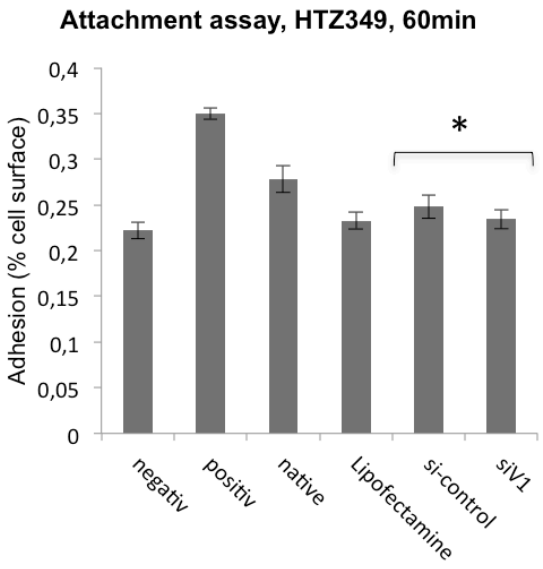

Figure 42: Attachment assay with HTZ349 and siV1-transfected cells. Experiments were run with 5,000 cells per well five-fold for each group. Analysis was performed 60 minutes after seeding. *p= 0.45

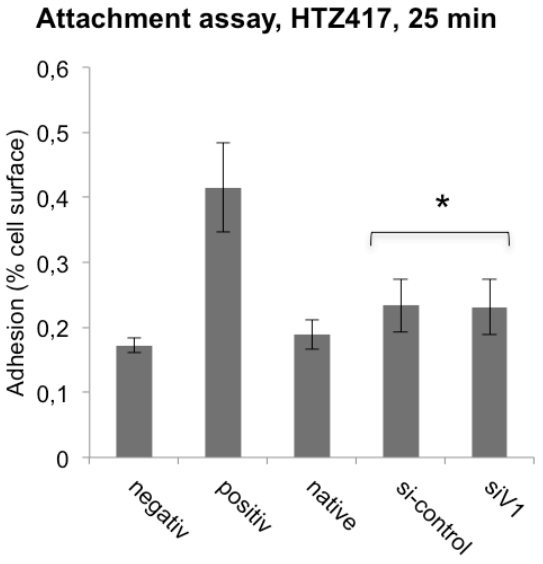

Figure 43: Attachment assay with HTZ419 and siV1-transfected cells. Experiments were run with 5,000 cells per well five-fold for each group. Analysis is performed 25 minutes after seeding. *p = 0.48

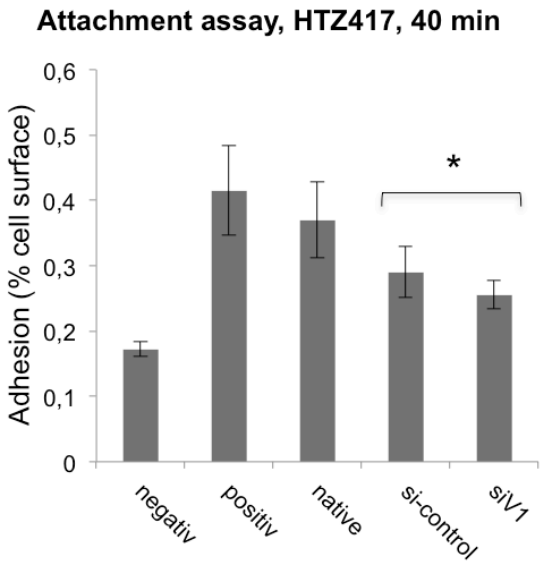

Figure 44: Attachment assay with HTZ419 and siV1-transfected cells. Experiments were run with 5,000 cells per well five-fold for each group. Analysis was performed 40 minutes after seeding. *p = 0.24

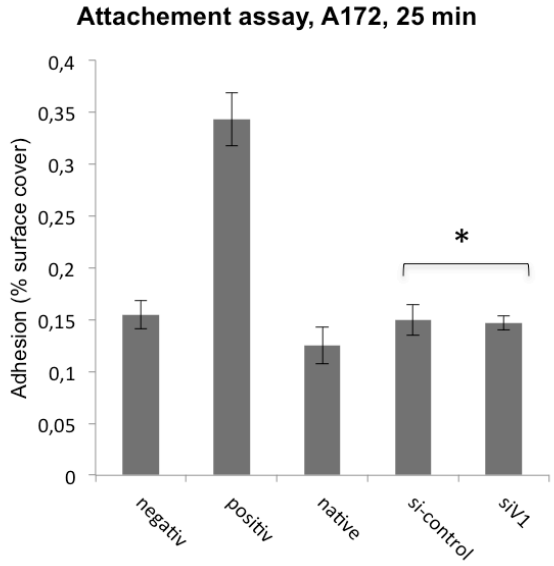

Figure 45: Attachment assay with A172 and siV1-transfected cells. Experiments were run with 5,000 cells per well five-fold for each group. Analysis was performed 25 minutes after seeding. *p = 0.45

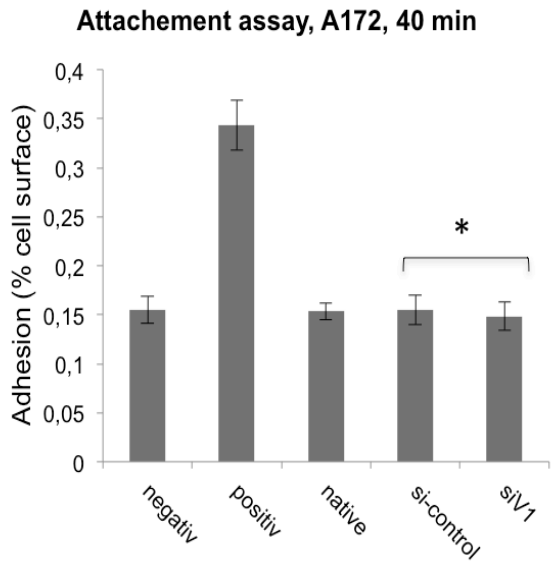

Figure 46: Attachment assay with A172 and siV1-transfected cells. Experiments were run with 5,000 cells per well five-fold for each group. Analysis was performed 40 minutes after seeding. *p = 0.44

I.12.7.2 Attachment assay for siv3-transfected cells

The attachment assay was performed with siV3-transfected cells in the same settings as described in the above (Figure 47, Figure 48). At 20 minutes no difference in the attachment behaviour was observed. At 40 minutes, native and Lipofectamine-treated cells showed an increase in cell number, whereas the number of si-control- and siV3-transfected cells remained the same. A statistically significant value could not be proven between si-control- and siV3-transfected cells.

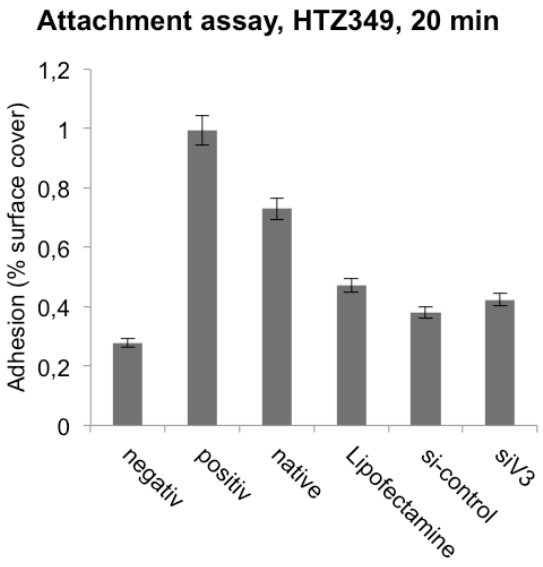

Figure 47: Attachment assay with HTZ349 and siV3-transfected cells. Experiments were run with 5,000 cells per well five-fold for each group. Analysis was performed 20 minutes after seeding. *p = 0.25

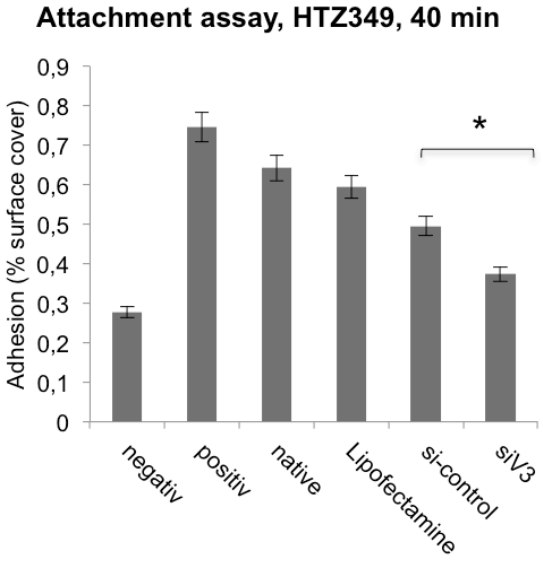

Figure 48: Attachment assay with HTZ349 and siV3-transfected cells. Experiments were run with 5,000 cells per well five-fold for each group. Analysis was performed 40 minutes after seeding. *p = 0.14

I.12.8 Migration assays

I.12.8.1 Scratch assay

The scratch assay was used as a two-dimensional migration assay, which is compatible with microscopy including live cell imaging.[101] Comparing the tracks of differently treated cells under the same experimental conditions allows the role of V1 in the regulation of directional cell migration to be determined. Figure 49 (left) shows nearly 100% confluent growing native cells, si-control transfected and siV1-transfected cells with a freshly made scratch.

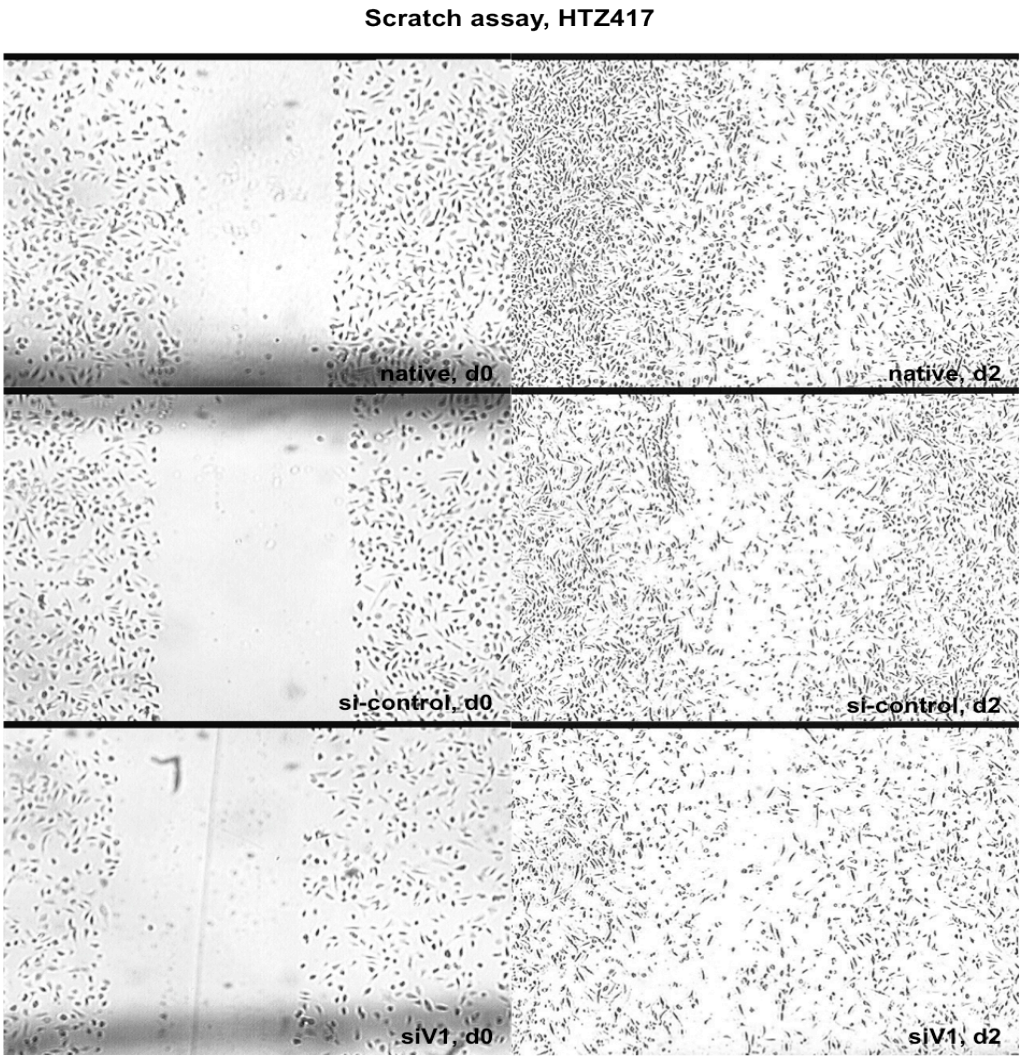

Figure 49: Scratch assay with HTZ419. The images were taken using a bright field microscope directly after placing the scratch (d0) and on day 2 (d2). Left: native cells, si-control-transfected cells and siV1-transfected cells immediately after placing the scratch on day 0. Right: migrated cells on day 2

The optimal experimental set-up for the scratch assay was determined observing different time points after seeding (12h, 24h, 36h and 48h). After two days, the cell population assembled with cells of the opposite side of the scratch. Statistical evaluation of migrated cells in the group of native cells, si-control-transfected cells and siV1-transfected cells showed impaired migratory activity in all treated cell populations. Additionally, siV1-transfected cells showed a further decrease in their migration rate, which is statistically highly significant ($p < 0.001$) in comparison to the si-control-transfected cells in cell lines HTZ349 and HTZ419 (Figure 50, Figure 51). In U87, a decreased migration rate was seen in siV1-transfected cells and si-control-transfected cells with a p value of 0.014 (Figure 52).

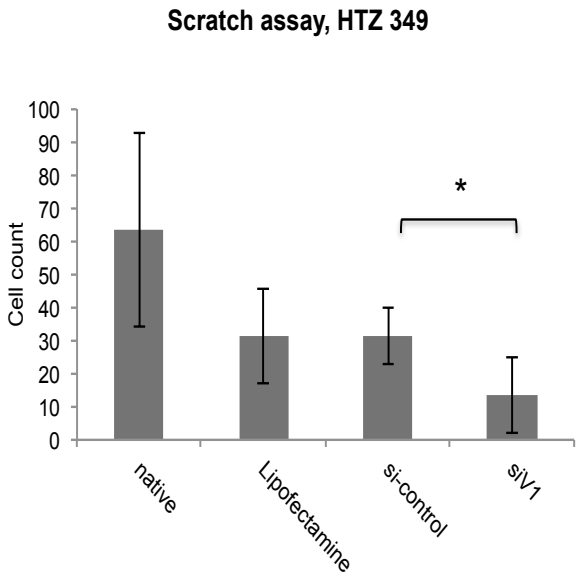

Figure 50: Statistical analysis of migrated cells in scratch assay with siV1-transfected HTZ349 cells. *p < 0.001

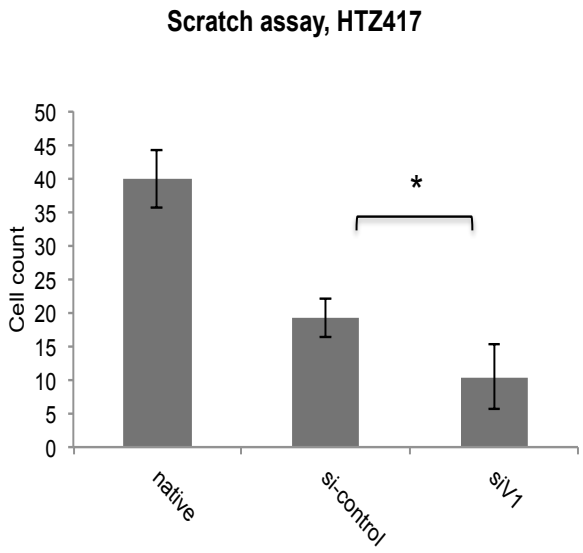

Figure 51: Statistical analysis of migrated cells in scratch assay with siV1-transfected HTZ417 cells. *p < 0.001

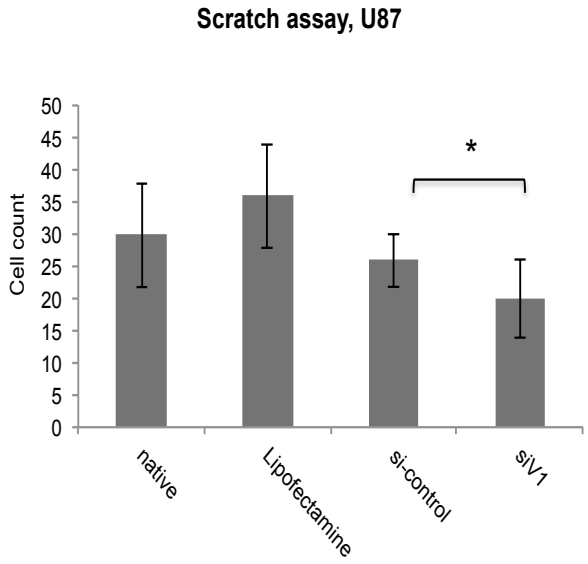

Figure 52: Statistical analysis of migrated cells in scratch assay with siV1-transfected U87 cells. *p = 0.014

The analysis of siV3-transfected cells in HTZ349 showed no changes in the migration behaviour of transfected cell populations compared to untreated cells (Figure 53).

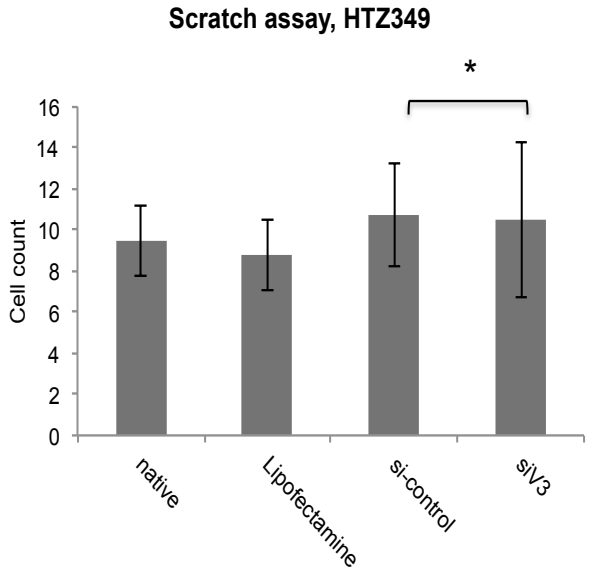

Figure 53: Statistical analysis of migrated cells in scratch assay with siV3-transfected HTZ349 cells. *p < 0.43

I.12.8.2 Boyden chamber assay

The Boyden chamber assay was performed for the three-dimensional analysis of the migratory ability in glioma cells. This allowed an analysis of cell migration separately from cell–cell interaction and proliferation.[102] As already demonstrated in the scratch assays described in the above, the results of the Boyden chamber assay confirmed the decrease in the migratory ability of siV1-transfected cells (Figure 55). Figure 54 shows the porous membrane at the end of the experiment. SiV1-transfected cells showed, in comparison to nonsense siRNA-transfected cells, a significant limitation in their migration ability (p = 0.001) in HTZ349 and in HTZ417 (Figure 56).

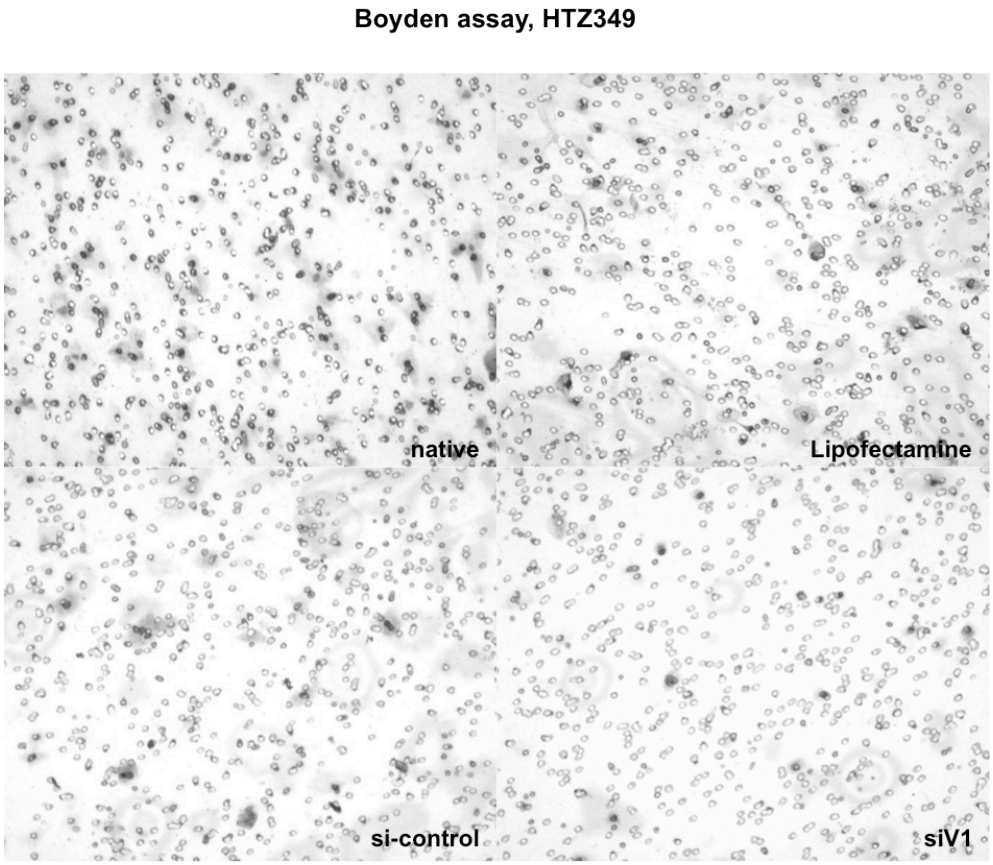

Figure 54: Boyden assay with HTZ349. Migration time: 4 hours. The experiment was run with native cells, si-control-transfected cells and siV1-transfected cells

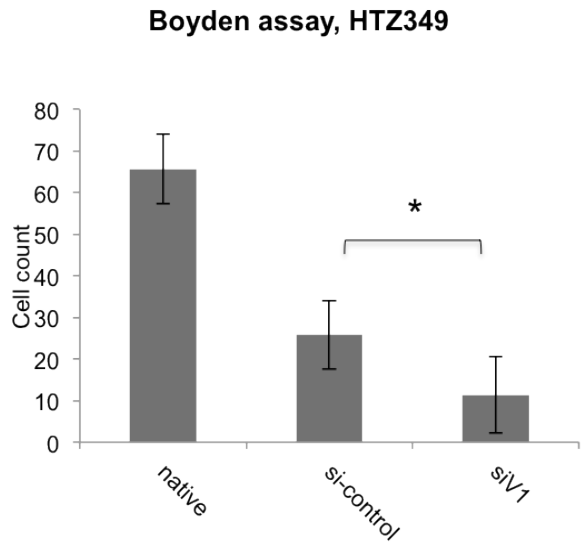

Figure 55: Statistical analysis of migrated cells in Boyden assay with siV1-transfected HTZ349 cells. *p = 0.001

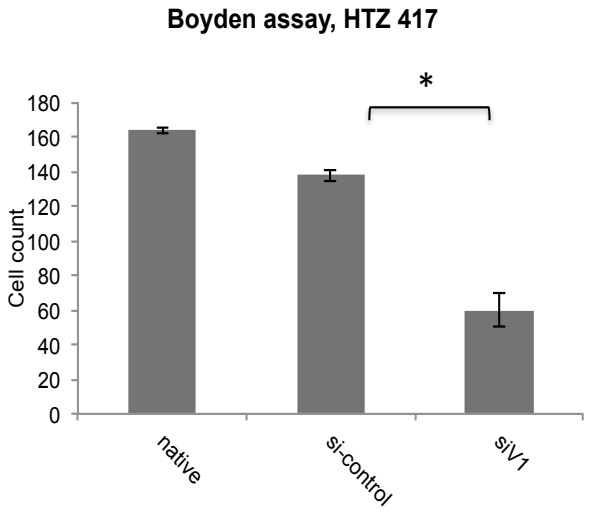

Figure 56: Statistical analysis of migrated cells in Boyden assay with siV1-transfected HTZ417 cells. Migration time: 4 hours. *p = 0.001

In the Boyden assay with siV3-transfected cells (Figure 57, Figure 58), siV3-transfected cells showed a mild increase in migrated cells compared with native cells, though this was without statistical significance. Also, the decrease in migrated cells in control siRNA-transfected cells showed no statistically significant results (p = 0.27). When the experiment was repeated again, the results remained with no significant change in migration ability compared with native cells.

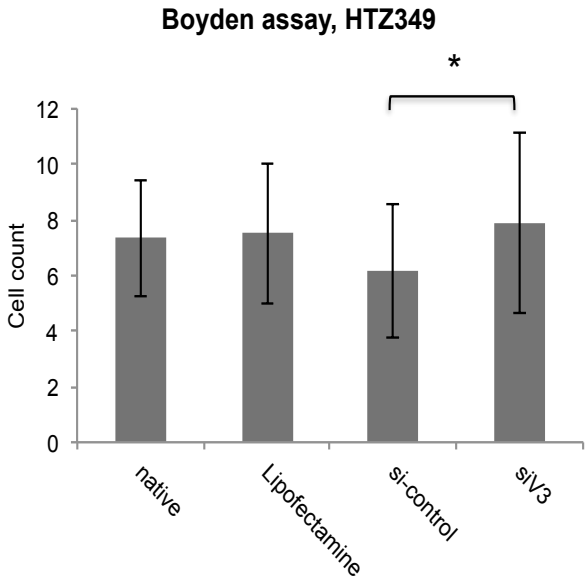

Figure 57: Statistical analysis of migrated cells in Boyden assay with siV3-transfected HTZ349 cells. Migration time: 4 hours. *p = 0.27

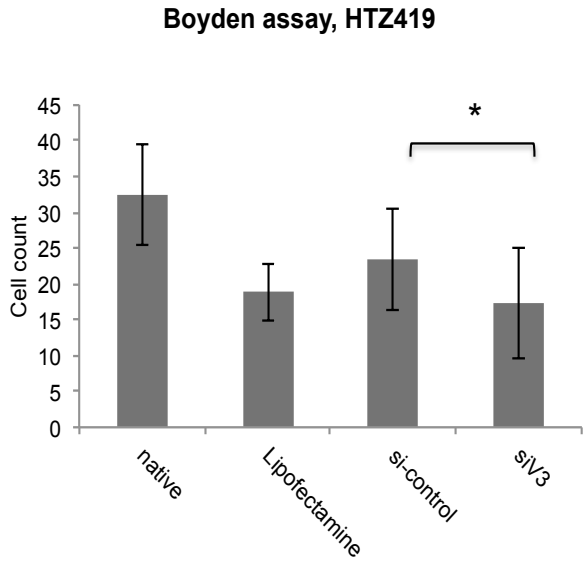

Figure 58: Statistical analysis of migrated cells in Boyden assay with siV3-transfected HTZ417 cells. Migration time: 4 hours.

Discussion

This thesis was able to show that siV1, but not siV3, significantly decreases the migration of glioma cells lines. This inhibition of migration is not attributable to the increased attachment of cells, one of the steps in tumour cell invasion. In addition, siV1 decreased proliferation in glioma cell lines. I therefore postulate that the versican isoform V1, but not V2 or V3, is an essential modulator of glioma cell migration and proliferation.

Extracellular matrix plays an important role in the aggressiveness of cancers, as it induces changes in cellular attachment, motility, invasion and proliferation. It is a well-known fact that versican has an increased expression level in cancer. Based on this and taking account of the results mentioned in the introduction, I planned to address the function of versican isoforms in malignant glioma cell lines.[103]

The isoforms of versican are found in various tissues and tumour cells. Previous publications and results from our laboratory already suggested that the isoforms of versican show different expression patterns, which might translate into different functions of the isoforms.[104] It has been reported that isoforms V0 and V1 are predominant forms in malignant glioma cells,[105] a finding that was reconfirmed in this work. The isoforms V0, V1, V2 and V3 were detected in all investigated cell lines (HTZ345, HTZ417, U87, A172) on the RNA level.

The proof of isoform V1 was easy, as it is described as the predominant isoform in glioma cell lines. The proof of V2 on PCR level did not succeed very well. It has ben reported that V2 is a major constituent of adult brain ECMs and has a characteristic expression pattern in myelinated fibre tracts of the CNS,[106,107] whereas the expression in glioma cells lines appears to be very low level.[108] The results of semi-quantitative PCR in this work confirmed the varying expression pattern of V2 in all cell lines used.

Only little information is available on the function of versican isoform V3 in glioma cell lines. Previously, isoform V3 was detected in activated endothelium, in arterial smooth muscle cells and melanoma cancer cells.[109] In view of the fact that V3 might play a dual role as an inhibitor of tumour growth and a stimulator of metastasis in melanoma cancer cells, it would be interesting to establish which role V3 might play in glioma cell lines.[110] Isoform V3 was detected on the semi-quantitative and quantitative PCR level in all investigated glioma cell lines, mandating an examination of its function.

Providing evidence of V1 on the protein level is a challenging task. V1 did not appear on the estimated protein lengths of 70kDa in western blots under current protein isolation techniques (Figure 14, Figure 15). Instead, I found various bands on the blot and it was not possible to clearly attribute the correct product. In literature different variants of harvesting methods and sample preparation before the run are described, i.e. some authors said that the digestion of a protein sample with Chondroitinase ABC would remove chondroitin side chains of V1 and might improve antibody binding. Despite implementing this method knowing that alternative splicing in the extracellular space generates the isoforms of versican, results still remained unsatisfactory. New harvesting methods were tested consecutively in order to increase the yield of pure protein. However, even protein augmentation via immunoprecipitation remained ineffective. Imagining a dissociation of versican isoforms from the cell to the surrounding culture medium led to the idea of that protein could be isolated from the culture medium. As it was impossible to isolate protein V1 and V2 out of FCS-containing medium, it is suggested that FCS covers binding sites of versican and consequently disables antibody binding. Further, the protein might stay attached to the bottom of the culture flask. Constant results in western blot were gained when the protein was scraped off the bottom of the culture flask and separated from the cell debris.

Both harvesting methods were tested in western blot using the antibody for V2. Analysis of samples consisting of cell lysate and samples, which were harvested using the method described for V1 isolation, also worked. The different expression patterns and difficulties inherent in the protein isolation of V1 and V2 raised questions concerning the exact localization of these proteins. To clarify the predominant position of V1 and V2 in the context with the cell surface or cytoplasm, immunostaining was performed with the same antibodies that were used in western blotting experiments. Methanol fixation detected the relevant proteins on the nuclear side and in the cytoplasm.

Under PFA fixation it became clear that the negative control consisting of cells incubated with fluorescent antibody only showed some fluorescent signal under the microscope. As in PFA fixation, cell walls remained intact, and unspecific binding of the fluorescent antibody on the cell surface of the negative control was proposed. Cells incubated with antibody Neo V1/0 and V2/0 showed a stronger signal across their whole surface and on the connection site with neighbouring cells. In contrast, in

the experiment with methanol fixation, there was a clear, vesicle-like formation visible in the cytoplasm of cells incubated with antibody Neo V1/0 (Figure 18). In contrast, in cells incubated with the antibody Neo V2/0, the nucleus showed a strong fluorescent signal, whereas no vesicles could be detected in the cytoplasm. This observation suggests that V1 is mainly located outside of the cell. The successful detection of V1 in western blot via V1-isolation out of the culture medium and the extraction of protein throughout scraping off of the cell layer confirmed its predominant role as a linking protein on the outside of the cells. The assumption of a pericellular sheath formed by cancer cells consisting of CD44 and hyaluronic acid/versican aggregates could possibly be confirmed as a result.[111] The localization of V1 on the cell surface und connection site enhances its function in cell–cell interaction as ECM protein involved in migration and adhesive processes in glioma cells.

In light of the different expression patterns of V2 on the PCR level, the question of the exact localization of versican isoform V2 in or around the cell gains in importance. V3 cannot be detected on the protein level, as no suitable antibody is available at this time.

The procession of versican isoforms by ADAMTS (A disintegrin and metalloprotease domain with thrompospondin motifs) proteases and other matrix-degrading metallo-enzymes have been discussed as an explanation for difficulties in the protein isolation in western blot and protein detection in immunostaining.[112] It has been shown that versican V0, V1 and V2 are cleaved by different proteases *in vitro*.[113] Further previous results suggest that versican V2 is present as multiple C-terminally truncated forms in normal brain tissue, with the full-length isoform apparently representing a quantitatively minor proportion of the total.[114] Since ADAMTS4 cleaves the Glu405–Gln406 bond of brain versican V2, it is possible that this enzyme, as well as ADAMTS 1, 5 or 9, may play an important role in the processing of this molecule.[115] We propose that processing versican isoforms leads to the failure of antibody binding.

SiRNA transfection was able to silence versican isoforms, which I was able to prove at the PCR and protein level. In sum, the transfection efficiency of glioma cell lines is pretty high and varies between 70% and 80%. Control groups in all experiments consisted of cells incubated with Lipofectamine only, cells transfected with a control-siRNA, native cells and untreated cells. These control groups were needed to establish whether changes in cell behaviour, especially in functional assays, are side

effects of the transfection procedure or can be regarded as specific effects of the siRNA.

The product V1 shows a clear down-regulation on the PCR level. Within the first three days after transfection, near-complete suppression occurred (Figure 23, figure 24). The down-regulation of V1 was seen at least until days 4-5 after transfection. Following that, the expression of V1 returned to its initial value as measured by the signal intensity of the PCR product in gel electrophoresis. As regards similarities between the structure and components of versican isoforms, undesired down-regulation of different isoforms by specific siRNA was suspected. Therefore, during initial testing of my siRNAs, PCRs were performed on all samples and primers targeting V2 and V3. I was able to show that the products showed no relevant off-target effects when it comes to the expression of isoforms V2 and V3 in siV1-transfected cells.

As already reported, the expression of versican isoform V2 on the PCR level appears to be very inconsistent. Regarding the more or less reliable results of V2 in western blotting, I tried to establish functional siRNA targeting V2. The results showed that the down-regulation of V2 failed and resulted in the regulation of V1 and V3. This is probably due to the fact that there is only little scope for creation of a specific siRNA targeting V2 regarding the homologies in the genome between V1, V2 and V3. Preserving the specific of a siRNA targeting V2 goes to the expense of their functionality, because not all criteria can be considered for a proper siRNA design.

The transfection with siRNA targeting V3 showed a complete down-regulation of V3 expression on the PCR level. As there is no antibody that detects V3, siRNA functionality was only proven on the PCR level, whereas possible off-target effects on the expression of V1 and V2 were additionally ruled out on the protein level. As regards the results of semi-quantitative PCR, V1 regulation was observed in siV3-transfected cells. Suggesting that V3 might play an opposite role in glioma cells than V1, I decided to run functional experiments to see whether the leakage of V1 and V3 outweighs the functional ability of the cells compared to single down-regulation of V1.

After successful transfection and down-regulation of versican isoforms V1 and V3, functional assays with siRNA-transfected cells were started. The selection of possible functional assays is dependent on the time limit, which is determined by the short-term effect of siRNA transfection in the cell. As I was able to show that the regulatory effect lasts at least four days, there was sufficient time for migratory assays like the

Boyden chamber assay and the scratch assay. Account must be taken of the fact that, so far, we do not have a full understanding of which side effects occur on account of the simple presence of siRNA inside the cell. For example, siRNA mediates the expression of double-strand protein kinases (PKR), which results in the up-regulation of interferon-expressing genes.[116] Changes in the migratory, proliferative and adhesive ability of transfected cells might also result from molecular changes mediated by the presence of a siRNA inside the cell. Therefore, the control groups in my experiments consisted of Lipofectamine-treated cells, control siRNA-transfected cells und untreated cells.

Cell proliferation assays were performed as described in the above to distinguish migratory effects from proliferative effects, as migration might be mimicked by severe proliferation. As I knew that the down-regulation of V1 lasts up to four days after transfection, proliferation assays were performed for up to six days to see whether cell motility is affected longer than the siRNA effect is seen on the PCR level. The experiments showed a decline in the cell number one day after seeding for all investigated groups, which was interpreted as being related to the previous harvesting, cell counting and transfection procedure. As shown in the above, the proliferation rate of siV1-transfected cells showed a proliferation stop within the first three days after transfection. In PCR, which was performed simultaneously with the samples of the run, regulatory effects of siRNA expired within these three days. On day 4, siV1-transfected cells started to proliferate less than the control groups. In the experiments, V3-transfected cells did not show any changes in their proliferation behaviour compared with the control groups.

It has been reported that versican is highly expressed in developing tissue where cells are metabolically active and proliferating.[117] It has also been shown that versican expression is elevated in brain tumour tissue compared to the surrounding normal tissue. Older papers have described that the increased proliferation rate in tumour cells depends on the G3 domain of versican.[118] It has been shown that the proliferation rate of U87 cells could be enhanced by adding a G3-domain-containing medium to the cell culture.[119] In another work, the G1-domain of versican appeared to be relevant for increased proliferation rates in fibroblasts.[120] Further, tumour growth, proliferation and angiogenesis can be enhanced by over-expression of the G3-domain in astrocytoma cancer cells.[121] As the G1- and G3-domain are part of each splice variant of versican, I intended to investigate whether the different

isoforms V1, V2 and V3 containing G3-domains have a similar or a distinct influence on proliferation rates in glioma cell lines.

My results suggest that V1 seems very important in the modulation of proliferation of malignant glioma cells. It is still not fully understood which components interact with versican isoform V1 in glioma cell lines and enhance the proliferation rate. Transferring data from other work on different cell populations, growth factor interaction might play a key role. It was shown that components like EGF-like motifs in the G3-domain of versican activate EGF-receptors.[122] This mechanism was interpreted as an indicator of increased proliferation rate in endothelial cells.[123] I hypothesize that the impaired proliferation rate under V1 down-regulation might result from the loss of complexes between G3-domains of V1 and other cellular and extracellular components, like growth factor receptors. In sum, my results reconfirmed these observations, which were already made in NIH-3T3 and astrocytoma cells *in vivo.*[124,125] My results showed that V1 is essential for proliferation in high-grade glioma cell lines *in vitro*.

No data are yet available on the influence of V3 on the proliferation rate in glioma cell lines. Diverse effects of V3 in different cell populations have been described in the literature. V3 reduces cell growth *in vivo* and *in vitro* and promotes metastasis in melanoma cancer cells.[126] Given that siV3 transfection leads to co-regulation of V1 and V3, I expected a stable and an increasing proliferation rate, respectively. My experiments showed that under siV3 transfection, the proliferation rate remained stable. Consequently, Iwe suggested that V3 negates the adverse effect of V1, meaning V3 tends to lower the proliferation rate in glioma cell lines.

Diffuse invasion of glioma cells is a limiting factor in brain tumour survival. Detachment and migration has been described as a very complex combination of processes, including modulation of the ECM, proteinase activity and interaction between cell surface and extracellular matrix.[127] Changes in the synthesis, degradation and modification of matrix adhesion molecules, as well as those of their receptors have been shown to be involved in various aspects of malignant cancer cell behaviour.[128] Cell migration is mediated by the complex interplay of detachment, adhesion and motility that involves a number of different proteases and other enzymes. Because of the close connection of cellular processes in cell adhesion and migration, I will discuss my results of attachment and migration assays together.

Before starting the attachment experiments with transfected cells, the optimal time point for adhesion after seeding was determined for each cell line used. The experiments were performed as described in the above. Interestingly, no significant changes in the adhesive behaviour of siV1- and siV3-transfected cells were observed compared to the control groups in all the cell lines investigated. The adhesive potential was further checked at different times in each cell line. Here, the adhesive ability of si-control, siV1- and siV3-transfected cells was slightly increased at early time points compared to native cells in the cell lines A172 and HTZ419 (Figure 43, Figure 45). As this phenomenon was observed in si-control transfected as well as in cells transfected with a target-siRNA, it could be interpreted as an effect of the transfection procedure. However, no statistical significance is available to confirm that impression.

The G1-domain of versican is able to reduce cell adhesion in glioma cells[129]. Some publications have shown that in glioma cells, the G3-fragment of versican contains EGF-like motifs and ß1-integrin. All of these components are able to bind to U87 and enhance cell attachment.[130] On the other hand, in osteosarcoma cells, it has been shown that versican acts as an anti-adhesive molecule.[131] These findings contradict observations from melanoma cells, where V3 increases cell adhesion on hyaluronic acid.[132] In view of the results of this work, it can be said that selective down-regulation of V1 and V3 in different glioma cell lines does not affect the adhesive behaviour in these cells in a statistically significant manner. The adhesive potential of glioma cells seems to be related to the G3-domain of the versican isoforms, which could not be proven in our experiments. As V1 and V3 contain both a G1- and a G3-domain, it can be suggested that within intracellular modification (i.e. phosphorylation), these domains exist in active and non-active forms.

Migratory ability is also facilitated by the fact that versican-rich ECMs exert an anti-adhesive effect on tumour cells[133]. Versican shows anti-adhesive effects in tumour cells, which enables cells to migrate and proliferate. Besides EGFR, tenascin, CD44, integrins and hyaluronan, TGF-ß2 was identified as an interaction partner of versican isoform V1 during migration. Our group has already shown that TGF-ß2 induces migration of glioma cells.[134] After adding TGF-ß2, versican isoforms V0 and V1 were unregulated, resulting in significantly higher migration rates compared to the untreated controls.[135] The scratch assay was used for two-dimensional analyses of directional migration. The Boyden chamber assay was additionally performed to

gather more information on the migration behaviour of transfected glioma cells in a three-dimensional setting.

The transfection procedure itself diminishes the migration rate in all investigated cell lines compared to the untreated, native cell population. The results of siV1-transfected cells were therefore compared to the results of the si-control transfected cell population. SiV1-transfected cells showed significantly lower migration rates than control groups in all investigated cell lines in the scratch assay. Certainly, account needs to be taken of the fact that the results in the two-dimensional migratory scratch assay were influenced by different factors, i.e. the cell-cell interaction and cell proliferation. During the 36 hours the experiment ran, cells passed through a complete cell cycle, so the gap in the scratch assay was likely to be closed by proliferating cells. My results showed that cell proliferation was diminished in siV1-transfected cells in a statistically significant manner compared to the control groups.

Thus, migration ability needs to be investigated separately from the influence of proliferation and cell–cell interaction. The Boyden chamber assay was established for this purpose, and clearly confirmed the results of the scratch assays. SiV1-transfected cells migrated significantly less than cells in the control groups. Based on my results, I suggest that versican isoform V1 is a very important component in the migratory process of malignant glioma cells.

Investigating the role of V3 in migration assays, my results showed that siV3-transfected cells did slightly increase in their migration ability, but statistical analysis did not prove the results to be statistically significant. Still considering that siV3 transfection also has a down-regulatory effect on V1 expression, the inhibiting effect of siV1 on migration ability in glioma cell lines can be interpreted as being counteracted by an adverse effect of siV3. An additional effect of versican isoform V1 and V3 in migratory processes can definitively be ruled out.

In summary, my results demonstrate the predominant role of versican isoform V1 in regard to the migration and proliferation ability of malignant glioma cell lines. The importance of versican isoforms V1 and V3 was illuminated in different functional assays. As the effect of siRNA lasted at least three to four days, time appeared to be a limiting factor in my experiments. The internal control of counter-regulation mechanisms during transfection is currently done using primers and antibodies targeting V1, V2 and V3, respectively.

For further long-term experiments, a short hairpin vector system was established for stable transfection in glioma cells. This tool offers many opportunities, for example the investigation of cells in a long-lasting functional experiment and transfer of the vector systems *in vivo*. I was able to show a clear down-regulation of versican isoform V1 in the cells that were transfected with a short hairpin vector targeting V1. Results were confirmed on the RNA level and in western blots.

Future *in vivo* experiments may help to detect physiological changes in a living organism throughout transfection, which is not accessible in *in vitro* experiments. In the nude mice model, inoculation of shV1-transfected glioma cells would offer the opportunity to analyse cell invasion via live-cell imaging. It will be interesting to see whether *in vitro* assays are reproducible *in vivo.* Moreover, toxicity in living animals needs to be examined.

Some further questions could be addressed by means of *in vivo* experiments. On the one hand, it will be necessary to elucidate whether cells develop counter-regulation mechanisms to cover the function of down-regulated molecules. Further, it will be interesting to elucidate which signalling pathways are involved, which could shed light on other possibly important molecules. Further, it will be of great interest to see whether versican isoform V1 has interfaces with known important molecules (e.g. p53, PTEN, EGFR, CDKN2A/2B and NF1[136]) and pathways and whether its role in regard to tumour migration and proliferation is reconfirmed *in vivo*.

The stem cell model in tumour genesis has recently been gaining in importance. The underlying cancer stem cell hypothesis postulates that malignancies are maintained by a rare subpopulation of stem cell-like cells deriving from the cell of origin of a given tumour.[137] As the origin and characteristics of these cells are still not fully understood, the more precise scientific term, namely cancer-initiating precursors, is used.[138] Besides findings of cancer stem cells in haematopoietic cancer, recently cells with stem cell-like qualities have been found in brain tumours, for example in high-grade glioma, ependymoma and medulloblastoma.

Inherent differences in the sensitivity of clonogenic cells are hypothesized as an explanation for clinical drug failure, tumour heterogeneity and age-response relationships.[139] The capacity to culture brain tumour stem cells *in vitro* could give us the opportunity to devise new and more specific therapeutic approaches to targeting incurable brain tumours.

Knowing about the role of versican in the fate of embryonic stem cells and its role in glioma cell lines *in vitro*, it would be interesting to investigate the role of versican and its isoforms in glioma stem cells as a possible target for tumour therapy.

List of figures and tables

List of literature

[1] Louis DN (2007) WHO classification of tumours of the central nervous system. *International Agency for Research on Cancer*, 4:1-309

[2] Des Rosiers PM, Timmerman RD (2003) Primary brain tumors. *Handbook of advanced cancer care,* 289

[3] Kleihues P, Soylemezoglu F, Schäuble B, Scheithauer BW, Burger PC (1995) Histopathology, classification, and grading of gliomas. *Glia,* 15: 211-221

[4] Kleihues P, Ohgaki H (1999) Primary and secondary glioblastomas: From concept to clinical diagnosis. *Neuro-Oncology,* 1: 44-51

[5] Supp R, Weber DC (2005) The role of radio- and chemotherapy in glioblastoma. *Oncology*, 28(6-7): 315-317

[3] Benjamin R, Capparella J, Brown A (2003) Classification of glioblastoma multiforme in adults by molecular genetics. *Cancer Journal,* 9: 82-90

[7] Lefranc F, Brotchi J, Kiss R (2005) Possible future issues in the treatment of glioblastomas: Special emphasis on cell migration and the resistance of migrating glioblastoma cells to apoptosis. *Journal of clinical oncology,* 23: 2411-2417

[8] Lefranc F, Brotchi J, Kiss R (2005) Possible Future Issues in the Treatment of Glioblastomas: Special Emphasis on Cell Migration and the Resistance of Migrating Glioblastoma Cells to Apoptosis. *Journal of Clinical Oncology*, 23(10): 2411-2422

[9] Hill C, Hunter SB, Brat DJ (2003) Genetic markers in glioblastoma: Prognostic significance and future therapeutic implications. *Adv Anat Pathol,* 10: 212-217

[10] Fuller GN, Hess KR, Rhee CH, et al. (2002) Molecular classification of human diffuse gliomas by multidimensional scaling analysis of gene expression profiles

parallels morphology based classification, correlates with survival, and reveals clinically-relevant novel glioma subsets. *Brain Pathology,* 12: 108-116

[11] Gabriely G et al. (2008) MicroRNA 21 promotes glioma invasion by targeting MMP regulators. *Molecular and Cellular Biology,* 9: 5369-5380

[12] Rao JS (2003) Molecular mechanism of glioma invasiveness: the role of proteases. *Nature Review,* 3: 489-501

[13] Bellail AC, Hunter SB, Bart DJ, Tan C, Van Meir EG (2004) Microregional extracellular matrix heterogeneity in brain modulates glioma cell invasion. *The International Journal of Biochemistry and Cell Biology,* 36: 1046-1069

[14] Rao JS (2003) Molecular mechanism of glioma invasiveness: the role of proteases. *Nature Review,* 3: 489-501

Gabriely G, Wurdinger T, Kesari S et al. (2008) MicroRNA 21 promotes glioma invasion by targeting matrix metalloproteinase regulators. *Molecular and cellular Biology,* 28(17): 5369-5380

[15] Louis DN (2006) Molecular pathology of malignant gliomas. *Annual Review Pathology,* 1: 97-117

[16] Ulrich TA, de Juan Pardo EM, Kumar S (2009) The mechanical rigidity of the extracellular matrix regulates the structure, motility, and proliferation of glioma cells. *Cancer Research,* 69(10): 4167-4174

[17] Burger PC, Heinz ER, Shibata T, Kleihues P (1988) Topographic anatomy and CT correlations in the untreated glioblastoma multiforme. *Journal of Neurosurgery,* 68: 698–704

[18] Ingber SN, Folkman SN (1989) How does extracellular matrix control capillary morphogenesis? *Cell,* 58(5): 803-805

[19] Powell SK and Rivas RJ (1998) The generation of polarity in neuronal cells. *Advances in molecular and cell biology,* 26: 157-180

[20] Aruga J, Yokota N, Mikoshiba K (2003) Human SLITRK family genes: genomic organization and expression profiling in normal brain and brain tumor tissue. *Gene*, 315: 87-94

[21] Burgoyne RD, Cambray-Deakin MD (1998) The cellular neurobiology of neuronal development: The cerebellar granule cell. *Brain Research,* 472(1): 77-101

[22] Ricciardelli C et al. (2009) The biological role and regulation of versican levels in cancer. *Cancer Metastasis Review,* 28: 233-245

[23] Rutka JT, Apodaca G, Stern R, Rosenblum M (1988) The extracellular matrix of the central and peripheral nervous systems: structure and function. *Journal of Neurosurgery,* 69: 155–170

[24] Fryer HJ, Kelly GM, Molinaro L, Hockfield S (1992) The high molecular weight Cat-301 chondroitin sulphate proteoglycan from brain is related to the large aggregating proteoglycan from cartilage, aggrecan. *Journal of Biol. Chem,* 267: 9874–9883

[25] Aquino DA, Margolis RU, Jargolis RK (1984) Immunocytochemical localization of a chondroitin sulfate proteoglycan in nervous tissue. II. Studies in developing brain. *Journal of Cell Biology,* 99: 1130–1139

[26] Margolis RK, Margolis RU (1979) Complex Carbohydrates of Nervous Tissue. *Plenum Press,* 45–73

[27] Buckley KM *et al.* (1983) A synaptic vesicle antigen is restricted to the junctional region of the presynaptic plasma membrane. *Proc. Natl Acad. Sci. (USA),* 80: 7342–7346

[28] Bunge RP, Bunge MB (1983) Interrelationship between Schwann cell function and extracellular matrix production. *Trends Neuroscience,* 6: 499–505

[29] Rollins BJ, Cathcart MK, Culp LA (1982) The Glycoconjugate (ed. Harowitz, M. I.) *Academic Press (NY),* 3: 289–329

[30] Bellail AC et al. (2004) Microregional extracellular matrix heterogeneity in brain modulates glioma cell invasion*. IJBCB,* 36: 1046-1069

[31] Bellail AC et al. (2004) Mircroregional extracellular matrix heterogenity in brain modulates glioma cell invasion. IJBCB 36, 1046-1069

[32] Iozzo BP (1984) Proteoglycans and neoplastic–mesenchymal cell interactions. *Human Pathology,* 15: 2–10

[33] Toole BP, Goldberg RL, Chi-Rosso G, Underhill CB, Orkin RW (1984) The Role of Extracellular Matrix in Development. *Liss (NY),* 43–66

[34] Akiyama et al. (2001) Hyaluronate Receptors Mediating Glioma Cell Migration and Proliferation. *Journal of Neuro-Oncology*, 53(2): 115-127

[35] Chintala SK, Sawaya R, Gokaslan ZL, Fuller G, Rao JS (1996) Immmunohistochemical localization of extracellular matrix proteins in human glioma, both *in vivo* and *in vitro*. *Cancer Lett.,* 101: 107–114

[36] Ruosssslahti E, Pierschbacher MD (1987) New perspectives in cell adhesion: RGD and integrins. *Science,* 238: 491–497

[37] Gladson CL, Cheresh DA (1991) Glioblastoma expression of vitronectin and the αvβ3 integrin. Adhesion mechanism for transformed glial cells. *J. Clin. Invest.,* 88: 1924–1932

[38] Berens ME, Rief MD, Loo MA, Giese A (1994) The role of extracellular matrix in human astrocytoma migration and proliferation studies in a microliter scale assay. *Clin. Exp. Metastasis,* 12: 405–415

[39] Prieto AL, Edelman GM, Crossin KL (1993) Multiple integrins mediate cell attachment to cytotactin/tenascin. *Proc. Natl Acad. Sci. (USA),* 90: 10154–10158

[40] Newton HB (2006) Handbook of brain tumor chemotherapy. 1: 103-104

[41] Tucker RP (1993) The *in situ* localization of tenascin splice variants and thrombospondin 2 mRNA in the avian embryo. *Development,* 117: 347–358

[42] Wehrle-Haller B, Koch M, Baumgartner S, Spring J, Chiquet M (1991) Nerve-dependent and -independent tenascin expression in the developing chick limb bud. *Development,* 112: 627–637

[43] Tritschler I, Gramatzki D, Capper D, Mittelbronn M, Meyermann R, Saharinen J, Wick W, Keski-Oja J, Weller M (2009) Modulation of TGF-beta activity by latent TGF-beta-binding protein 1 in human malignant glioma cells. *Int J Cancer,* 125(3): 530-540

[44] Zimmermann DR, Ruoslahti E (1989) Multiple domains of the large fibroblast proteoglycan, versican. *EMBO Journal,* 8(10): 2975-2981

[45] Isogai Z, Shinomura T, Yamakawa N (1996) 2B1 antigen characteristically expressed on extracellular matrices of human malignant tumors is a large chondroitin sulfate proteoglycan, PG-M/versican. *Cancer Reseach,* 56(17): 3902-3908

[46] Arslan F, Bosserhoff AK, Nickl- Jockschat T (2007) The role of versican isoforms V0/V1 in glioma migration mediated by transforming growth factor- β2. *Cancer Research (UK),* 96: 1560-1568

[47] LeBaron RG (1996) Versican. *Perspectives on Developmental Neurobiology,* 3(4): 261–271

[48] Matsumoto K, Shionyu M, Go M, Shimizu K, Shinomura T, Kimata K et al. (2003) Distinct interaction of versican/PG-M with hyaluronan and link protein. *Journal of Biological Chemistry,* 278(42): 41205–41212

[49] LeBaron RG (1996) Versican. *Perspectives on Developmental Neurobiology,* 3(4): 261–271

[50] www.ncbi.nlm.nih.gov/bookshelf/picrender.fcgi

[51] LeBaron RG, Zimmermann DR, Ruoslahti E (1992) Hyaluronate binding properties of versican. *Journal of Biological Chemistry*, 267(14): 10003–10010

[52] Wight TN (2002) Versican: a versatile extracellular matrix proteoglycan in cell biology. *Current Opinions in Cell Biology*, 14(5): 617–623

[53] Wu YJ, La Pierre DP, Wu J, Yee AJ, Yang BB (2005) The interaction of versican with its binding partners. *Cell Research*, 15(7): 483–549

[54] Aspberg A, Adam S, Kostka G, Timpl R, Heinegard D (1999) Fibulin-1 is a ligand for the C-type lectin domains of aggrecan and versican. *Journal of Biological Chemistry*, 274(29): 20444–20449

[55]Olin AI, Morgelin M, Sasaki T, Timpl R, Heinegard D, Aspberg A (2001) The proteoglycans aggrecan and Versican form networks with fibulin-2 through their lectin domain binding. *Journal of Biological Chemistry*, 276(2): 1253–1261

[56] Hirose J, Kawashima H, Yoshie O, Tashiro K, Miyasaka M (2001) Versican interacts with chemokines and modulates cellular responses. *Journal of Biological Chemistry*, 276(7): 5228–5234

[57] Perissinotto D, Iacopetti P, Bellina I, Doliana R, Colombatti A, Pettway Z, et al. (2000) Avian neural crest cell migration is diversely regulated by the two major hyaluronan-binding proteoglycans PG-M/versican and aggrecan. *Development*, 127(13): 2823–2842

[58] Sheng W, Wang G, Wang Y, Liang J, Wen J, Zheng PS et al. (2005) The roles of versican V1 and V2 isoforms in cell proliferation and apoptosis. *Molecular Biology of the Cell*, 16(3): 1330–1340

[59] Sheng W, Wang G, Wang Y et al. (2005) The roles of versican V1 and V2 isoforms in cell proliferation and apoptosis. *Molecular Biology of the Cell,* 16(3): 1330-1340

[60] Wu Y, Sheng W, Chen L, Dong H, Lee V, Lu F et al. (2004) Versican V1 isoform induces neuronal differentiation and promotes neurite outgrowth. *Molecular Biology of the Cell*, 15(5): 2093–2104

[61] Y Wu, W Sheng, L Chen, H Dong et. al (2004) Versican V1 Isoform Induces Neuronal Differentiation and Promotes Neurite Outgrowth. *Mol Biol Cell.,* 15(5): 2093–2104

[62] Asher RA, morgenstern DA, Shearer MC, Adcock KH, Pesheva P, Fawcett JW (2002) Versican is upregulated in CNS injury and is a product of oligodendrocyte lineage cells. *J. Neurosci.,* 22: 2225-2236

[63] Ricciardelli C, Russell DL, Ween MP, Mayne K, Suwiwat S, Byers S, Marshall VR, Tilley WD, Horsfall DJ (2007) Formation of hyaluronan- and versican-rich pericellular matrix by prostate cancer cells promotes cell motility. *Journal of biological chemisty,* 282(14): 10814-10825

[64] Ween MP, Hummitzsch K, Rodgers RJ, Oehler MK, Ricciardelli C (2011) Versican induces a pro-metastatic ovarian cancer cell behavior which can be inhibited by small hyaluronan oligosaccharides. *Clinical and experimantal Metastasis*, 28(2): 113-125

[65] Makatsori E, Lamari FN, Theocharis AD, Anagnostides S, Hjerpe A, Tsegenidis T et al. (2003) Large matrix proteoglycans, versican and perlecan, are expressed and secreted by human leukemic monocytes. *Anticancer Research*, 23(4): 3303–3309

[66] Voutilainen K, Anttila M, Sillanpaa S, Tammi R, Tammi M, Saarikoski S et al. (2003) Versican in epithelial ovarian cancer: relation to hyaluronan, clinicopathologic factors and prognosis. *International Journal of Cancer*, 107(3): 359–364

[67] Riccardelli C, Brooks JH, Suwiwat S et al. (1998) Elevated levels of versican but not decorin predict disease progression in early stage prostate cancer. *Clinical Cancer Research,* 4: 963-71

[68] Sakko AJ, Ricciardelli C, Mayne K, Tilley WD, LeBaron RG, Horsfall DJ (2001) Versican accumulation in human prostatic fibroblast cultures is enhanced by prostate cancer cell derived transforming growth factor beta1. *Cancer Research*, 61(3): 926–930

[69] Lemire JM, Merrilees MJ, Braun KR, Wight TN (2002) Overexpression of the V3 variant of versican alters arterial smooth muscle cell adhesion, migration, and proliferation in vitro. *Journal of Cell Physiology*, 190(1): 38–45

[70] Serra M, Miquel L, Domenzain C, Docampo MJ, Fabra A, Wight TN et al. (2005) V3 versican isoform expression alters the phenotype of melanoma cells and their tumorigenic potential. *International Journal of Cancer*, 114(6): 879–886

[71] Miquel-Serra L, Serra M, Hernandez D, Domenzain C, Docampo MJ, Rabanal RM et al. (2006) V3 versican isoform expression has a dual role in human melanoma tumor growth and metastasis. *Laboratory Investigation*, 86(9): 889–901

[72] Arslan F, Doerfelt A, Bogdahn U, Hau P (2006) The regulatory effect of transforming growth factor- beta 2 in malignant glioma invasion via modulation of extracellular matrix. *Proc Am Assoc Cancer Res,* 47: 3285

[73] Carmela Ricciardelli, Andrew J. Sakko, Miranda P. Ween, Darryl L. Russell und David J. Horsfall (2009) The biological role and regulation of versican levels in cancer. *Cancer and Metastasis Reviews,* 28(1-2): 233-245

[74] Carmela Ricciardelli, Andrew J. Sakko, Miranda P. Ween, Darryl L. Russell und David J. Horsfall (2009) The biological role and regulation of versican levels in cancer. *Cancer and Metastasis Reviews,* 28(1-2): 233-245

[75] Arslan F, Doerfelt A, Bogdahn U, Hau P (2006) The regulatory effect of transforming growth factor- beta 2 in malignant glioma invasion via modulation of extracellular matrix. *Proc Am Assoc Cancer Res,* 47: 3285

[76] Arslan F, Bosserhoff AK, Nickl- Jockschat T (2007) The role of versican isoforms V0/V1 in glioma migration mediated by transforming growth factor- β2. *Cancer Research (UK),* 96: 1559-1565

[77] Arslan F, Bosserhoff AK, Nickl- Jockschat T (2007) The role of versican isoforms V0/V1 in glioma migration mediated by transforming growth factor- β2. *Cancer Research (UK),* 96: 1559-1565

[78] Arslan F, Bosserhoff AK, Nickl- Jockschat T (2007) The role of versican isoforms V0/V1 in glioma migration mediated by transforming growth factor- β2. *Cancer Research (UK),* 96: 1559-1565

[79] Gregory J. Hannon (2002) RNA interference. *Nature* 418: 244-251

[80] Morris KV, Chan SWL, Jacobsen SE, Looney DJ (2004) Small Interfering RNA-Induced Transcriptional Gene Silencing in Human Cells. *Science,* 5688: 1289-1292

[81] http://www.boc.uu.se/boc14www/res_proj/RNAi.html

[82] Paddison PJ, Caudy AA, Bernstein E et al. (2002) Short hairpin RNAs (shRNAs) induce sequence-specific silencing in mammalian cells. *Genes Dev.,* 16: 948-958

[83] Jankovic R, Radulovic S, Brankovic-Magic M (2009) siRNA and miRNA for the treatment of cancer. *J B.U.ON.,* 14(1): 43-49

[84] Bogdahn U, Apfel R, Hahn M, Gerlach M, Behl C, Hoppe J, Martin R (1989) Autocrine tumor cell growth-inhibiting activities from human malignant melanoma. *Cancer Res.,* 49(19): 5358-5363

[85] Experimental Biosiences, Introductory labratories BioC-211, counting chamber

[86] Experimental Biosiences, Introductory labratories BioC-211, counting grid

[87] Roche (2005) Cell Proliferation Kit II (XTT)- Colorimetric assay (XTT based) for the non-radioactive quantification of cell proliferation and viability. Cat. No. 11 465 015 001

[88] Fedorcsák I, Ehrenberg L (1966) Effects of diethyl pyrocarbonate and methyl methanesulfonate on nucleic acids and nucleases. *Acta Chem Scand.,* 20(1): 107-112

[89] http://www.ncbi.nlm.nih.gov/tools/primer-blast/

[90] Roux H (2009) Optimization and troubleshooting in PCR. *Cold Spring Harb Protoc.*, 4: 66

[91] http://www.ncbi.nlm.nih.gov/genome/seq/BlastGen/BlastGen.cgi?taxid=9606

[92] Eppendorf North America. Using Gradient PCR To Determine The Optimum AnnealingTemperature. *Inc.102 Motor Parkway, Hauppauge, NY,* 11788-5178

[93] Marten NW, Burke EJ, Hayden JM, Straus DS (1994) Effect of amino acid limitation on the expression of 19 genes in rat hepatoma cells. *FASEB J.,* 8: 538-544

[94] Elbashir SM, Harborth J, Lendeckel W, Yalcin A, Weber K, Tuschl T (2001) Duplexes of 21-nucleotide RNAs mediates RNA interference in cultured mammalian cells. *Nature,* 411: 494-498

[95] http://www.fermentas.com/techinfo/electrophoresis/pproteintransfer.htm

[96] Product: Versican V0/V1 Neo. *Thermo Fisher Scientific Inc.* ContactInfo: PO Box 117, Rockford, IL 61105 USA

Product: Versican V0/V2 Neo. *Thermo Fisher Scientific Inc.* ContactInfo: PO Box 117, Rockford, IL 61105 USA

[97] Larionov A, Krause A, Miller W (2005) A standard curve based method for relative real time PCR data processing. *BMC Bioinformatics,* 21(6): 62

[98] adapted from Yamagata L (2005) *Journal of Neuroscience*

[99] Park YK, Park SM, Choi YC, Lee D, Won M, Kim YJ (2008) AsiDesigner: exon-based siRNA design server alternative splicing. *Nucleic Acids Res.,* 1(36): 97-103

[100] Marten NW, Burke EJ, Hayden JM, Straus DS (1994) Effect of amino acid limitation on the expression of 19 genes in rat hepatoma cells. *FASEB J.,* 8: 538-544

[101] Liang CC, Park AY, Guan JL (2007) In vitro scratch assay: a convenient and inexpensive method for analysis of cell migration in vitro. *Nature Protocols,* 2: 329-333

[102] Chen HC (2005) Cell migration. *Methods in Molecular Biology,* 294(II): 15-22

[103] Ricciardelli C, Andrew J, Sakko MP (2009) The biological role and regulation of versican levels in cancer. *Cancer metastasis rev*., 28: 235

[104] Arslan F, Doerfelt A, Bogdahn U, Hau P (2006) The regulatory effect of transforming growth factor- beta 2 in malignant glioma invasion via modulation of extracellular matrix. *Proc Am Assoc Cancer Res,* 47: 3285

[105] Dours- Zimmermann MT, Zimmermann DR (1994) A novel glycosaminoglycan attachment domain identified in two alternative splice variants of human versican. *J. Biol. Chem.,* 269(52): 32992-32998

[106] Schmalfeldt M, Bandtlow CE, Dours-Zimmermann MT, Winterhalter KH, Zimmermann DR (1998) Versican V2 Is a Major Extracellular Matrix Component of the Mature Bovine Brain. *The Journal of Biological Chemistry*, 273: 15758-15764

[107] Schmalfeldt M, Bandtlow CE, Dours-Zimmermann MT, Winterhalter KH, Zimmermann DR (2000) Brain derived versican V2 is a potent inhibitor of axonal growth*. Journal of Cell Science,* 113: 807-816

[108] Wu Y, Sheng W, Chen L, Dong H, Lee V, Lu F, Wong CS, Lu WY, Yang BB (2004) Versican v1 isoform induces neuronal differentiation and promotes neurite outgrowth. *Molecular Biology of the cell*, 15(5): 2093-2104

[109] Ricciardelli C, Andrew J, Sakko MP (2009) The biological role and regulation of versican levels in cancer. *Cancer metastasis rev*., 28: 235

[110] Serra M, Miquel L, Domenzain C, Docampo MJ, Fabra A, Wight TN, Bassols A (2005) V3 isoform expression alters the phenotype of melanoma cells and their tumorigenic potential. *International journal of cancer,* 114(6): 879-886

[111] Ricciardelli C, Russel DL, Ween MP et al. (2007) Formation of hyaluronan and versican- rich pericellular matrix by prostate cancer cells promotes cell mobility. *Journal of Biological Chemistry,* 282(14), 10814-10825

[112] Dutt S, Kléber M, Matasci M, Sommer L, Zimmermann D (2005) Versican V0 and V1 guide migratory neural crest cells. *Journal of biological chemistry,* 12126: 18-21

[113] Ricciardelli C, Andrew J, Sakko MP (2009) The biological role and regulation of versican levels in cancer. *Cancer metastasis rev*., 28: 237

[114] Westling J, Gottschall PE, Thompson VP, Cockburn A et al. (2004) ADAMTS4 (aggrecanase-1) cleaves human brain versican V2 at Glu405–Gln406 to generate glial hyaluronate binding protein. *Biochem. J.,* 377: 790–793

[115] Westling J, Gottschall PE, Thompson VP, Cockburn A et al. (2004) ADAMTS4 (aggrecanase-1) cleaves human brain versican V2 at Glu405–Gln406 to generate glial hyaluronate binding protein. *Biochem. J.,* 377: 792

[116] Sledz CA, Holko M, de Veer MJ, Silverman RH, Williams BRG (2003) Activation of the interferon system by short-interfering RNAs. *Nature Cell Biology,* 5(9): 834-839

[117] Paulus W, Baur J, Dours- Zimmermann MT, Zimmermann DR (1996) Differential expression of versican isoforms in brain tumors. *J. Neuropathol. Exp. Neurol*., 55: 528-533

[118] Zheng PS, Wen J et al. (2004) Versican / PG- G3 domain promotes tumor growth and angiogenesis. *FASEB journal*, 18(6): 754-756

[119] Zheng PS, Wen J et al. (2004) Versican / PG- G3 domain promotes tumor growth and angiogenesis. *FASEB journal*, 18(6): 754-756

[120] Cattaruzza S, Schiappacassi M, Kimata K, Colombatti A, Perris R (2004) The globular domains of PG-M/versican modulate the proliferation-apoptosis equilibrium and invasive capabilities of tumor cells. *FASEB J.,* 18(6): 779-781

[121] Ang LC, Zhang Y, Cao L, Yang BL (1999) Versican enhances locomotion of astrocytoma cells and reduces cell adhesion through its G1 domain. *Journal of neuropathology and experimental neurology*, 58(6): 597-605

[122] Wu YJ, La Pierre D, Wu J, Yee AJ, Yang BB (2005) The interaction of versican with its binding partners. *Cell Research,* 15: 483–494. doi:10.1038/sj.cr.7290318

[123] Zheng PS, Wen J et al. (2004) Versican / PG- G3 domain promotes tumor growth and angiogenesis. *FASEB journal,* 18(6): 754-756

[124] Zhang Y, Cao L, Yang BB (1999) The G3 domain of versican enhances ell proliferation via epidermal growth factor- like motifs. *Journal of biological chemistry,* 72(2): 210-220

[125] Zheng PS, Wen J et al. (2004) Versican / PG- G3 domain promotes tumor growth and angiogenesis. *FASEB journal,* 18(6): 754-756

[126] Miquel- Serra L, Serra M, Hernadez D et al. (2006) V3 versican isoform expression has a dual role in human melanoma tumor growth and metastasis. *Laboratory Investigation,* 86(9): 889-901

[127] Yamagata M, Kimata K (1994) Repression of a malignant cell substratum adhesion phenotype by inhibiting the production of the ant- adhesive proteoglycan, PG –M/ versican. *J cell Sci,* 107: 2581-2590

[128] Hynes RO (1992) Integrins: Versatility, modulation, and signaling in cell adhesion. *Cell,* 69: 11-25

[129] Ang LC, Zhang Y, Coa L et al. (1999) Versican enhaces locomotion of astrocytoma cells and reduces cell adhesion through its G1 domain. *Journal of Neuropathology and Experimental Neurology,* 58(6): 597-605

[130] Wu Y, Chen L, Zheng PS, Yang BB (2002) 1-Integrin-mediated Glioma Cell Adhesion and Free Radical-induced Apoptosis Are Regulated by Binding to a C-terminal Domain of PG-M/Versican. *J Biol Chem.,* 14: 12294–12301

[131] Yamagata M and Kimata K (1994) Repression of a malignant cell-substratum adhesion phenotype by inhibiting the production of the anti-adhesive proteoglycan, PG-M/versican. *Journal of Cell Science,* 107: 2581

[132] Miquel-Serra L, Serra M, Hernandez D, Domenzain C, Docampo MJ, Rabanal RM, de Torres I, Wight TN et al. (2006) V3 versican isoform expression has a dual role in human melanoma tumor growth and metastasis. *Laboratory Investigation,* 86: 889–901

[133] Yamagata M, Kimata K (1994) Repression of a malignant cell substratum adhesion phenotype by inhibiting the production of anti- adhesive proteoglycan, PG-M/ versican. *J Cell Sci,* 107: 2581-2590

[134] Arslan F, Bosserhoff AK, Nickl- Jockschat T (2007) The role of versican isoforms V0/V1 in glioma migration mediated by transforming growth factor- β2. *Cancer Research (UK),* 96: 1559-1565

[135] Arslan F, Bosserhoff AK, Nickl- Jockschat T (2007) The role of versican isoforms V0/V1 in glioma migration mediated by transforming growth factor- β2. *Cancer Research (UK),* 96: 1559-1565

[136] The Cancer Genome Atlas Research Network TCGA (2008) Comprehensive genomic characterization defines human glioblastoma genes and core pathways. Nature, 455: 1061-1068

[137] Beier D, Hau P, Proescholdt M , Lohmeier A , Wischhusen J, Oefner PJ et al. (2007) CD133+ and CD133- glioblastoma-derived cancer stem cells show differential growth characteristics and molecular profiles. *Cancer Res,* 67: 4010–4015

[138] Sang KL et al. (2009) Glioblastoma multiforme: a perspective on recent findings in human cancer and mouse models. *BMB reports,* 158-164

[139] Rosenblum ML, Dougherty DV, Reese C, Wilson CB (1981) Potentials and possible pitfalls of human stem cell analysis. *Cancer Chemotherapy and Pharmacology,* 6(3): 227–235